TÉCNICO LISBOA

Development of a smart node IoT for agriculture appliances

João Pedro Ramos Tagaio

Thesis to obtain the Master of Science Degree in

Electrical and Computer Engineering

Supervisor(s): Prof. Doutor António Manuel Raminhos Cordeiro Grilo
Prof. Doutor Marcelino Bicho dos Santos

Examination Committee

Chairperson: Prof. Doutor Francisco André Corrêa Alegria
Supervisor: Prof. Doutor Marcelino Bicho dos Santos
Member of the Committee: Prof. Doutor Pedro Manuel Brito da Silva Girão

November 2019

Declaration

I declare that this document is an original work of my own authorship and that it fulfills all the requirements of the Code of Conduct and Good Practises of the Universidade de Lisboa.

Dedicated to my parents which always supported me

Acknowledgments

I would first like to thank my thesis supervisors, professor António Grilo and professor Marcelino Santos, for all their support during the writing and development of this thesis. Professor António Grilo with a precious help for the communication protocol and professor Marcelino for all the electronics questions that emerge during the writing of the thesis. They allowed this thesis to be my own work, but guided me to the right direction whenever they thought I needed it. I would also like to thank Paulo Ilhéu from Muvu Technologies which helped creating a network server for the LoRaWAN protocol. Also for his great sense of humor and motivation that helped this thesis to gain form. I would like to acknowledge Muvu Technologies that supported all the financial costs of the thesis. From the components to the PCB's a word of gratitude for enabling this thesis to have a final physical product. A special thanks to António Gonçalves and Tiago Santos from Muvu Technologies that believed in this thesis and for giving me the opportunity to work in Muvu Technologies during the writing and development where all the necessary tools were made available. A special thanks to Igor Fernandes, Alexander Fernandes, Diogo Santos, Luís Lota and all the Muvu Technologies employees that supported me during the writing of the thesis. I would also like to thank Pedro Neves from SiliconGate which helped soldering the most difficult components which required the use of a heat gun. I will never forget the help provided and the time that Pedro spent to solve the problems that emerge during the hardware test phase. Finally, I must express my profound gratitude to my parents and my brother for giving me unconditional support and encouragement throughout my years of study. This thesis would not have been possible without any of you. Thank you all.

Resumo

Atualmente com as alterações climáticas, juntamente com o crescimento populacional, é necessário reduzir o desperdiço de recursos utilizados na agricultura. A utilização de sistemas de informação pode ser útil na redução do desperdício de água e na utilização excessiva de fertilizantes que podem esgotar os recursos hídricos e levar à erosão dos solos. Com os recentes desenvolvimentos nas áreas de microelectrónica e protocolos de comunicação, é atualmente possível criar sistemas de monitorização que comunicam a uma distância de vários quilómetros e com uma duração de vários anos utilizando apenas uma carga de bateria. Novos protocolos, como por exemplo, a rede LoRaWAN ou Sigfox permitem este alcance de vários quilómetros. Nesta tese é apresentado um sistema embebido com uma corrente em modo de suspensão muito baixa de forma a otimizar a duração da bateria. Deste modo, é usado um sistema que desliga o microcontrolador ficando apenas o relógio de tempo real em funcionamento. Visto que as variáveis físicas num campo agrícola variam lentamente, um sistema embebido utilizado em agricultura de precisão passa grande parte do tempo em suspensão. A suspensão do sistema é conseguida através do desligar de todos os componentes expecto o relógio de tempo real. É também utilizado um conversor de tensão contínua de forma a melhorar a eficiência do sistema para módulos com consumos mais elevados. Finalmente, o sistema utilizado teve em consideração os sensores utilizados em agricultura de precisão.

Palavras-chave: Sistema Embebido, Ultra baixo consumo, LoraWAN, Gestão de Energia

Abstract

In the present, with the growth of population and the climate change, it is necessary to create more efficient ways of farming. The use of information systems can reduce the waste in the agriculture process such as the water waste and the use of excessive fertilizers that stresses the water resources and contribute to the erosion of soils. With new advancements in microelectronics and communication protocols, it is now possible to create ultra low power systems able to get data from sensors and transmit it to the Internet. New Low-Power Wide-Area Network protocols such as LoRaWAN and Sigfox allow each node to have a range of several kilometres. In addition, the use of low power regulators, with low quiescent currents, and a real time clock to generate interruptions, allow the system to achieve long periods of operation using a single battery charge. This thesis work proposes a embedded system with a ultra low power sleep mode. Considering that physical variables in a farm present slow variation, an embedded system used for precision agriculture can spend most of its time in a sleep state. The ultra low power is achieved by disabling all the modules except the real time clock. In addition, the use of a DC-DC converter to power demanding modules allows optimal efficiency. The system was design to support sensors that are used in precision agriculture.

Keywords: Embeded System, Ultra Low Power, Low-Power Wide-Area Network Protocols, Power Management

Contents

List of Tables

List of Figures

Glossary

I^2C	Inter-integrated Circuit Protocol - A protocol intended to allow multiple slaves to communicate with one or more masters. The slaves and the masters are integrated circuits
IoT	Internet of Things - is the network of devices such as vehicles, and home appliances that contain electronics, software, actuators, and connectivity which allows these things to connect, interact and exchange data.
MCU	Microcontroller Unit - A microcontroller contains one or more CPUs (processor cores) along with memory and programmable input/output peripherals. It uses on-chip embedded Flash memory in which to store and execute the program.
MPU	A MPU incorporates the functionality of a clock, central processing unit (CPU), arithmetic logic unit (ALU), floating point unit (FPU), control unit (CU), memory management unit (MMU), interrupts, input/output interfaces, and cache. However it requires an external memory module in order to store the the program and the programming variables.
One-wire	Device communications bus system designed by Dallas Semiconductor Corp. that provides low-speed (16.3kbps) data, signaling, and power over a single conductor.

RF Radio Frequency - any of the electromagnetic wave frequencies that lie in the range extending from below 3 kilohertz to about 300 gigahertz and that include the frequencies used for communications signals (as for radio and television broadcasting and cell-phone and satellite transmissions) or radar signals

SPI Serial Peripheral Interface - An interface bus used to send data between microcontrollers and small peripherals such as sensors, and SD cards. It uses a separate clock and data lines, along with a select line to choose the device you wish to talk to.

UART Universal Asynchronous Receiver/Transmitter - A physical circuit inside a integrated circuit. The main propose is to transmit and receive serial data

USB Universal Serial Bus - Used to designate a kind of standard interface for connecting peripherals to a computer

Chapter 1

Introduction

1.1 Motivation

The Internet of Things is becoming one of the most interesting subjects when talking about technology. With the ability to connect several devices to the Internet that can transmit data from sensors or control the state of specific actuators, previous objects that were static are now becoming intelligent. Finding a way to connect them to the Internet is one of the main challenges that needs to be surpassed. At the same time, the development of a system that uses the right hardware is also a challenge to be taken into account. It is necessary to consider the hardware used in terms of processing data, communication capabilities, and connections to external elements such as sensors and actuators. In addition to this, an IoT project requires the use of an online platform where the data from the sensors can be processed in order to transmit valuable information to the end user. Having that in mind, this thesis focuses on the development of an IoT board to be used in an agriculture system. An IoT agricultural system uses several sensors such as light, humidity, temperature, soil moisture and others in order to monitor the crop field. These sensors help farmers to monitor the state of the farm, and to act accordingly, but they also help the agriculture field to tackle the challenges that it faces. With the growing in population, there is a need to produce more food. For that reason the production must be optimized in order to reduce the waste of natural resources.

1.2 Muvu Technologies

Muvu Technologies is a company in the field of information and communication technologies. Its market consists on areas such as Web and Mobile Applications, Information Technologies Infrastructures, Internet of Things and Industry 4.0. The main objective of this thesis is the design of an hardware system that can last for several years with a single battery charge in order to monitor an agriculture field. Furthermore, the ability to connect different sensors is an important aspect to be taken into consideration. Muvu Technologies proposed this thesis with the aim to obtain a product targeting the market and also to be used by them to gather information in order to apply machine learning algorithms and data science. It

is then important to create a reliable system that can extract the information from the sensors and send it to a gateway/server.

1.3 Topic Overview

The agriculture field will face many challenges in the years ahead. The climate change alongside with population grown create challenges that need to be overcome. It is necessary to reduce the waste of resources in agriculture, more precisely the use of water and fertilizers. With the use of sensors and actuators it is possible for the farmer to monitor the state of the farm. From the collected information it is possible to take a more accurate action that optimizes the resources. For instance the data extracted from the field can point to the necessity of watering the plants or the need of a fertilizer in some parts of the field. With this application in mind it is important that the hardware involved can operate for long periods of time using a single battery charge. For that to happen, the use of hardware parts that are highly efficient and operate in ultra-low power whenever possible are required. By deploying several of this nodes in a agriculture field a good amount of information can be gathered to inform the farmer and reduce its costs and improve the overall efficiency of the agriculture activity.

1.4 Objectives

In this thesis two main topics will be studied. The first one is the development of an embedded system that can be integrated in an agriculture precision monitoring system. The main challenges consist in the design of a system that needs to sustain external environmental effects such as temperature and humidity. A possible architecture will be proposed for an embedded system aiming to be supplied for several days from a single battery charge. Existing systems used in agriculture and their characteristics are presented as well. The second topic refers to the different Internet of Things (IoT) communication protocols. In recent years, several protocols emerged in the market clamming power saving features and long ranges. In this thesis, a study will be conducted in terms of IoT protocols. The final objective is to have a, fully functionally embedded system that can be used in an agriculture field to monitor different physical variables such as temperature and humidity of the soil.

1.5 Thesis Outline

In the next chapter, the current state of IoT systems used for monitoring agriculture fields are presented. The hardware, the sensors, and the different protocols are detailed. Additionally, different implementations of precision agriculture systems supported by sensors to gather information from the agriculture field are presented.

The third chapter, the design of the embedded system is presented. The power management of the system is discussed selecting the appropriate voltage regulators targeting maximum efficiency. In addition, the microcontroller and the communication protocol are presented as well as the sensors.

The fourth chapter, the system is detailed both in terms of hardware and software. Chapter five presents the different tests that were conduct in order to verify the correct functionality of the system.

Finally, chapter six presents the conclusions and points at possible future improvements.

Chapter 2

Background

The agricultural market is facing numerous challenges related to the food production. The increase of population requires the use of more sophisticated methods to reduce the waste and to increase the efficiency of the agricultural process. Through this chapter, the needs of the agriculture market are presented, as well as the IoT systems that are being used in several agriculture applications to increase the productivity and to reduce the waste. In addition, the different communication protocols and the hardware used in these IoT systems are discussed

2.1 Agriculture challenges

With the population growth, it is necessary to produce more food. This can only be achieve with a reduction of the resources wasted, namely water, food for cattle, etc. It is expected that the world population will increase 2.3 billion from 2009 to 2050 [1]. It is estimated that this growth will happen in sub developed countries, especially on southeast Asia and sub Saharan Africa. Not only the population in these places is expected to grow but also their economical situation. The growth of purchase power in sub development countries will also have impact in the food consumed [2]. On the other hand, food consumption in developed countries is heavily based on meat and it will continue like that in the following years [2]. It is important to understand the consumption of calories, per person per year, in the different parts of the word. Normally, countries that have developed economics have a higher intake of calories and sub developed countries present a minor intake. However, in sub developed countries the intake of calories is expected to increase. This rise of calories consumed needs to be followed by an increase of food production, which means an increase of agriculture production. Figure 2.1 taken form [2] represents the food consumption per capita. In Figure 2.1 it is possible to understand the food consumption per capita in different parts of the word. The dark blue represents the consumption of food in interval from 2005 to 2007. The blue light represents the food consumption in the year 2050. It is possible to see that the food consumption increases in all parts of the word (develop and sub develop countries). Following the same topic, it is now important to understand the type of food that people around the world consume. For instance in India and Muslim countries there is a lower intake of meat because of religious questions

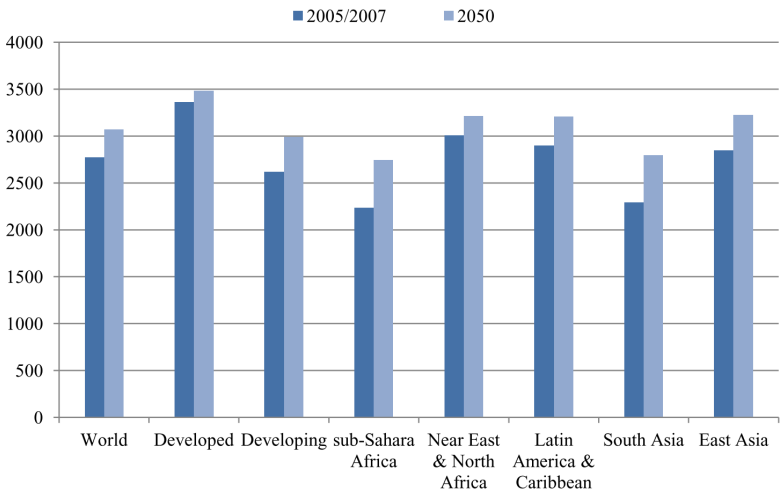

Figure 2.1: Food consumption per capita (kcal/person/year) [2]

(pork is forbidden for Muslims and cow is sacred for the Hindu people). In contrast, in western countries, there is a enormous intake of meat (Europe and North America are the two biggest responsible). The diet of these two regions is heavily based on meet. China and Brazil, followed the diet of the western world during their development [2]. However the same evolution is not expected for other sub developed countries. In Figure 2.2, the different types of agriculture products that people consume are presented.

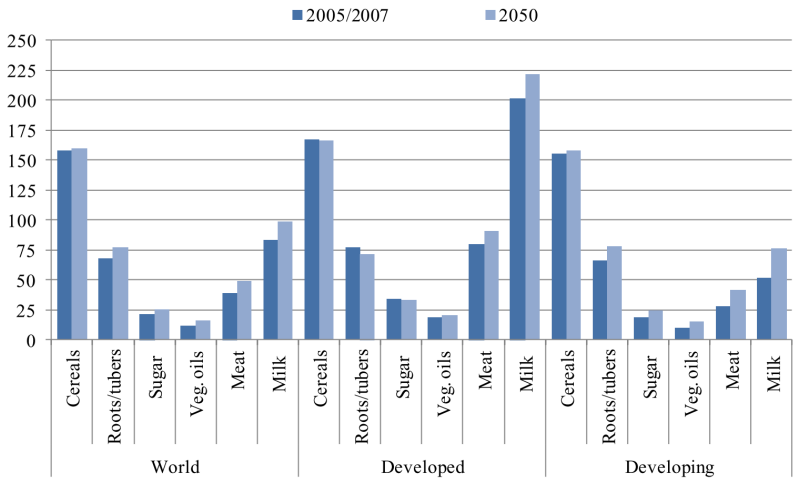

Figure 2.2: Types of food per capita (kcal/person/year) [2]

The dark blue lines are relative to the period from 2005 to 2007 where light blue line are relative to the year of 2050 and it is an estimate. As we can see, there is an increase in all food products although the products that have an higher increase are milk, roots/tubers and meat. The production of this products is related with cattle (milk and meat), open field agriculture (tubers) and greenhouses(roots). As a consequence, there is a need for a more efficient way to produce these types of food. It points then to the concept of precision agriculture.

2.1.1 Precision agriculture

It is very important to define the concept of precision agriculture. The Home Grown Cereals Authority (HGCA) defines precision farming as management of farm practices that uses computers, satellite positioning systems and remote sensing devices to provide information from which the farmer takes his decision. On the other hand, the United States Department of Agriculture (USDA) refers to this type of agriculture as being needed and it uses the following definition: A management system that is information and technology based, is site specific and uses one or more of the following sources of data: soils, crops, nutrients, pests, moisture or yield for optimum profitability, sustainability and protection of the environment. Precision agriculture can be summarized as the use of information technologies in agriculture (computers, sensors, drones and others) to collect data and to produce a valuable output for the farmer. For example, a sensor that is collecting data related to soil moisture can alert the farmer when it is necessary to locally water the farm. In order to monitor an agriculture field, a set of sensors can be used to measure different physical variables such as temperature, PH and moisture of the soil, humidity of the air and temperature, light and concentration of C02 [3]. In [3], in section Case Studies, different projects of precision agriculture are described. From a bee monitoring system that uses a microcontroller and some sensors to monitor the temperature of a bee hive, to a system that uses temperature, humidity sensors, light sensors, carbon dioxide concentration sensors, soil temperature sensors and PH sensors to monitor a greenhouse, there are many different projects in precision agriculture where a microcontroller and sensors are used to monitor an agricultural system. On the other hand, there are also drones used that acquire pictures from the air and use image processing algorithms to evaluate the conditions of the soil [4].

2.1.2 Internet of Things

The Internet of Things (IoT) is a system of interrelated computing devices, mechanical and digital machines, objects, animals or people that are provided with unique identifiers (UIDs) and the ability to transfer data over a network without requiring human-to-human or human-to-computer interaction [5]. These smart technologies allow everyday inanimate objects the possibility to think or process information and interact with the world. When the farmer puts sensors in his plantation, the farm starts to talk to him, giving information of the temperature, humidity, moisture, PH of soil and others. The term Internet of Things is one of the most interesting topics in technology nowadays and the number of articles about this topic is growing, namely addressing IoT in agriculture [6]. The different types of hardware used, alongside with the different communication protocols used, are discussed. Table 2.1 is based in [6] and presents frequently used hardware and communication protocols in precision agriculture namely, the microcontroller and the transceiver used. It is possible to see that different types of microcontrollers, like the MSP430 from Texas Instruments alongside microcontrollers from Atmel are widely used. On the other hand, most of the boards used in precision agriculture have an IEEE 802.15.4 transceiver module, except the LoPy platform that already has a LoRaWAN transceiver. When taking into consideration the application of sensors nodes in agriculture, important aspects include the accuracy and the shield against

environmental factors, which can either produce false information or permanently destroy the node [6]. On the other hand, it is also important to have in consideration the power source of the node. Normally, these nodes run on a finite source, such as a single battery charge or, on the other hand, they can use mechanisms of energy harvesting such as solar panels or wind turbines to generate energy and recharge its batteries. It is also important to have in consideration that the ability for the farmer to reach the node and change the battery is very limited [6]. Having in consideration the previous reasons presented, the design of an hardware system to be used in precision agriculture needs to take in consideration the power consumption. The important aspects of a sensor node are its durability, stability, the number of inputs (analog and digital), the capacity to hold the energy of the battery for long periods of time and the ease to program the device [6]. It is also important to consider the characteristics of different communication protocols in order to choose which best fits an agriculture application.

Table 2.1: The most usual platforms used in precision agriculture [6]

Platform name	Microcontroller	Transceiver	Program, Data Memory	Flash, EEPROM, Ext. Memory	Sensor Connections	Sleep Current
IMote 2.0	Marvell PXA271 ARM 11-400 MHz	TI CC2420 IEEE 802.15.4/ZigBee compliant radio	32 MB SRAM	32 MB	UART, SPI, I2C, GPIOS	Data not available
Iris Mote	ATmega 1281	Atmel AT86RF230 802.15.4/ZigBee compliant radio	8 KB RAM	128 KB	ADC, UART, GPIOS, I2C, SPI	$8\mu A$
TelosB/T-Mote Sky	Texas Instruments MSP430 microcontroller	250 kbit/s 2.4 GHz IEEE 802.15.4 Chipcon Wireless Transceiver	8 KB RAM	48 KB	UART, SPI, I2C, USB, ADC	$1\mu A$
Zolertia Remote	CC2538 ARM Cortex-M3	Dual Radio: 802.15.4/CC1200 869/915 MHz	32 KB RAM	512 KB	UART, I2C, SPI, ADC	$1\mu A$ *to* $150nA$
Zolertia Z1	Texas Instruments MSP430 microcontroller	Chipcon Wireless Transceiver 2.4 GHz IEEE 802.15.4	8 KB RAM	92 KB	GPIOS, SPI, I2C, UART, USB	Data not available
WiSMote	Texas Instruments MSP430 microcontroller	TI CC2520 2.4 GHz IEEE 802.15.4	16 KB RAM	1-8 MB, 128, 192 or 256 KB	Data not available	Data not available
Waspmote	ATmega 1281	ZigBee/IEEE 802.15.4 DigiMesh RF, 2.4 GHz/868 MHz/915 MHz	8 KB SRAM	128 KB, 4 KB EEPROM, 2 GB SD card	Analog, GPIOS, UART, I2C, SPI, USB	$7\mu A$
Arduino Uno/Mega/Nano	ATmega328P ATmega168 ATmega328P	External modules	2 KB SRAM/8 KB SRAM/2 KB SRAM	32 KB, 1 KB/256 KB, 4 KB/32 KB, 1 KB	Analog, I2C, SPI, UART, Digital	Data not available
Arduino Yun (2 processors)	ATmega32U4/Atheros AR9331	Ethernet, Wifi	2.5 KB, 64 MB DDR2	1 KB/16 MB	Analog, I2C, SPI, UART, Digital	Data not available
Raspberry Pi (various versions)	ARMv6 (1-core, 700MHz) ARMv7 (4-cores, 900MHz) ARMv8 (4-cores, 1.2 GHz)	Onboard LAN, "Wifi/Bluetooth" ("RPi 3 only")	256 MB - 1 GB SRAM (@400 MHz)	SD card	I2C, SPI, UART, GPIOS	Data not available
LoPy (2 processors)	Xtensa (2-cores, 160 MHz)	Onboard Wifi, SX1272 LoRa, Bluetooth (BLE)	256 KB	1 MB (internal) 4 MB (external)	Analog, GPIO, UART, SPI	$10\mu A$
NodeMCU	ESP8266/LX106	Onboard Wifi	20 KB RAM	4 MB Flash	Analog, GPIO, UART, SPI	$20\mu A$
Arietta G25	ARMv9 (4-cores, 400 MHz)	External Wifi adapter	128-256 MB RAM	SD card	Analog, I2C, UART, SPI	$9.1mA$
WIOT Board	ATmega32U4 ESP8266 (for Wifi)	Wifi	2.5 KB SRAM	32 KB, 1 KB	Analog, GPIOS	Data not available

2.2 Communication Protocols

In [6] and [7] the communication protocols are divided in the following categories.

- Celular - The use of the GSM, 3G, 4G and 5G technologies to allow the sensor nodes to communicate with the Internet. It offers reliable communication and a good support. However it presents an higher cost of operation and it uses more power than the others.
- Mesh Protocols - In this typology if the sensor is too far away from the gateway it can not communicate with the gateway directly. It uses the closest node and it sends the information to that node. Then the node that received the information will send the information to the node that is closer to the gateway and so on. When finally the information reaches a node close to the gateway the information is transmitted to the gateway and then to the Internet. Very used in home automation, smart lightning, HVAC systems (climatization), security, energy management and others.
- Point-to-point - Used to establish a direct communication between two nodes. It connects two devices directly without the need for a host. An example is the RFID technology that uses radio waves to transmit a reduce amount of data from a tag to the reader. Widely used in transportation, agriculture, industry and others.
- Wireless Personal Area Networks (WPAN) - A network that connects devices that are closer to each other and have some kind of radio communication. They have reduce range (approximately 10 meters) and require communication on the line of sight. Bluetooth, Zigbee, IrDA (infrared) are all examples of WPAN.
- Wireless Regional Area Networks (WRAN) - The protocol IEEE 802.22 is the most known protocol that is WRAN. This network is defined as a network technology that uses parts of the radio frequency spectrum that are considered white spaces in order to provide connectivity to the internet. White spaces refers to portions of licensed radio spectrum that licensees do not use all the time in the same localization. This category is also associated with cognitive radio (CR) meaning that is a radio that can be setup to use the wireless channels that present the best characteristics in order to avoid congestion and interference.
- Low-Power Wide-Area Network (LPN/LPWAN) - It connects devices that are battery powered providing low bit rates over long ranges. Especially created for the market of IoT these protocols provide a long range to the sensor node creating a start topology network. The sensor nodes are able to connect to the gateway directly meaning that they do not communicate with each other. Examples of these networks are LoRaWAN, SigFox, MIOTY and NB-IoT.

The Figure 2.3 that was taken from [7] is a comparative of the different categories presented before. In 2.3 the vertical axis represents the data rate and power consumption of the protocol. The higher position represents an higher data rate and power consumption: on the other hand, a lower position means a low data rate and power consumption. In the horizontal axis a representation of the range of the protocol is made. On the right the protocols that show and higher range and on the left the ones that present a

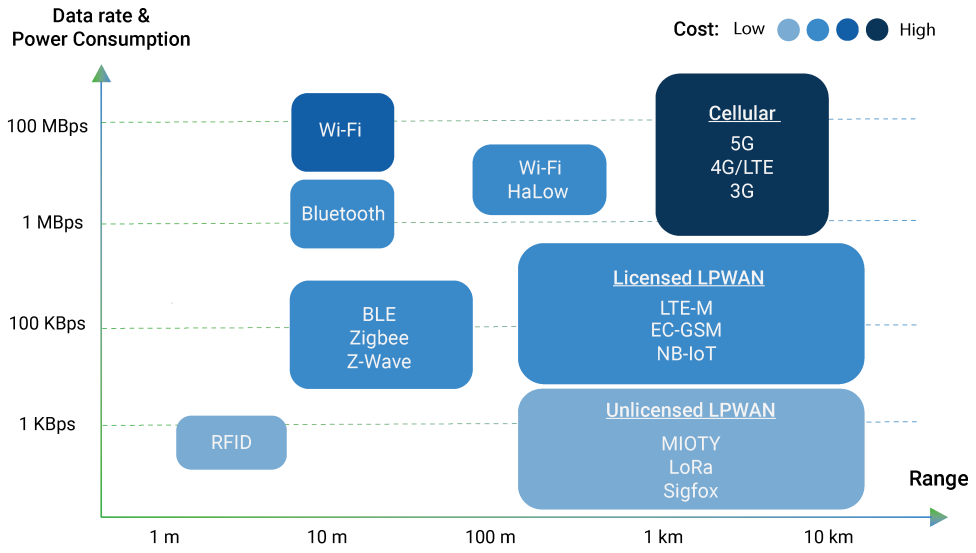

Figure 2.3: Wireless Technology used in IoT) [2]

smaller range. The most interesting protocols are the LoRa, Sigfox and MIOTY do to the long range an power consumption that they present. The LTE-M, NarrowBand-IoT (NB-IoT) and Extended Coverage Global System for Mobile Communications (EC-GSM) are also very interesting because they present a middle ground between power consumption and data rate. For these reasons they are all presented in the following sections in terms of strengths and flaws.

2.2.1 Sigfox

The Sigfox protocol is a proprietary technology developed by a French company called Sigfox. It uses Ultra Narrow Band combine with DBPSK (Differential Binary phase-shift keying) and GFSK (Gaussian frequency-shift keying) to allow the devices to connect to a gateway. It operates on the 868 MHz frequency band (868 to 869 MHz) in Europe and on the 915 MHz in North America (902 to 928 MHz). Each message sent by the gateway or the node is 100 Hz wide and transferred at 100 or 600 bits per second (data rate). Each end device can send up to 140 messages per day, accordingly with Sigfox website. For the uplink the message has a maximum of 12-bytes of payload and a downlink of 8 bytes [8]. For a 12 bytes data payload, a SIGFOX frame will use 26 bytes in total. The protocol does not acknowledge every uplink message. For that reason it is used time/frequency diversity and transmission duplication to guarantee that the messages sent by the nodes are received by the gateway [8]. Each message is sent three times in different frequency channels [8]. According to [9] the company Sigfox claims a coverage of 30 to 50 km in rural areas and 3 to 10 km in urban areas. The company also states a low power consumption due to the simplicity of the communication between the node and the gateway. The coverage of Sigfox around the world can be consulted here [10]. It is possible to see in [10] that all the Western Europe has Sigfox coverage. In other parts of the world, like United States of America, New Zealand, Japan and Iran there are some parts with Sigfox coverage and it is expected that in the following years the coverage of these countries will increase. Also in the website of Sigfox company is possible to see the different manufactures of transceivers chips [11]. The Table 2.2 shows the different transceivers available and their

characteristics.

Table 2.2: Transceiver available to be used with Sigfox protocol

Transceiver Company	Chip reference	Shutdown current	Standby current	Sleep current	Maximum Transmission current	Maximum Reception current	Maximum Sensitivity (dBm)
STMicroelectronics	S2-LP[12]	2.5 nA	500 nA	700 nA	29 mA	7.2 mA	-128
Microchip	ATA8520E[13]	5 nA	50 uA	-	31.8 mA	10.4 mA	-121.5
NXP Semiconductors	OL2385[14]	-	-	1.5 uA	38 mA	11 mA	- 124
Texas Instruments	CC1310[15]	185 nA	0.8 uA	-	25.1 mA	5.5 mA	- 121

2.2.2 LoRaWAN protocol

LoRaWAN is a network that uses LoRa modulation created by Lora-Alliance. LoRa uses spread spectrum modulation using the unlicensed sub-GHZ band. In Europe it uses the 868 MHz frequency band (868 to 869 MHz) and in America the 915 MHz frequency band (902 to 928 MHz) The LoRa modulation is based on Chirp Spread Spectrum Modulation(CSS) [8]. A chirp is a wideband frequency modulated pulse where the frequency increases with time (up chirp) or decreases (down chirp). The network LoRaWAN gives six spreading factors that go from 7 to 12 in order to achieve a longer range. The trade-off is the decrease of the data rate [8]. A higher spreading factor means a higher range but a reduced data rate. According to [8] the data rate can vary from 300 bps to 50 kbps and the maximum payload of each message is 243 bytes. In terms of robustness the LoRaWAN technology uses several techniques. The first is that all the gateways in range of a sensor node receive the message from the node. Then the network server is responsible to remove the extra messages and choose the gateway that presents the better signal. Furthermore the network server and the sensor node use special keys to improve the security of the network. The range of the LoRaWAN network varies from 5 km in urban areas and 20 km in rural areas. [8]. It is also important to take in consideration the different classes that the LoRaWAN network presents.

- Class A - It is the default class of a sensor node and must be supported by all LoRaWAN device. In this class the communication is always initiated by the end node and is fully asynchronous. When a sensor node sends an uplink message it opens two downlink windows to receive a message from the network server. This means a bi-directional communication and is a ALOHA type of protocol. In this class the sensor node can enter in a low power mode since the communication is initiated by the node. For this reason this is the class that presents the lowest power consumption.

- Class B - is very similar to class A. The only different is that the sensor node has more windows to receive data from the network server. The network server sends periodic beacons opening windows at schedule times. With this mechanism the network server is able to know when the end device is listening to the medium and send a message at the schedule time. Compared to the class A this class presents an higher consumption.

- Class C - is the most expensive class in terms of energy. The sensor node is always listening to the medium and can not enter power saving modes. For this reason the class C is suitable for an application where the device as some kind of energy source.

The only companies that produce LoRaWAN transceiver modules are Microchip and Semtech. The Table 2.3 presents one chip from each company. It is important to refer that the LoRa protocol belongs to the

Table 2.3: Transceivers available for LoRaWAN network

Transceiver Company	Chip reference	Shutdown current	Standby current	Sleep current	Maximum transmission current	Maximum reception current	Maximum sensitivity (dBm)
Microchip	RN2483[16]	50 nA	2.8 mA	1.6 uA	38.9 mA	-	- 146
Semtech	SX1262[17]	160 nA	0.6 mA	600 nA	118 mA	8.2/10.1 mA	- 134

company Semtech. The LoRaWAN network, on the other hand, is open source meaning that all the details are publicly available.

2.2.3 MiOTY

MiOTY is a LPWAN communication solution that is designed for industrial and commercial IoT deployments. There is little information about this protocol. It was developed by a company called Behr Technologies Inc. (BTI) and presents similar characteristics to LoRaWAN and SigFox. The company brochure [18] highlights some of the qualities of the protocol. It presents a low power consumption that can support up to 20 years of battery life and a range of 15 km. Also it is only necessary the deployment of a few base stations to cover vast areas. One of the interesting points is the ability to connect to a moving sensor nodes. The brochure claims that they can travel up to 120 km/h. Also the protocol says that it can achieve maximum spectral efficiency by using a technique called Telegram Splitting. This technique was patented by Fraunhofer which is a non-profit research German association. Also according to the company brochure the protocol is compatible with sub-GHz transceiver chipsets from a variety of manufacturers like Silicon Labs. An application example of this technology can be found here [19]. In this example a Mioty node is connected to a Raspberry Pi and from this hardware configuration the whole system is tested.

2.2.4 NarrowBand Internet of Things (NB-IoT)

The NarrowBand IoT is a communication protocol developed for the IoT market. It is, along side Sigfox, a narrowband protocol occupying one resource block in GSM and Long Term Evolution (LTE) technology. The NB-IoT protocol is based in the same technology as the LTE. For that reason the NB-IoT can operate in three distinct areas of the mobile network.

- Stand alone operation: It uses the GSM frequency bands that are not being used by the mobile operator to connect the devices
- Guard band operation: It uses the guard band of a carrier in LTE technology to connect the sensor nodes
- In-band operation: It uses non-allocated resources in the LTE technology

The protocol uses the same functionalities as the LTE technology although they are reduce and improve for the IoT application [8]. It can connect more than 100 000 devices per cell [8] and uses Quadrature

Phase-shift Keying (QPSK) modulation. For the uplink the protocol uses Frequency Division Multiple Access (FDMA) and for the downlink uses Orthogonal Frequency Division Multiple Access (OFDMA). The maximum throughput rate is 200kps for the downlink and 20kbps in the uplink. Each message can have a payload of 1600 bytes. The protocol claims 10 years of battery life with 200 bytes per day. [8]. The hardware depends on the mobile network and it needs to take in consideration the characteristics of the mobile network. For instance in Portugal, the only available operator is Altice Portugal [20]. The hardware used depends on the frequency band that the operator works. In Portugal the frequency bands of the Altice operator can be consulted in ANACOM site, the regulator of telecommunications in Portugal [21]. Altice uses the frequency bands of 900 MHz and 1800 MHz which corresponds to the LTE frequency bands B3 and B8. For that reason any chip compatible with these two bands can operate with the NB-IoT from Altice Portugal. The following table shows two possible chips from Quectel that can be used for an NB-IoT application. Both devices present in Table 2.4 are compatible with B3 and B8 LTE frequency bands.

Table 2.4: Compatible NarrowBand IoT chips with Altice Portugal network

Transceiver Company	Chip reference	Standby current	Sleep current	Maximum transmission current	Maximum reception current	Maximum sensitivity (dBm)
Quectel	BG96	16 mA	2.3 mA	78 mA	-	- 113
Quectel	BC66	To be defined (TBD)	TBD	TBD	TBD	TBD

2.2.5 Long Term Evolution for Machines (LTE-M)

The LTE-M protocol is another Internet of Things protocol. Machine to machine communication (M2M) refers to a direct communication between two devices using any type of communication channels. The communication can be establish between wired or wireless network. This type of communication does not require the assistance of a human and enables different devices to communicate with each other [22]. The protocol was introduce by Nokia, Qualcom and Ericson [22]. The protocol extends the specifications of LTE technology to M2M communications. It does it by improving battery life, extended coverage and a large number of devices per cell [22]. The devices using LTE-M communicate along side the devices that use LTE. There are different forms for a device to communicate using LTE-M [22].

- A device can communicate with another device in the network
- A device communicates directly to the application server over the LTE-M network
- A device can form a capillary network with other M2M devices that have similar characteristics and connect to the server via a gateway

A M2M gateway has the same characteristics as other M2M devices. Although it performs protocol translation and data aggregation before transmitting the messages to the network server [22]. A nLTE-M base station provide a way to access the LTE-M devices and gateways. Base stations are devices deployed by a cellular company giving LTE-M coverage. There were two main releases of the LTE-M protocol, release 8 and release 13. The 8 release only introduce some changes in the uplink and downlink. On the

other hand release 13 introduce several changes and a new protocol, the NB-IoT. The following table compares the LTE-M protocol to the NB-IoT protocol. As it is possible to see in Table 2.5 the LTE-M

Table 2.5: Comparison between NB-IoT and LTE-M

	Release/Category	
	Release 13	Release 13
	Cat-M (LTE-M)	Cat-NB-IoT
Downlink peak rate	1 Mbps	200 kbps
Uplink peak rate	1 Mbps	144 kbps
Duplex	Half Duplex	Half Duplex
Number of antennas	1	1
Transmit Power (UE)	20 dBm	23 dBm
Receive Bandwith (UE)	1.4 MHz	20 MHz

protocol provides higher data rates for the uplink and down link. However compared to the NB-IoT protocol it uses more energy. The NB-IoT protocol was developed having in mind the idea to reduce the energy consumption and proving energy saving features [22]. In Portugal there is no support for LTE-M protocol and for that reason no chips are presented for this protocol.

Chapter 3

Agriculture Node Design

On the market, there are different types of platforms that can be used in precision agriculture. They have multiple input and output ports, and support both digital and analog sensors. They make use of sleeping, low power states in order to reduce the power consumption of the system, powering down some modules. They also support different communication protocols and aim for several years of operation using a single battery charge. Many of the systems are heavily based on Atmel microcontrollers in order to use the Arduino bootloader which enables the use of the Arduino IDE. This simplifies the programming process and makes it easier for the user to program the microcontroller. However, this creates an abstraction from the hardware part since the Arduino IDE uses already built-in functions such as the Wire function that is the implementation of the I^2C protocol. In addition the Arduino IDE is based in C++ which compared to Assembly or C is less efficient. Although the user can use the ISCP to program the Atmel microcontroller using C or Assembly, many products use the Arduino interface to simplify the programming task. Furthermore, many of the systems available on the market do not power down the microcontroller. They use the sleep state of the microcontroller in order to reduce the current consumption of the system but they do not cut the power from the microcontroller. Also they require the use of a mechanism to turn off sensors and the transceiver module. Other systems use a separated regulator that has an enable pin that can be used to turn on or off the regulator. By turning off the regulator, modules that are powered by the regulator are disabled. Nonetheless, they still keep the power at the microcontroller and use external interruptions to wake up the microcontroller from the sleep state. This means that many systems use a regulator to power up a RTC (to generate interruptions) and the microcontroller. The proposed solution in this thesis uses a different solution in order to achieve a lower consumption when in sleep state. The proposed solution is to turn off the microcontroller, the transceiver module, and the sensors without the need of any additional hardware such as a separated regulator or transistors. Additionally, the system only uses two regulators. One of them is only used to power the RTC, which is always on. A second regulator is used to power the microcontroller, transceiver module, and the sensors. It uses the mechanism of a DC-DC regulator, that when disable, disconnects the load from the input and a RTC to generate interruptions at specific periods of time to enable the DC-DC. The aim of this design is to reduce the sleeping current since the system spends most of its time in sleep

state. In addition, it aims to reduce the hardware used in order to decrease the cost of the whole system. In this chapter, it will be presented the design of the embedded system. The design is divided in the following sections:

- Power management
- Real Time Clock
- Communication module
- Microcontroller
- Sensors interface
- Analog to digital conversion
- Working principle of the system

Figure 3.1 is a block diagram of the embedded system of this thesis.

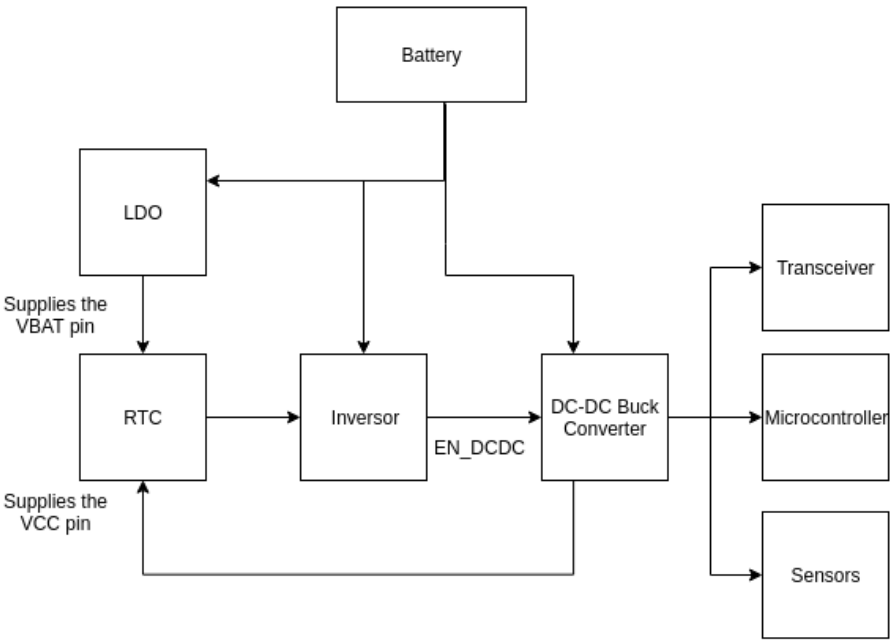

Figure 3.1: System block diagram

3.1 Power management

As already stated, the main objective of this thesis is the development of and embedded system to work for several years with a single battery charge. As a result, power management is one of the most import aspects to be optimized.

There are different types of regulators that perform different voltage translations. A voltage regulator is an electronic system that maintains a constant voltage at its output. There are different types of

regulators such as LDO (Low-Dropout Regulator) and DC-to-DC that converts a direct current (DC) from one voltage level to another voltage level. LDOs always convert an higher input voltage to a lower output voltage. On the other hand, DC-DC converters can convert from a higher voltage to a lower voltage, as well as convert from a lower voltage to a higher voltage. The first corresponds to a buck converter and the second is called a boost converter. It is important to consider the efficiency of the regulators to be used as well as their quiescent currents (currents of the electronic system when there is no load at its output). Consequently, the different possibilities are going to be studied in terms of efficiency and quiescent current in order to choose the best one for each regulator required by the system. When dealing with battery powered systems, one of the questions that emerges is the possibility to use or to use voltage regulators. Many systems prefer not to use voltage regulators and to supply the system directly from the battery. This has the benefit of reducing the consumption of the system, because there are no losses and quiescent currents in the regulators. Although this may be true, the system swings from the higher voltage level of the battery to the lower voltage, which means that when the battery is fully charge the system has an higher voltage at its inputs. This means that the quiescent currents during sleep mode are higher since more integrated circuits are active. On the other hand, by having regulators that convert the battery voltage to a lower voltage, the system can work with lower voltages at its inputs. As a result the quiescent current is lower and the operation of the system also requires less energy. Therefore, a comparison between a sub-system with regulators and a sub-system without regulators is presented in Table 3.1.

Table 3.1: Comparison between using or not using a regulator

Sub-system with regulator	**Sub-system without regulator**
Stable voltage	Voltage swings as the battery discharges
More hardware components used	Less hardware used
Compliant with higher supply voltages	Limited to the supply voltage that the sub-system can support
Quiescient currents at the regulators	No quiescent currents at the regulators
Lower quiescent current in the system	Higher quiescent current in the system

Although the use of a regulator implies higher quiescent current the fact that most components are not compliant with the complete range of the power supply, forces the use of these regulators. For that reason and considering the recent regulators available on the market that present lower quiescent current, the system purposed uses two regulators. One for the RTC and another to supply the microcontroller, sensors and transceiver. By doing this it is possible to guarantee a constant voltage of operation, and in the case of the RTC, it is possible to use the low power modes by providing a low voltage to the chip. In the next subsections, different types of voltage regulators are presented.

3.1.1 Low dropout regulator (LDO)

Nowadays targetting applications as the Internet of Things there is a necessity to develop voltage regulators that are highly efficient and present low quiescent currents. It is important to understand what

defines the efficiency of a low dropout regulator. The following equation taken form [23] represents the efficiency of a LDO.

$$Efficiency = \frac{I_{out}}{I_{out} + I_{GND}} \times \frac{V_{OUT}}{V_{IN}} \times 100 \tag{3.1}$$

It is important to define the ground current. The following equation is the definition of ground current

$$I_{GND} = I_{IN} - I_{OUT} \tag{3.2}$$

The ground current is the difference between the input current and the output current and includes the quiescent currents and all the internal losses of the regulator. In order to fully understand the working principle of a LDO, the Figure 3.2 shows its block diagram.

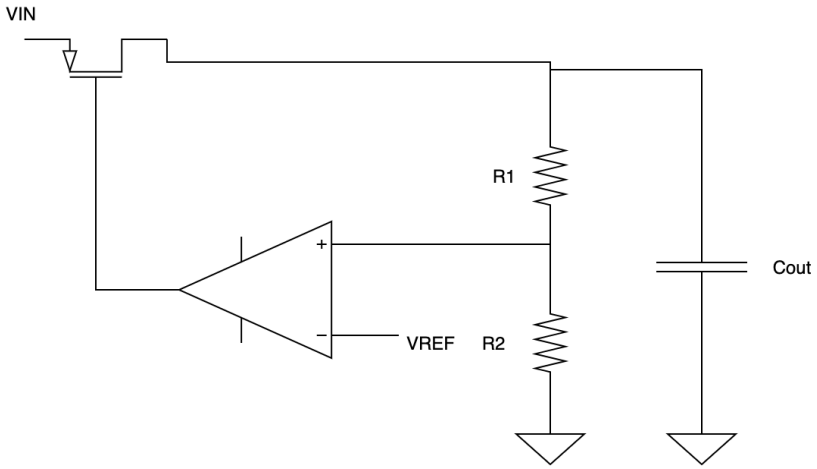

Figure 3.2: Block diagram of a LDO

The basic operation of an LDO is based on a comparison of the output voltage with an internal voltage reference. When the saturation of the driver circuit occurs the regulator starts to work in the dropout region. For an LDO to work properly the voltage at is input must follow the following equation

$$V_{IN} \geq V_{OUT} + V_{DROPOUT} \tag{3.3}$$

When V_{IN} is lower than the dropout voltage plus the output voltage, the LDO works in the dropout region. With a power device properly designed $V_{DROPOUT}$ can be in the range of 100 to 200 mV. In this region the regulator cannot keep its output voltage regulated. Additionally, the ground current increases due to the saturation of the driving circuit of the LDO. Another important aspect is the difference between the input voltage and the output voltage. When the input voltage is much higher than the output regulated voltage, the LDO presents a lower efficiency. For example, for a system with a 3.3V at

its output and 5V at the input, the efficiency cannot be higher than 66%,

$$\eta = \frac{P_{out}}{P_{in}} = \frac{I_{out} \times V_{out}}{I_{in} \times V_{in}} < \frac{V_{out}}{V_{in}} = \frac{3.3V}{5V} = 0.66 \tag{3.4}$$

In summary, to limit losses when using an LDO, it is important to have a small difference between the input and the output voltage or to limit its use to low output currents.

3.1.2 DC to DC converter (DC-DC)

Boost converter

The boost converter translates a lower voltage at its input to a higher voltage at the output. It uses a inductor to store energy and then release it to the load. Figure 3.3 shows a simple representation of power stage of a boost converter. The NMOS and PMOS transistors are used as a switch. When the

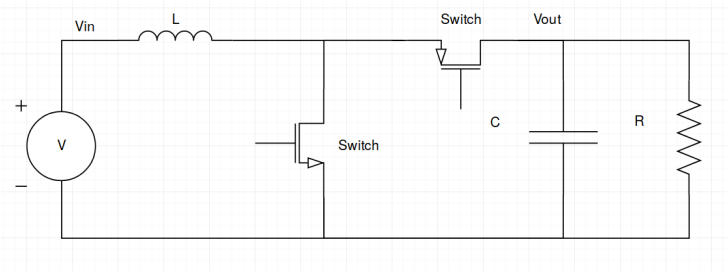

Figure 3.3: Representation of a boost converter

NMOS switch is closed and the PMOS switch is open, the inductor is charged through the input voltage. When the NMOS transistor opens and the PMOS closes, the inductor is charged an the output voltage is equal to

$$V_{IN} + V_L - V_{R_{DS(ON)}}, \tag{3.5}$$

where $V_{R_{DS(ON)}}$ is the voltage drop at the PMOS transistor. The output voltage is controlled by controlling the inductor energy, modulating the time that the transistors are ON and OFF. Since the duty cycle is the relation between the conduction time and the period, the voltage at the output of the boost convert follows the following equation

$$V_{out} = \frac{V_{IN}}{1 - D}, \tag{3.6}$$

where D is the duty cycle:

$$D = \frac{t_{ON}}{t_{ON} + t_{OFF}}, \tag{3.7}$$

where t_{ON} is the time when the NMOS is conducting and the t_{OFF} the time when it is off. The efficiency of the converter is given by the following equation

$$Efficiency = \frac{P_{IN} - P_{LOSSES}}{P_{IN}}, \tag{3.8}$$

Where the P_{LOSSES} are the MOSFET conduction losses, the switching losses at the MOSFET and the inductor resistance. There are boost converts on the market that reach 96% efficiency such as the

TPS61291 [24] from Texas Instruments.

Buck converter

The buck converter is used to convert an higher input voltage into a lower output voltage. It uses two power switches to transfer charge to the output capacitor. Figure 3.4 is a block diagram with a simple representation of a buck converter. The voltage at the output is controlled by acting on the time each

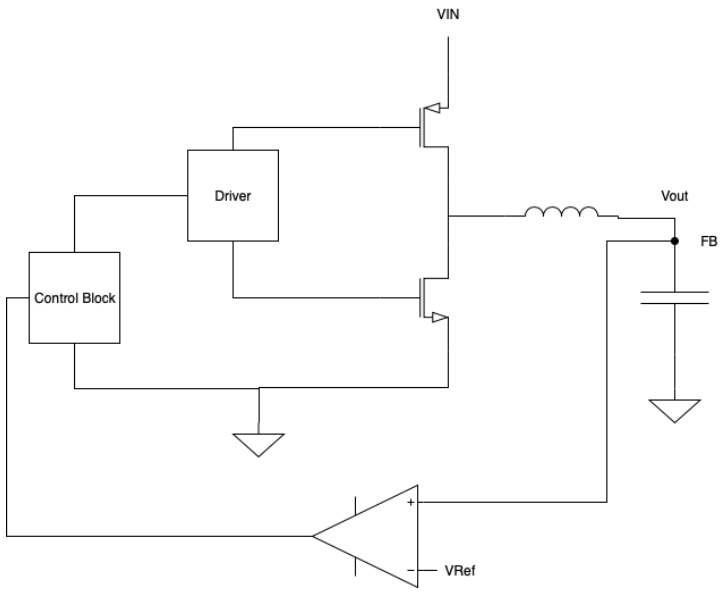

Figure 3.4: Representation of a buck converter

power switch is turned on. When the PMOS is ON the NMOS is OFF and the current in the inductor rises. On the contrary, when the NMOS is ON the PMOS is OFF and the current in the inductor falls. There are two modes of operation: PFM (Pulse Frequency Modulation) and PWM(Pulse Width Modulation). In the first mode of operation the inductor current pulses are spaced in time but they have the same amplitude and duration which means that the frequency changes but the width of the pulses stays the same. When the load increases, the PFM mode can not keep up since the width does not change and the frequency can not be increased. For this reason the PWM mode is used. In this mode the width of the pulses changes but the period is the same. Therefore, if the load increase,s the time ON of the PMOS switch increases. If the load decreases the time ON of the PMOS decreases and the time ON of the NMOS switch increases. The equation,

$$Efficiency = \frac{V_{OUT} \times I_{OUT}}{V_{OUT} \times I_{OUT} + P}, \tag{3.9}$$

(3.9) represents the efficiency of a buck converter, where P is the total power losses given by the MOSFET losses both in PMOS and NMOS, capacitor losses, inductor losses and control loop required energy. The efficiency of a buck converter can reach 96% such as the TPS627431 [25] from Texas instruments.

Power Management Unit (PMU)

A PMU is an integrated circuit that has several regulators in a single chip. LDOs and DC-DCs are used to provide different voltage levels to the system. PMUs can have internal digital logic to control the different regulators or use external pins for enabling/disabling the regulators. They also include some monitoring functions such as battery monitoring voltage level or power fail. Figure 3.5 is a representation of power management unit from Texas Instruments, namely the TPS6502x. A PMU includes several regulators

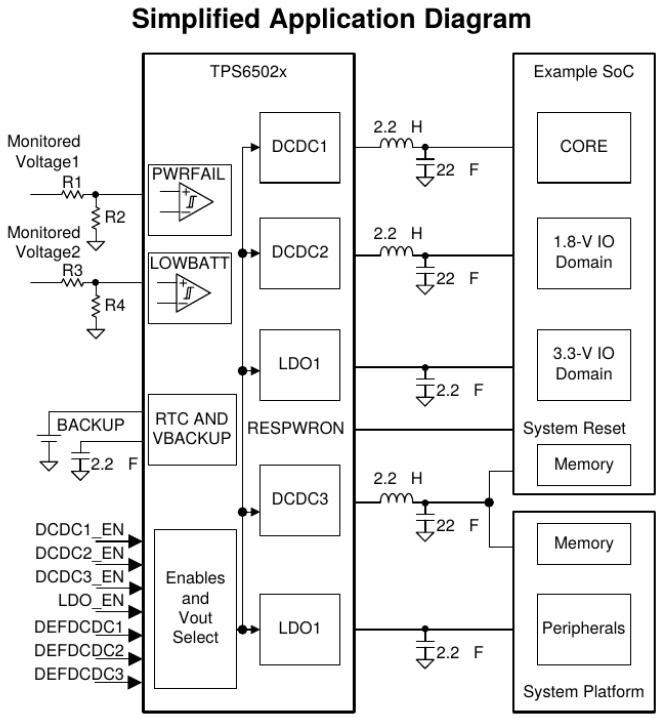

Figure 3.5: Block diagram of a PMU, TPS6502x from Texas Instruments [26]

and allows the reduction of the occupied space in a PCB. For that reason, a power management unit is ideal for an IoT system.

3.1.3 Power management design

Since the LDO has a limited efficiency ($< \frac{Vo}{Vi}$), LDO losses are only acceptable for lower currents. LDOs are ideal to regulate the voltage of always on and low power integrated circuits such as the RTC. The RTC is used to keep the time and to generate alarms in order to wake up the system. LDOs are not appropriated to supply current demanding circuits such as the microcontroller or the radio frequency circuit. For that reason another regulator should be used to increase the efficiency of the overall system. In Table 3.2, three different LDO's are compared in terms of input voltage range, quiescent current, output voltage level, dropout voltage and the output current.

Table 3.2: Low Dropout Regulator

	MCP1810 [27]	TVL755P [28]	LD39015 [29]
Input voltage range:	2.5V to 5.5V	1.45V to 5.5V	1.5V to 5.5V
Quiescent current:	20 nA	25 nA	18 uA
Output voltage level:	1.2 V to 4.2 V	0.6 V to 5.0V	0.8V to 3.3V
Dropout voltage:	380 mV	325 mV	90 mV
Output current:	150 mA	500 mA	150 mA

The LDO that presents the lowest quiescent current is the MCP1810 from Microchip. Having in consideration that the LDO will be always on, the most important aspect is the quiescent current of the regulator. For that reason the MCP1810 from Microchip was used in this system. For the current demanding part of the system, a DC-DC regulator was selected. In Table 3.3 a series of two boost converters are present. On Table 3.4 a series of two buck converters are presented.

Table 3.3: DC-DC Boost Converter

	TPS61291 [24]	MCP16252 [30]
Input voltage range:	-0.3V to 5.5V	0.82V to 5.5V
Quiescent current:	57 uA	0.6 uA
Output voltage level:	3.3 V	1.8 V to 5.5 V
Output current:	250 mA	125 mA to 225 mA

Table 3.4: DC-DC Buck Regulator

	TPS627431 [25]	MIC23051 [31]
Input voltage range:	2.15V to 5.5V	2.7V to 5.5V
Quiescent current:	360 nA	20 uA
Output voltage level:	1.2V to 3.3V	0.72V to 3.3V
Output current:	400 mA	600 mA

In order to choose between a boost converter and buck convert it is necessary to compare the range of input/output voltages and efficiency of the regulators for higher loads. The system uses AA alkaline batteries (at fully charge provide 1.5V) as power source. Normally a discharged alkaline battery has a voltage level of 0.8V. The system can also work with lithium batteries. For these batteries the voltage swings from 4.2V (fully charged) to 3.0V (discharged). Looking at the main modules of the system such as the microcontroller, the transceiver module and the RTC, it is important to understand the input voltage range of these modules. The microcontroller works from 1.8V to 3.6V, the transceiver module works from 2.1V to 3.6V and the RTC works from 1.71V to 5.5V. The LDO will lose regulation when the input voltage is less than the output plus the dropout voltage. As for the DC-DC it will only lose the regulation when the input voltage is lower than the output voltage plus the Auto 100% Mode leave

detection threshold which in the case of the TPS627431 is equal to 200 mV. Therefore, when the voltage of the battery is equal to 3.5V the buck regulator will lose the regulation and it will enter in the Auto 100% Mode. In this operation mode the DC-DC stops the regulation and the input voltage appears at the output of the regulator. Figure 3.6 shows the different modes of operation of the TPS627431 buck converter

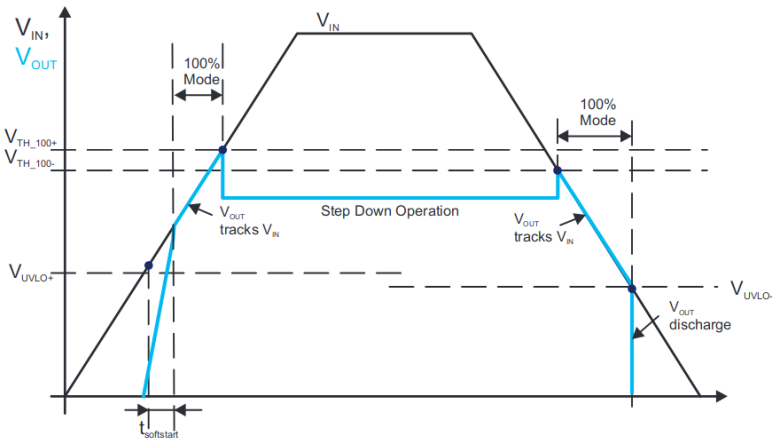

Figure 3.6: TPS627431 operation modes [25]

Moreover, when the battery level is equal to 1.925V the buck DC-DC enters in under-voltage lockout meaning that the DC-DC is shutdown.

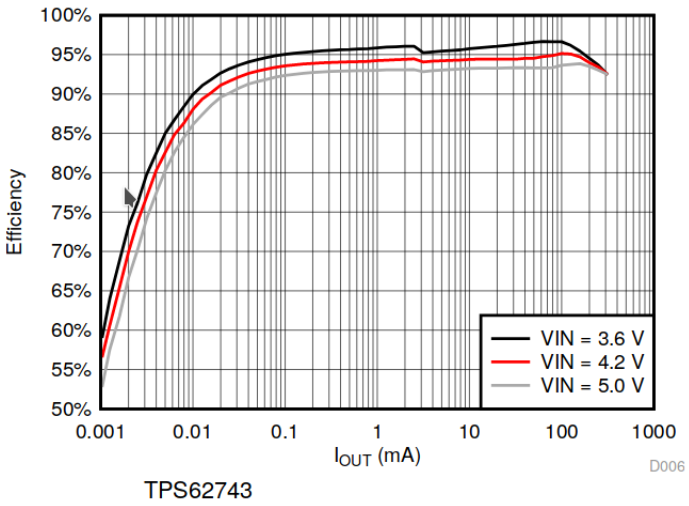

Figure 3.7: Efficiency curves of TPS627431 buck converter [25]

Alternatively, it is possible to use a boost converter with the purpose of using the full range of a single alkaline battery. Also the number of alkaline batteries used is less than the ones that are used by a buck converter. As for the efficiency, in Figure 3.8 it is possible to visualize the efficiency of the boost converter for different input voltages and different loads. Figure 3.7 shows different curves of efficiency for different loads and input voltages. Also, as for the boost converter the output voltage is 3.3V. Comparing Figures 3.8 and 3.7 we can see that the buck converter presents generally a higher efficiency for different input voltages. It is important to notice that the efficiency of the buck is typically higher than 90 %.

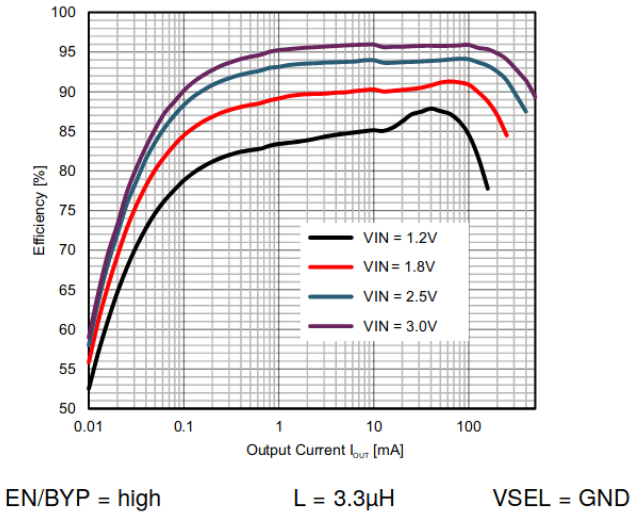

Figure 3.8: Efficiency curves of TPS61291 boost converter [24]

Additionally, it is more efficient to use more alkaline batteries or a lithium battery in order to use a buck converter than using a single battery for a boost converter. Also taking in consideration that the DC-DC will supply the demanding current part of the system, a buck convert should be used with three alkaline batteries or a lithium battery. Finally, it was also considered the possibility to use a PMU in order to reduce the space occupied by the two regulators. However, the quiescent currents of the available PMUs on the market are very high for a low power IoT system. Table 3.5 shows three different available PMU's.

Table 3.5: Power Management Units

Reference:	TPS65024x [32]	TPS65021 [33]	MAX14720/MAX14750 [34]
Number of regulators	3 DC-DC Buck converter 3 LDO	3 DC-DC Buck converter 2 LDO	1 DC-DC Buck-Boost Converter 2 Buck Converters
Quiescent currents	85 uA	85 uA	1.2 uA (Off current) 4.4 uA (On current)
Number of external enables	1 for each DC-DC 1 for LDO one Two and a separate one for the third LDO	1 for each DC-DC; 1 for all the LDOs	None (Controlled via I2C)
Input voltage	2.5 V to 6 V	2.5 V to 6 V	1.8V to 5.5V

Considering all the information, a combination of a LDO and a DC-DC buck converter is used to regulate the voltage in the system. The DCDC TPS627431, from Texas Instruments, is used to regulate the supply of the microcontroller, transceiver, and sensors. The LDO MCP1810, from Microchip, is used to regulate the supply of the Real Time Clock since this domain requires low current.

3.2 Real Time Clock and Calendar

In order to generate interruptions to wake the system, to enable the DC-DC buck converter that powers the microcontroller, to enable the LoRaWAN module and the sensors, a real-time clock is used. A RTC is an integrated circuit that performs the time keeping and generates interruptions through the use of alarms. The configuration of the RTC is performed, using I^2C or SPI, by writing or reading the

appropriate registers. Some RTCs have an input pin called Vbat that is used to reduce the consumption of RTC by turning off the registers and the communication module. The only modules that continue to work are the time keeping and the alarm. Most of the RTCs available on the market count the seconds. minutes, hours, day of the week, day of the month, month and year. RTCs have different types of alarms such as alarms on the seconds, minutes, hours and day of the week. Additionally, some RTCs have a block of memory used to store information. It is also important to refer that all the interrupt and communication pins are open drain, meaning that it is necessary to use a pull-up resistor to a supply in order for these pins to work properly. It also means that when an alarm is set the RTC pulls the interrupt pin to ground forcing a logical zero. For that reason, and since the RTC is used to wake up the DC-DC, it is necessary to use an inverter to translate this logical zero to a one. The combination of a RTC with an inverter allows the RTC to enable the DC-DC in order to power the microcontroller, the RF circuit and the sensors. By doing this, it is then possible to transmit the values of the sensors to the gateway. Table 3.6 presents two different real time clocks and their main characteristics.

Table 3.6: Real Time Clocks

	DS1339A [35]	MCP7940N [36]
Input Voltage:	-0.3V to 6.0V	-0.6V to 6.5V
Timekeeping current:	-	1.2 uA
VBAT voltage:	1.3V to 3.7V	1.3V to 5.5V
IBat current	10nA to 200 nA	850 nA to 9000 nA
Number of Alarms	2	2

The RTC chosen for the system was the DS1339A from Maxim Integrated. The reason that lead to this choice was the ability of the DS1339A RTC to support higher voltages at the pins of SDA, SCL (I^2C) and the square-wave interrupt pin. The MCP7940N from Microchip only supports a voltage at the interrupt pin that is equal to the power input supply plus 1V. For that reason, and considering the threshold of the enable pin of the DC-DC, it is necessary to supply a higher voltage at the interrupt pin. The inverter part chosen was the NC7SZ14 from ON Semiconductor. It presents a quiescent current lower than 1.0 uA and an input voltage range from -0.5 V to 6.0V. It is a single inverter with Schmitt trigger input. The device uses CMOS technology to achieve high speed with high output drive while maintaining low static power dissipation over a very broad input voltage range. [37]

3.3 Communication Module

Since the LoRaWAN network is open-source, and it can be used for free, this was the protocol chosen for the system. Although the Sigfox protocol presents better characteristics, it is a paid protocol which requires a contract with the Sigfox company. Since the LoRaWAN network is free to use, it is ideal to prove the concept of the Long Range Networks. If, in the future, another protocol is to be used, the only change required in the system is the change of the transceiver module. For this reason, the module

selected for the system was the RN2483 from MicroChip due to the fact that it presents the lowest consumption from the LoRaWAN chips presented in Table 2.3. It is suitable for simple, long range, sensor applications with an external MCU. The communication with the host MCU and the transceiver module is accomplish by sending commands from the MCU to the transceiver via UART. The transceiver then responds to the command letting the microcontroller know the result of the command given. The module is only compatible with LoRaWAN class A and supports LoRa modulation, GFSK (Gaussian Frequency Shift Keying) and FSK (Frequency Shift Keying) modulation. It has an operation frequency band from 863 MHz to 870 MHz or from 433.050 MHz to 434.790 MHz. The maximum sensitivity is -146 dBm which gives a range of 15 km at suburban zones and 5 km at urban zones. The module presents a wide list of commands [38]. The datasheet of the RN2483 module can be consulted online [39].

3.4 Microcontroller

Since Muvu Technologies wanted to work with Microchip, the microcontroller selected is the PIC18LF46K22, a 8 bit microcontroller from Microchip. The PIC microcontroller is one of the microcontrollers on the market that presents the lowest consumption. With their technology called Extreme Low Power (XLP) the microcontroller has a sleep current of 20 nA. The operation current depends on the modules in use. In the datasheet of the microcontroller it is possible to see the different consumptions of the different modules present on the microcontroller. With a crystal of 1 MHz the supply current of the microcontroller is 0.5 mA (parameter D033). Since a crystal of 8MHz is used the real consumption of the microcontroller will be higher. As for other characteristics, the microcontroller has 1024 bytes of EEPROM, four crystal modes, it can support a crystal with a frequency up to 64 MHz, an Analog to Digital converter (ADC), two analogue comparators and a Digital to Analogue Converter (DAC). The microcontroller only needs external components for the MCLR pin and for the the supply pins where a decoupling capacitor is needed. For the digital part, the microcontroller has $I2C$, SPI, EUSART (Enhanced Universal Synchronous Asynchronous Receiver Transmitter) and input/output ports. In addition, it has several analogue input ports that can be connected to an ADC in order to convert an analogue signal to a digital one. As for the programming, the microcontroller is programmed using ICSP (In System Programming). In the case of a PIC microcontroller a Pickit can be used to transfer the program from a computer to the flash memory of the device. The Pickit requires 5 pins that are the MCLR (Master Clear Pin External Reset), VCC, Ground, Programming Data and Programming Clock. There are two modes for programming the microcontroller. High voltage programming, where a high voltage is applied to the MCRL pin in order to prepare the chip for programming, or using Low Power Programming where a code is exchanged with the microcontroller in order to program it. The program is stored in the flash memory which contains 65536 bytes. As for the data memory, the microcontroller has 3896 bytes available to store program variables. The PIC18LF46K22 also includes interruptions that allow the microcontroller to handle important events that require its immediate attention. Furthermore, it has different operations modes such as run mode, idle mode and sleep mode. Finally the microcontroller has an EEPROM memory that can be used to store non-volatile. In the case of the PIC18LF46k22 it has 1024 bytes of EEPROM to be used. The

datasheet of the microcontroller is available online [40]

3.5 Sensors Interface

Since the microcontroller has different ports, digital and analogue, all type of sensors can be connected to the system. The only constrain is the voltage supply that each sensor requires. The system only provides a 3.3V voltage supply coming from the DC-DC regulator. This means that, if a sensor requires an higher voltage, it will be necessary to use an external power supply for the sensor. For the communication with the microcontroller there are output pins for the EUSART, $I2C$, SPI and digital pins that can be define as outputs. On the other hand, for input pins, there are comparators, analogue pins, and digital pins that can be used to receive/measure data from the sensors. As stated in the chapter 2 in the section 2.1.1 several sensors are used in precision agriculture such as soil moisture, light, C02 concentration, temperature and others. Table 3.7 presents some of the available sensors on the market that can be used in precision agriculture.

Table 3.7: Different types of sensors

	BME688	Capacitive Soil Moisture Sensor	Watermark soil moisture sensor	Decagon 5TM VWC	SEN-10972	LDR	SCD30	DS18B20
Type of sensor	Gas, pressure, temperature & humidity sensor	Soil Moisture Sensor	Soil Moisture Sensor	Soil Moisture Sensor	PH Sensor	Ligth Sensor	Carbon Dioxide Sensor	Temperature Sensor
Operating Voltage	1.71V to 3.6V	3.3V to 5.5V	0V to 3V	3.6V to 15V	3.3V to 5V	Any voltage	3.3V to 5.5V	3V to 5V
Communication protocol	I2C / SPI	Analog Sensor	Analog Sensor	SDI-12	UART/I2C	Analog Read	I2C/UART	One-Wire

All the sensors in Table 3.7 are compatible with the microcontroller of this system. The sensors that will be used in the embedded system are the capacitive soil moisture sensor and the DS18B20 from Maxim Integrated. The first one is an analog sensor meaning that the analog part of the microcontroller (ADC) will be used to translate a voltage level to a digital signal. The temperature sensor uses One Wire to communicate with a microcontroller.

3.5.1 Analog to digital conversion

The PIC microcontroller can connect the input of the ADC to any analog port. The following figure is a representation of the analog input model present in the datasheet of the microcontroller [40]

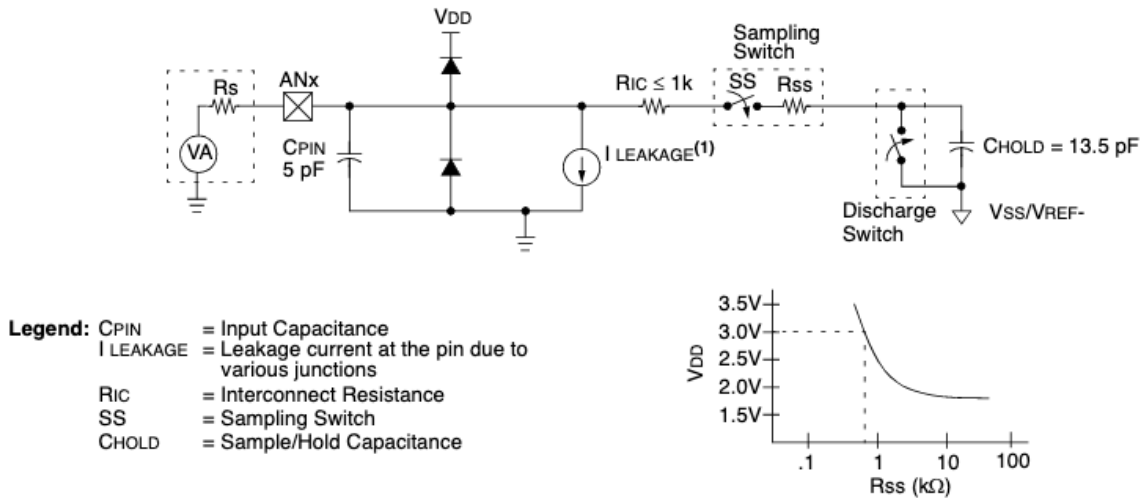

Figure 3.9: ADC input schematic [40]

The analog source is represented in the figure as a voltage generator in series with a resistor. The resistor represents the resistance associated to the analog signal. The $5pF$ capacitor is present representing the input capacitance of the pin. Following the input capacitance, is the ESD (Electrostatic discharge) protection diodes the current leakage and the interconnection resistance. The ADC itself has a sampling switch with a resistance that varies with the applied voltage and a hold capacitor in parallel with a discharge switch. In order for the ADC of PIC microcontroller to work properly, it is necessary that the impedance of the analog source do not exceed $3k\Omega$. For that reason, a buffer is used to allow the use of high output impedance sources. The AD8244 from Analog devices provides four buffers that can be used to adjust the impedance for compatibility with the ADC. Since a buffer has an higher input impedance and a lower output impedance it can make the connection between the sensors and the ADC [41].

3.6 Schematic of the system

After presenting the different parts selected, and referring some of their characteristics, it is now possible to introduce the system has a whole and to explain its working principle. Figure 3.1 is repeated here for the reader convenience. The battery powers the DC-DC, the LDO, the inverter, and the interrupt pin of the RTC. The LDO is responsible to translate the higher voltage level of the battery to 1.8V, which powers the VBAT pin of the RTC. As for the DC-DC, it is responsible to convert the input battery voltage to 3.3V that powers the microcontroller, the VCC pin of the RTC, the sensors and the LoRaWAN module. The combination of the RTC with the inverter is used to generate an enable signal to enable the DC-DC. However, it is necessary to use a switch (SW2) to change the source of the enable pin of the DC-DC. When the microcontroller and the RTC are not programmed, the switch should be in the ON position. In this position it connects the battery of the system to the enable pin of the DC-DC. This mechanism allows the system to be programmed for the first time. After the system joins the network, transmitting the first message, and performing the configuration of the RTC, the system is fully programmed and the switch should be put in the RTC position. In this position, the enable of the DC-DC is connected to the

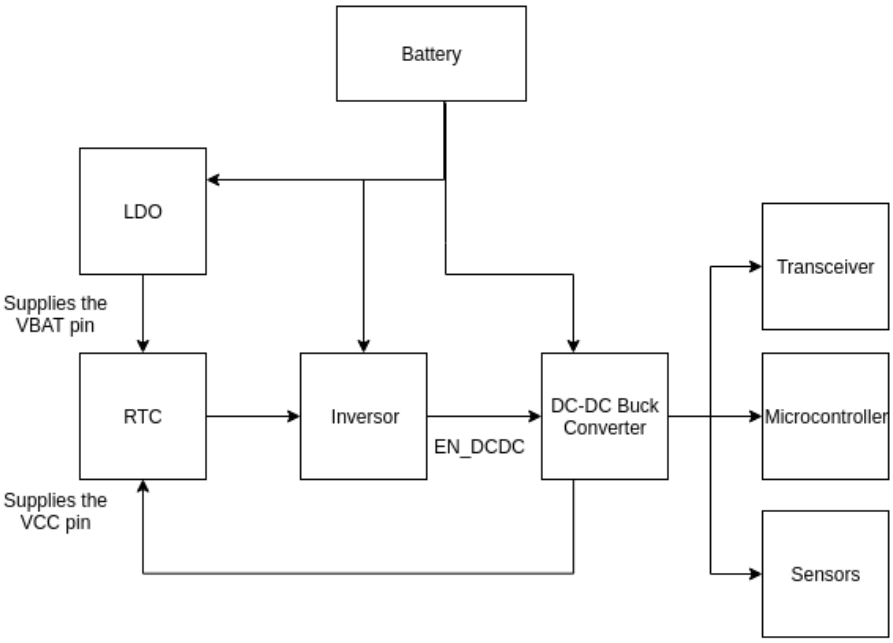

Figure 3.10: System block diagram

output of the inverter. Figure 3.11 presents a graphical representation of the above logic. The ON and RTC are written in the PCB silkscreen in order to guide the user.

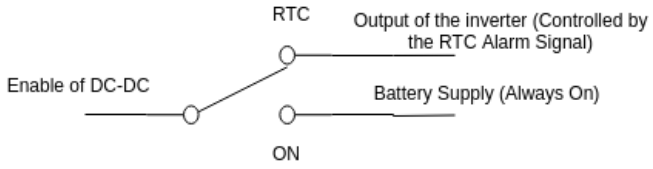

Figure 3.11: Switch logic

Additionally, a push up switch is present in order to reset the microcontroller when needed. Moreover, there are two crystals used in the system: one for the RTC and the other for the microcontroller in order to provide a clock signal. As for the communication, the RN2483 module is used to connect the system to a LoRaWAN network. There are decoupling capacitors used to filter the noise from the power supply, pull up resistors used to define logical levels of certain pins and an inductor used by the DC-DC to produce the desired voltage regulation. A detailed electrical schematic of the system it is present in the Appendix A.

Chapter 4

Implementation of the agriculture node

In this chapter, the PCB design to implement the embedded system is presented as well as and the software developed for the system to work properly.

4.1 PCB design

In order to connect the different elements of the embedded system, namely the RTC, microcontroller, transceiver module, and sensors a PCB was design and produced. In Figure 4.1 a 3D image of the PCB is presented. All the different modules used are identified.

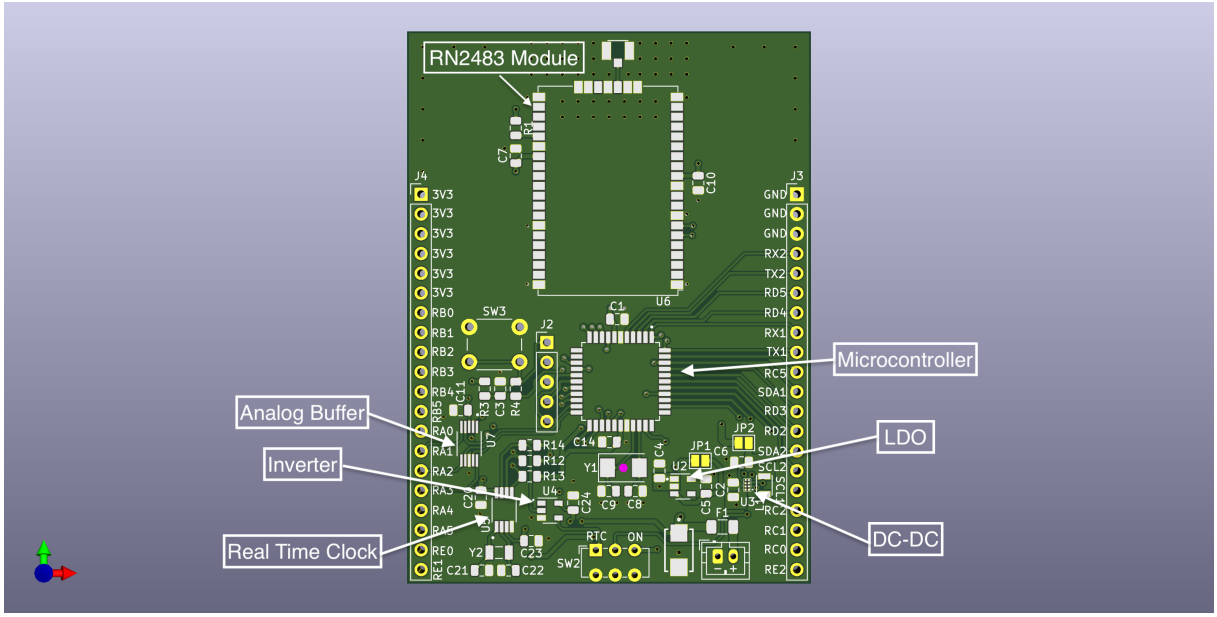

Figure 4.1: 3D view of the PCB

The microcontroller is the master of the system and it is responsible for reading values from the sensors and transmitting them via the transceiver module. There is also a connection between the microcontroller

and the RTC and between the microcontroller and the Analog buffer. For that reason, and considering all the connections that the microcontroller does, it is placed in the center of the PCB. At the top of the PCB it was placed the transceiver module. This location was chosen having in consideration the location of the DC-DC. The DC-DC is at the right bottom of the PCB and the switching of the DC-DC can generate noise that can interfere with the transceiver module. For that reason the DC-DC and the transceiver are far apart. Close to the DC-DC is the LDO an all the circuit related to the power management. The protection diode, the fuse are all at the the right bottom corner of the PCB. On bottom left of the PCB it is possible to find the RTC, the inverter and the analog buffer It is also possible to see the connections from the sensors at the left and right of the PCB. In the silkscreen it is indicated the port of the microcontroller to witch that pin connects. So for example, to connect a sensor to the RB0 pin of the microcontroller, the 7 pin from the right top should be used. There are also power pins to connect the sensors. The three top pins at the right and the six pins at the top left are respectively GND and 3.3V. They can be used to power sensors or actuators. Jumper J2 is used to program the microcontroller. At the right of the jumper it is placed the SW3 that is used to reset the microcontroller. Finally, at the bottom center is possible to find the SW3 that is used to select the source of the enable of the DC-DC. Several considerations during the PCB design were made. A more detail explanation can be found in Appendix B. Finally it is presented a picture in Figure 4.2 taken to the solder PCB with all the components.

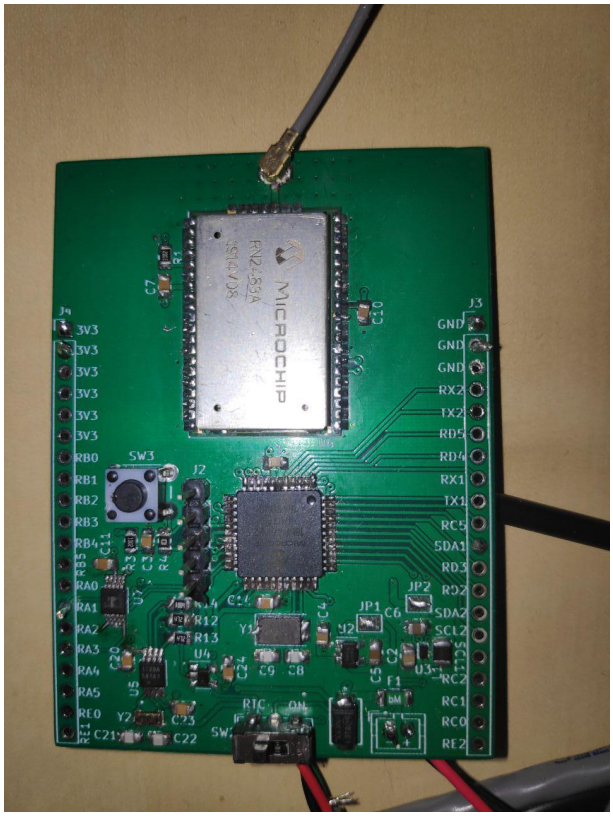

Figure 4.2: Picture of the soldered PCB

4.2 Programming the system

The program of the embedded system needs to follow a specific logic. Figure 4.3 is a graphical representation of the logic used to program the microcontroller. When the system is powered for the first time,

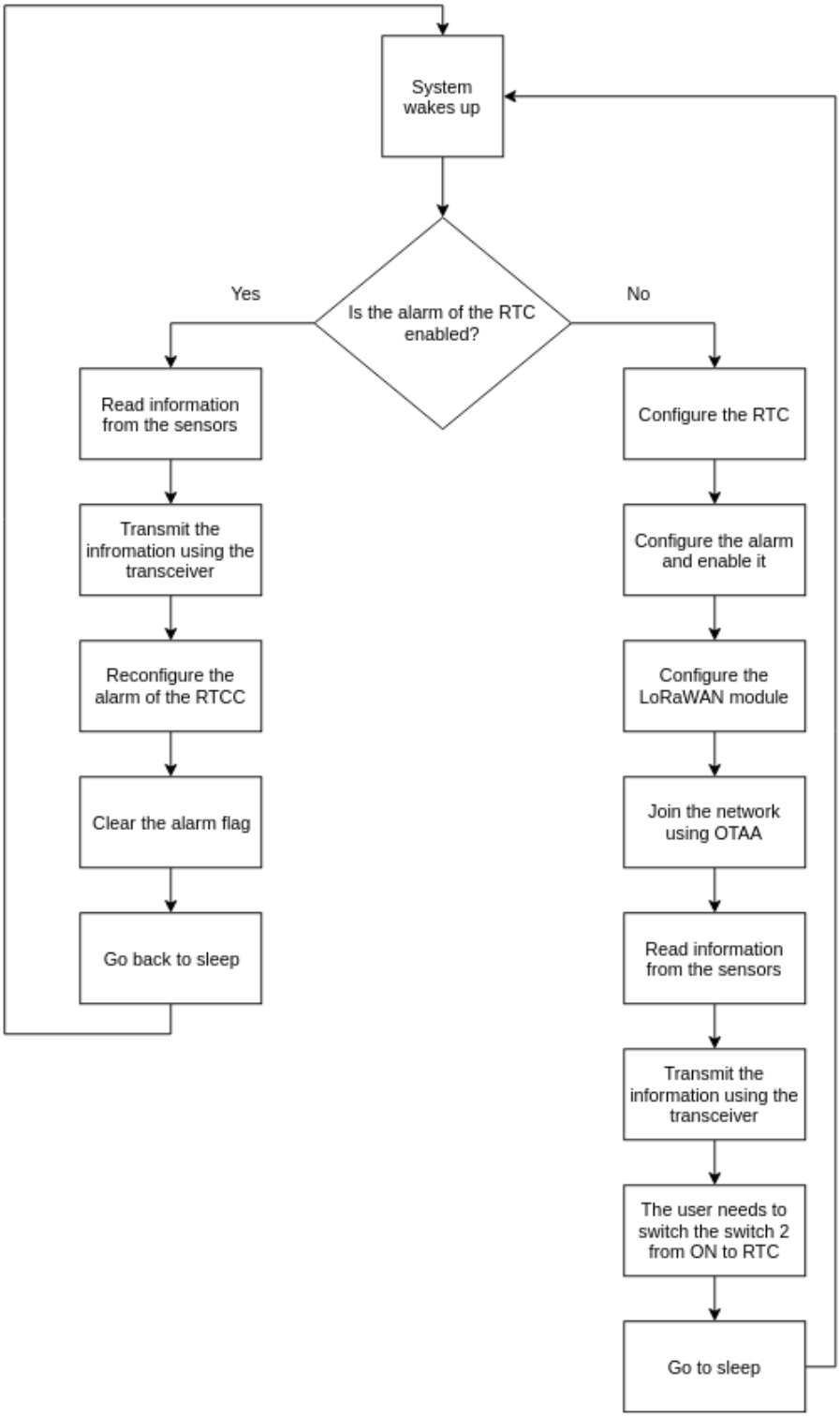

Figure 4.3: Program logic

the microcontroller and the RTC are not programmed. For that reason, and as stated in section 3.6, the switch SW2 should be in the ON position. Following that procedure it is now possible to use the PICKIT to flash the microcontroller with the program. After flashing the microcontroller the program will run for the first time. Since the RTC is not configured, the program will follow the right branch in the Figure 4.3. The user will need to look at the network server for a message of the node that is being configured. After receiving a message at the network server the user knows that the node has successfully join the network and that the configuration of the RTC has been performed. At this time the user needs to switch the SW2 to the RTC position. From that moment on, the system will wake up when the alarm of the RTC is set, it reads values from the sensors, it transmits those values using the transceiver and it goes back to sleep again. The user does not need to perform any action and the system will run until the battery runs out. In order to program the system, several software functions were created as described in the next subsections.

4.2.1 EUSART

Figure 4.4 represents the connections that are enabled by the EUSART (Enhanced Universal Asynchronous Receiver Transceiver) protocol.

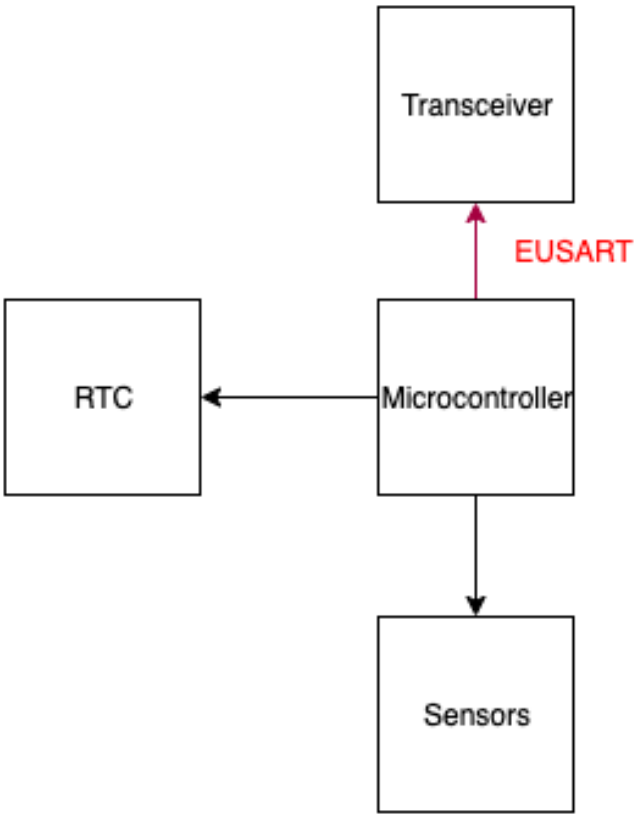

Figure 4.4: EUSART connection between the microcontroller and LoRaWAN module

The EUSART is the communication protocol used between the microcontroller and the LoRaWAN module. The microcontroller, via the EUSART, issues commands to the LoraWAN module and the

module writes to the EUSART the response. For that reason, it is necessary to configure the EUSART module of the microcontroller. The EUSART code flashed to the microcontroller presents an initialization function that configures the registers in order to turn on the EUSART. A write and read function that is used to write and read commands to and from the EUSART, and two checking functions to see if the EUSART is busy or not. Additionally, a clean buffer function was developed in order to clean the EUSART buffer from undesired messages. It will be presented where a simple working principle of the EUSART followed by the code created. The EUSART initialization function sets the baud rate, configures the ports of the microcontroller in order to work as EUSART input/output ports and configures the received and transmitting registers. The baud rate formula changes for different configurations. The Table 4.1 present in the datasheet of the microcontroller, shows the baud rate formula for different combinations of the SYNC (EUSART Mode Select bit), BRG16 (16-bit Baud Rate Generator bit) and BRGH (High Baud Rate Select bit) bits.

Table 4.1: Configuration bits for the EUSART

Configuration Bits			BRG/EUSART Mode	Baud Rate Formula
SYNC	BRG16	BRGH		
0	0	0	8-bit/Asynchronous	FOSC/[64 (n+1)]
0	0	1	8-bit/Asynchronous	FOSC/[16 (n+1)]
0	1	0	16-bit/Asynchronous	
0	1	1	16-bit/Asynchronous	FOSC/[4 (n+1)]
1	0	x	8-bit/Synchrounous	
1	1	x	16-bit/Synchronous	

Having in consideration Table 4.1, and the datasheet of the PIC [40], the following function for the initialization of the EUSART was developed. This function is equal for both the EUSARTs (1 and 2). Figure 4.5 shows a block diagram of the initialization function of the EUSART The block uses a register called SPBRG which contains the desired baud rate and then a series of bits that are used to generate the baud rate. This baud rate is used in combination with the Transmit Shift Register (TSR) to transmit information to the pin buffer and control. Having this block as a reference, the initialization function of the UART sets the pins used by the EUSART as digital by disable the analog block. Then, it sets the right configuration for the baud rate generator. After that, it sets both pins of the EUSART as inputs and configures both the receive and transmission registers. On the transmission control register the bit TXEN is set to one enabling the transmission and on the receiving control register the SPEN (Serial Port Enable) bit is set to one which configures the pins used for RX and TX as serial port pins and the CREN bit to one which in this case (Asynchronous mode) enables the receiver. It is also important to note that the SYNC bit is always zero meaning that this functions only supports asynchronous transmissions. Following the block diagram of the initialization function of the EUSART it is presented the the header of the function.

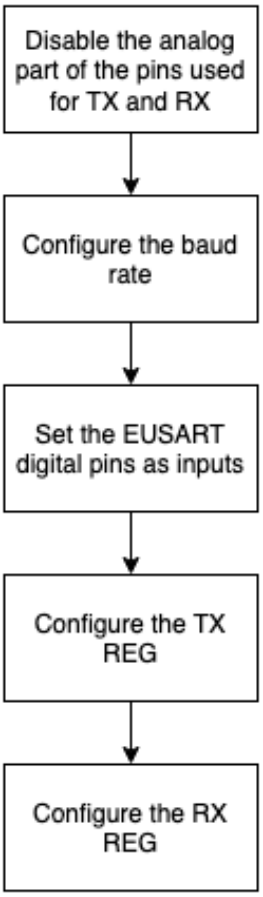

Figure 4.5: EUSART Initialization block diagram

```
/*
 * Function:  UART11_Init
 * ----------------------
 * Starts the UART 1 port by configuring the appropriate registers
 *
 * Arguments: Baudrate - Defines the baud rate to be used by the UART
 *            speedBaudRate: 0 - Low Speed; 1 - High Speed;
 *            baudRateNum: 1 - 16 bits baud rate; 0 - 8 bits baud rate;
 *
 * Returns: Returns 0 if it failed to configure the UART port
 *
 *
 */
uint8_t UART1_Init(uint32_t baudrate, uint8_t speedBaudRate, uint8_t baudRateNum);
```

In order to fully understand the EUSART block of a PIC microcontroller, Figure 4.6 shows the working principle of the EUSART transmitting block and the receiving block. For the writing operation, the program writes to the TxREG a block of eight bits, 1 byte, that in turns is immediately transferred to the TSR register. Then, the transmission is accomplish by using a start and stop bit sequence. When a transmission is occurring the TRMT bit from the control register has a logic level of 1. When the

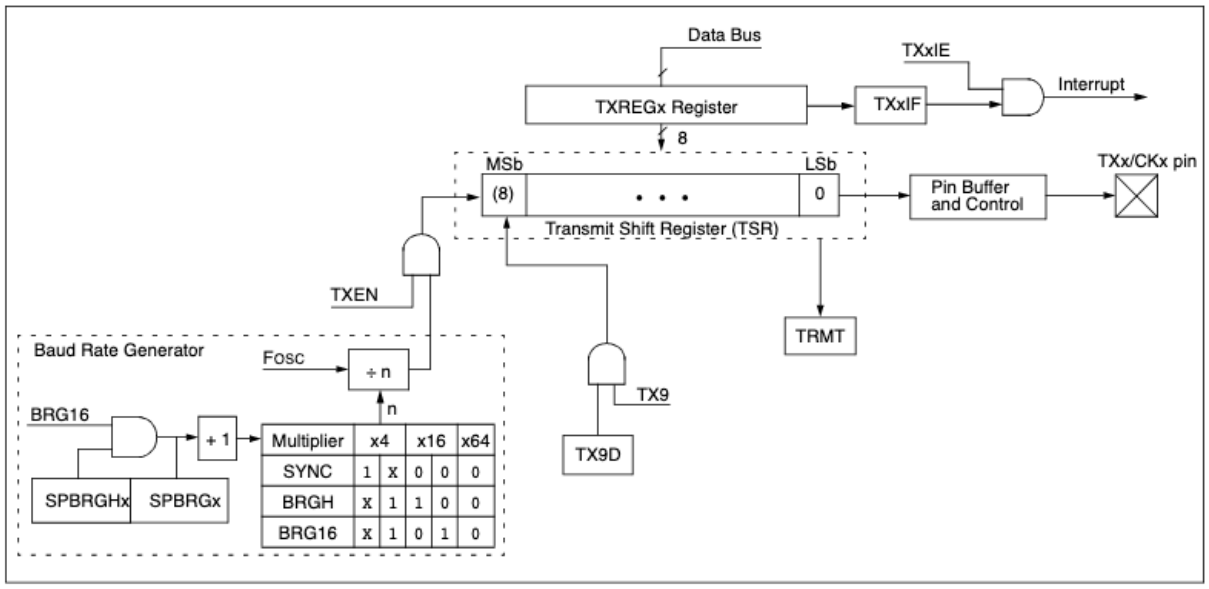

Figure 4.6: PIC EUSART transmitting block [40]

transmission finishes the hardware sets this bit to zero indicating that the TSR register is now empty and can be written again. A writing function of the EUSART receives the value to write in a buffer that is written to the TX1REG. Then, bit TX1IF (EUSART1 Transmit Interrupt Flag bit) of the PIR1 (Peripheral Interrupt Request Register) is set to zero indicating that the EUSART transmitting buffer is full. The program waits for the hardware to release the bit TRMT of the controller register indicating that the transmission is completed. After that, the EUSART write function writes a carriage return and new line character in order to indicate the end of a transmission. For example, the RN2483 UART command requires that all commands are terminated with a carriage return `\r` follow by a new line character `\n` in order to indicate the end of the command [38]. Figure 4.7 shows a block diagram of the writing function of the EUSART Following the block diagram of the writing function of the EUSART it is presented the the header of the function.

```
/*
 * Function:  UART1_Write
 * ----------------------
 * Writes a string to the UART buffer
 *
 * Arguments: A pointer to the string to be printed
 *
 * Returns: Nothing
 *
 *
 */
void UART1_Write(char *buffer);
```

In Figure 4.8, the internal block diagram for the receiving block of the PIC microcontroller is presented. The receiving block receives the information from the Pin Buffer and Control which goes to a data recovery block which is a high-speed shifter operating at 16 times the baud rate, whereas the serial

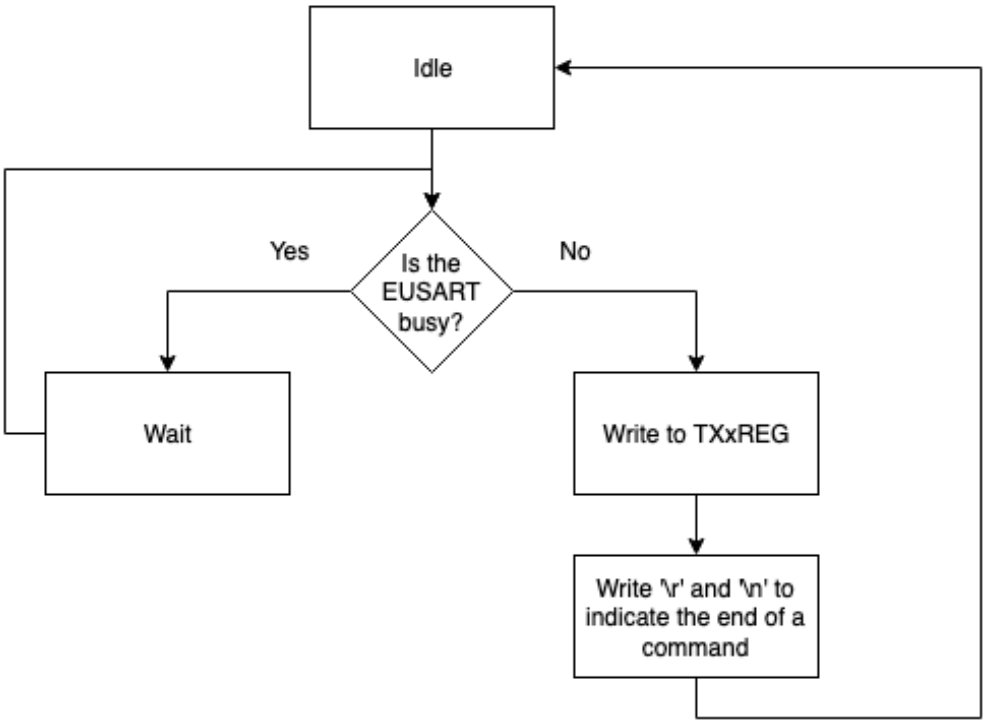

Figure 4.7: EUSART write function block diagram

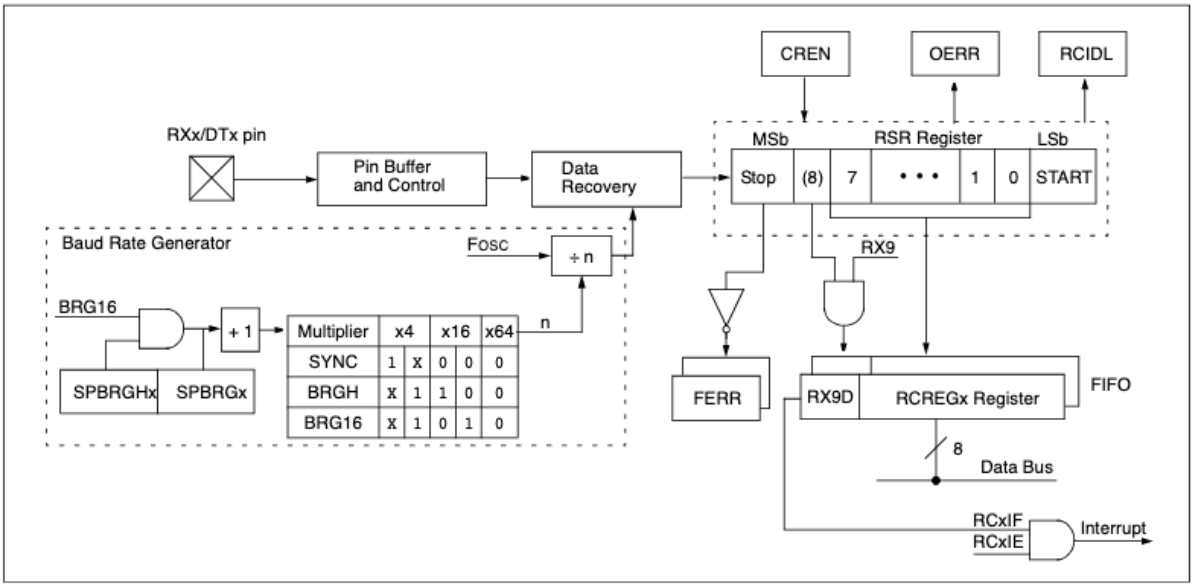

Figure 4.8: PIC EUSART receiving block [40]

Receive Shift Register (RSR) operates at the bit rate. The information in RSR register is written to the RCREGx register which can be read by the program to get the information that has been received. It is important to see also the FERR and OERR blocks which monitor the validity of the data received. In addition, the Baud rate generator block is also used here in order to keep the receiving block working with the appropriate baud rate. Since the received operation is more complex due to errors that can happen

during the transmission, it is necessary to look for overrun errors and framing errors. The EUSART receive buffer can hold two characters. If a third is received before reading the first one, an overrun error is generated. When this happens, it is necessary to restart the EUSART. The error is flagged by the hardware by setting the bit OERR (overrun error bit) of the control and status register. For this reason the OERR bit is checked when a character is received. If an overrun error has occurred the EUSART is reset by putting the CREN bit (Continuous Receive Enable bit) in the control and status register to zero and then enable the bit again by setting the same bit to one. In addition to an overrun error a framing error can also occur. A framing error is an error that indicates that a Stop bit was not seen at the expected time and it is flagged by the hardware by setting the FERR bit in the control and status register. For that reason it is also necessary to check the FERR bit. If it is set, it is necessary to restart the EUSART. The restart is achieved by clearing the EUSART buffer and then clearing the SPEN (Serial Port Enable bit) bit followed by setting the SPEN bit again. If none of this errors happen, after receiving a character, the flag RCIF in the PIR1 register is set to one indicating that a character has been received. When the EUSART received buffer is read this flag is set to zero again by the hardware. The following function was written in order to enable reads from the EUSART. Figure 4.7 shows a block diagram of the reading function of the EUSART. Following the block diagram of the reading function of the EUSART,

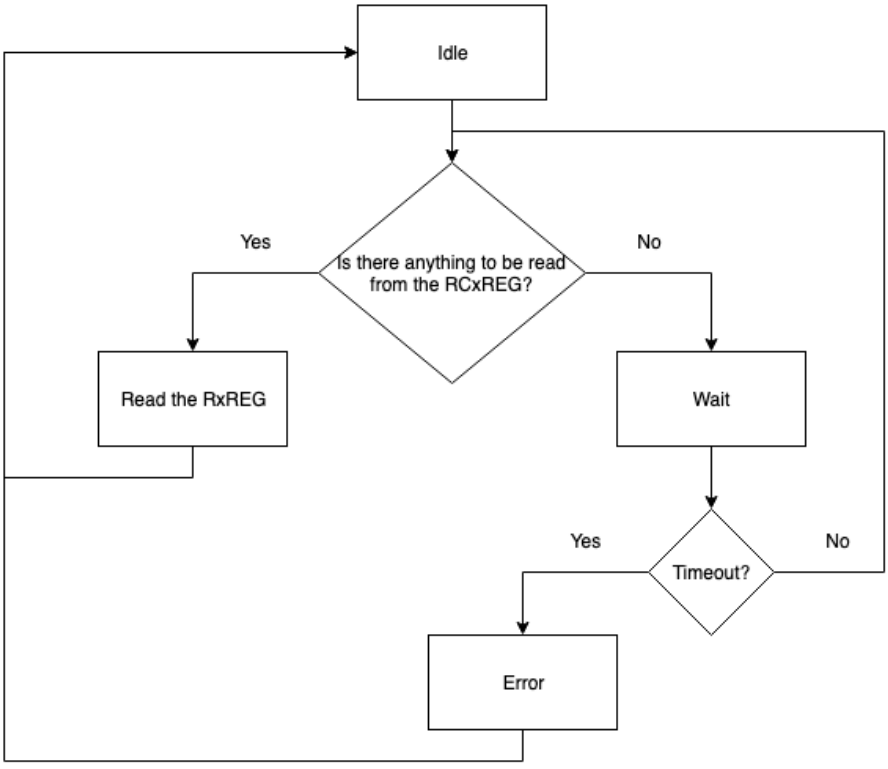

Figure 4.9: EUSART read function block diagram

the header of the function is presented.

```
1 /*
2  * Function:  UART1_Read
3  * ---------------------
```

```
4  * Reads a string from the UART buffer
5  *
6  * Arguments: A pointer to the string where the read information will be stored
7  *
8  * Returns: Nothing
9  *
10 *
11 */
12 void UART1_Read(char *buffer);
```

4.2.2 I^2C

Figure 4.10 represents the connections in the system that use the I^2C communication protocol. The I^2C

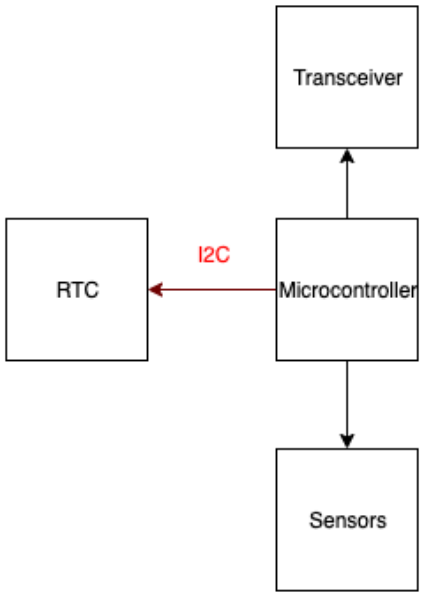

Figure 4.10: I^2C connection between the microcontroller and RTC module

is present in the Master Synchronous Serial Port Module of the microcontroller. It is a communication protocol used by several electronic devices. In this work, the RTC communicates with the microcontroller using I^2C. Additionally the development of an I^2C library can be useful for adding sensors that use the same protocol. The communication is performed between a master and a slave. In this case, the master is the microcontroller and the slave is the RTC or a sensor. The I^2C uses two open drain terminals called the SCL (Serial Clock) and the SDA (Serial Data). Since they are open drain terminals they required the use of a pull-up resistor. There are four modes of operation. The following list explains all the operation modes:

- Master Transmit Mode: In this mode the master (the microcontroller) transmits information to the slave.
- Master Receive Mode: In this mode the master (the microcontroller) receives information from the slave.
- Slave Transmit Mode: In this mode the microcontroller acts as a slave and transmits information to the master
- Slave Received Mode: The microcontroller receives information as a slave from a master

Since the microcontroller in the embedded system is the master, the first two modes will be used in order to transmit and receive information from the slave (Real Time Clock). Figure 4.11 and 4.12, taken from the data sheet of the microcontroller, represent a write and a read in the master mode. The master generates a start condition by keeping the SCL line pulled up while making a transition in the SDA line

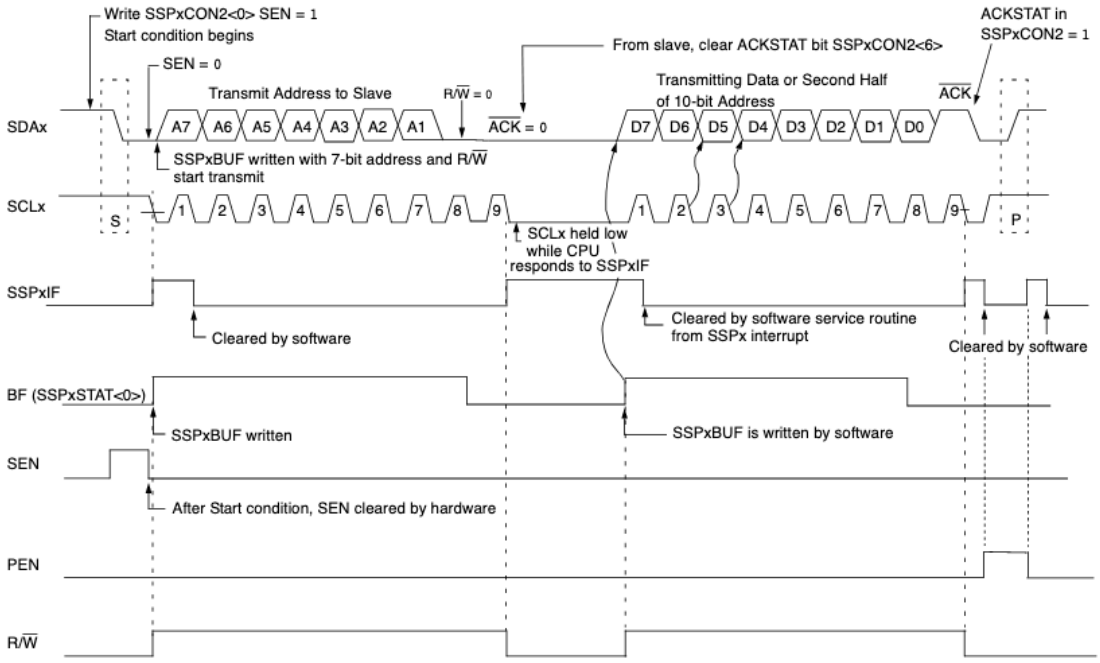

Figure 4.11: I^2C Master Transmitting Mode [40]

from high to low. After the start sequence, it transmits the write address of the slave using 9 clocks (7 bits). The 7 bits are transmitted in the first 8 clocks which corresponds to the slave address. On the 9th clock the master waits for the slave to pull down the SDA line indicating an acknowledge from the slave. If the slave does not pull down the line it means a not acknowledge and the transmission should be stopped. After this transmission and considering, that an acknowledge was received from the slave, it is possible to transmit information to the slave following the same sequence of 9 clocks (7 bits of information). When the master is done transmitting information to the slave, it sends a stop condition which is accomplished by having the SCL line pulled up while making a transition from low to high in the SDA line. Having all these concepts in mind, the following function to write in a slave using I^2C was developed.

```
/*
 * Function:  i2c_write_data
 * ------------------------
 * Writes a byte of data to the I2C buffer
 *
 * Arguments: The byte to be written to the I2C line
 *
 * Returns: Zero if the slave as acknowledge the data sent or one if the slave as not
    acknowledge the data sent by the master.
 *
 *
 */
uint8_t i2c_write_data(uint8_t data_out);
```

For the reading part, Figure 4.13 taken from the datasheet of the microcontroller, shows the digital

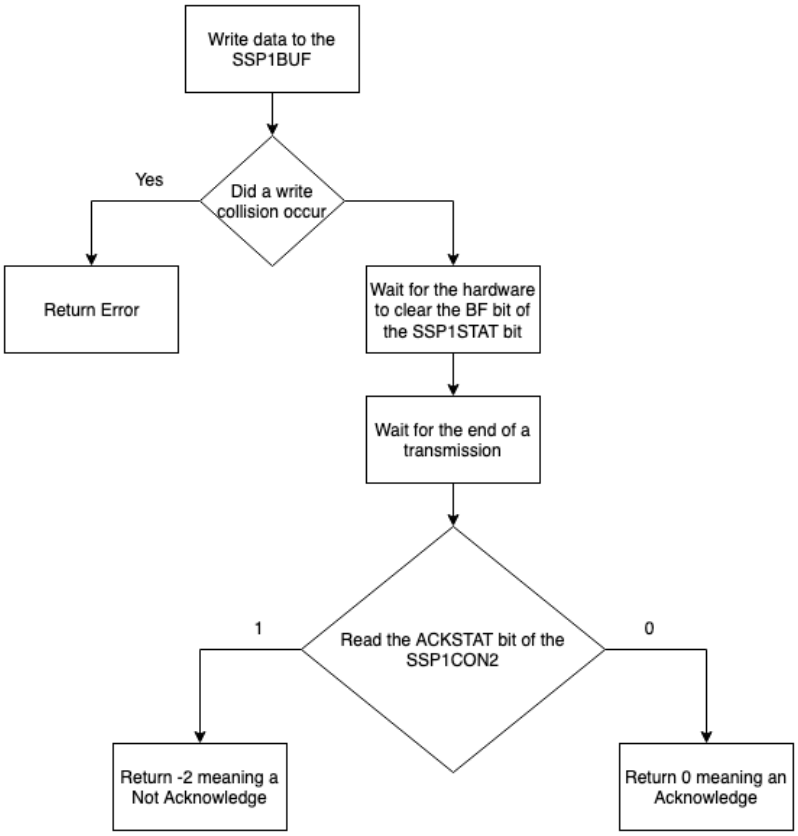

Figure 4.12: I^2C writing function block diagram

signals for the receiving part. The receiving is accomplished in two parts. In the first part, the master writes to the slave indicating a read operation. On the second part, it sends a repeated start condition and it starts receiving information from the slave. If the master wants the slave to keep transmitting information, after receiving the first 7 bits of information, it needs to send an acknowledge to the slave. If it wants the slave to stop sending information, the master should not send an acknowledge to the slave. After that a stop condition is generated by the master ending the transmission. Having in consideration the working principle of the protocol the following function was developed in order to receive information from a slave using I^2C. Figure 4.14 shows a block diagram of the I^2C function. Following the block diagram the header of the function is presented.

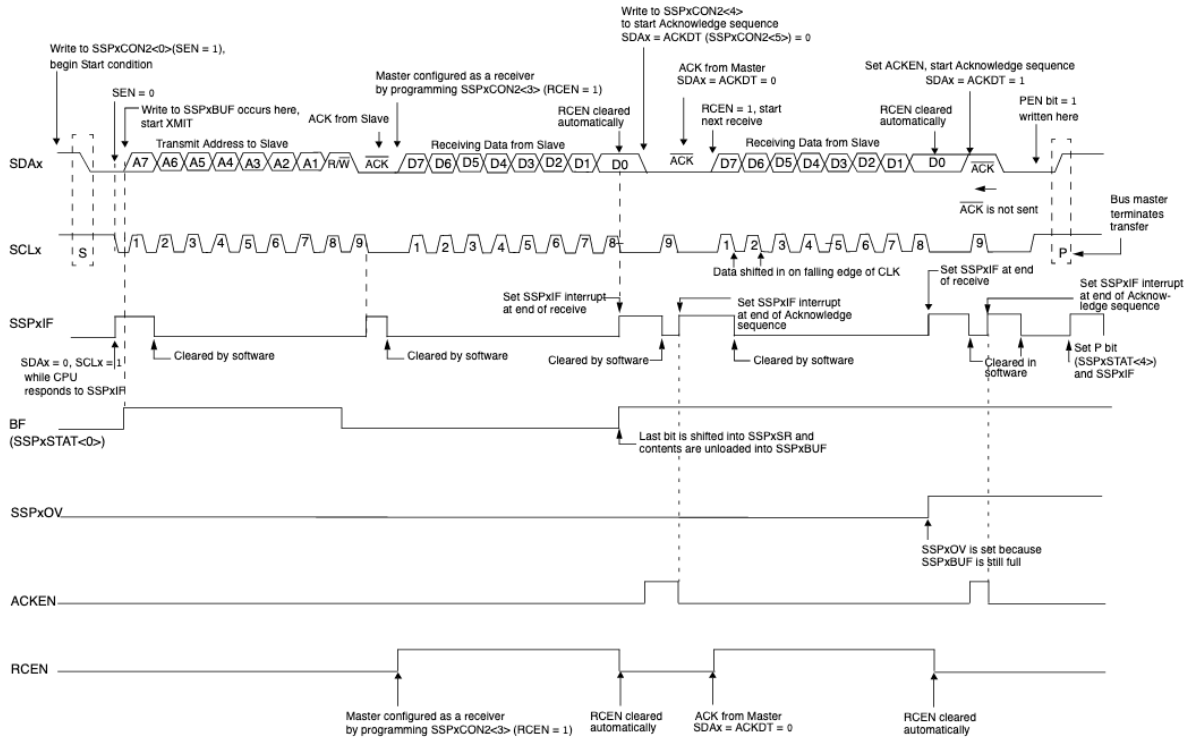

Figure 4.13: I^2C Master Receiving Mode [40]

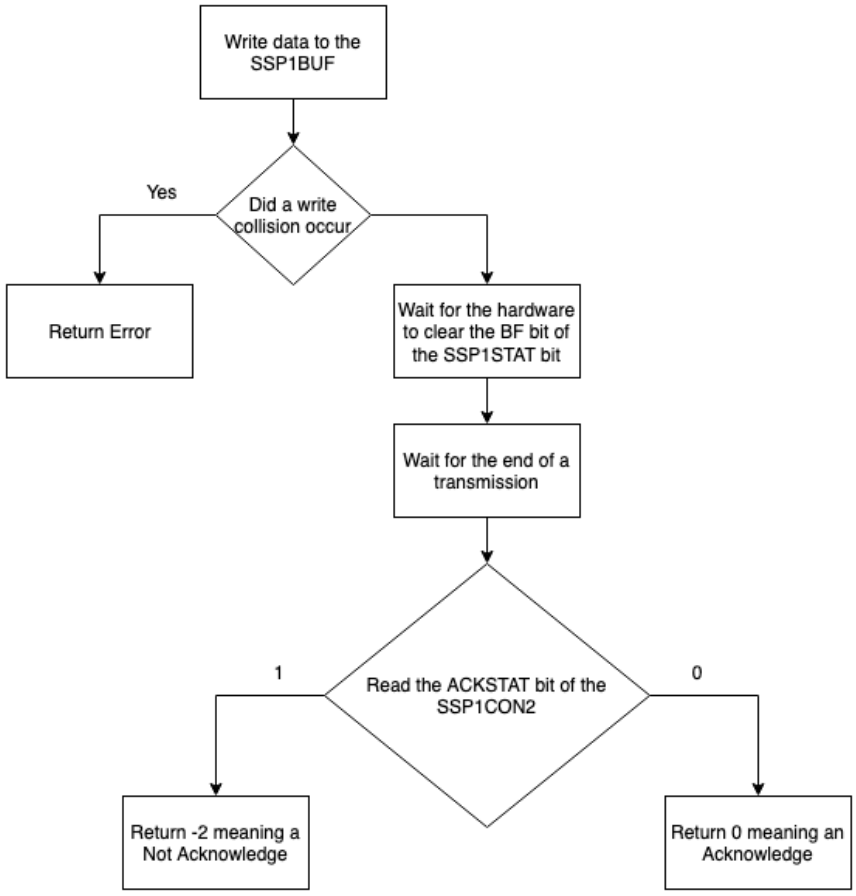

Figure 4.14: I^2C receive function block diagram

```
/*
 * Function:  i2c_read_data
 * --------------------
 * Reads a byte of data from the I2C buffer
 *
 * Arguments: Zero if an not acknowledge condition is to be sent to the slave, 1 if a
    acknowledge condition is to be sent to the slave
 *
 * Returns: The byte of data read from the I2C buffer
 *
 *
 */
uint8_t i2c_read_data( void );
```

4.2.3 One-Wire Protocol

The One-Wire protocol is a Dallas Semiconductor/Maxim Integrated communication protocol. It uses a single line to transmit information. The protocol requires a pull up resistor in order to pull up the voltage at the data line. It uses CMOS/TTL logic and can work between 2.8V to 6V. It is a half duplex transmission protocol which means that a master and a slave can only transmit one at a time. The master controls the transmission by initializing the transmission. It does not required a clock however it requires precise times in order to transmit or read information from the line. Figures 4.15 and 4.17, taken from the Dallas temperature sensor DS18B20, represent an initialization timing, a write of a zero or one bit, and the reading of a zero or one bit by the master. In this specific case, the master has a

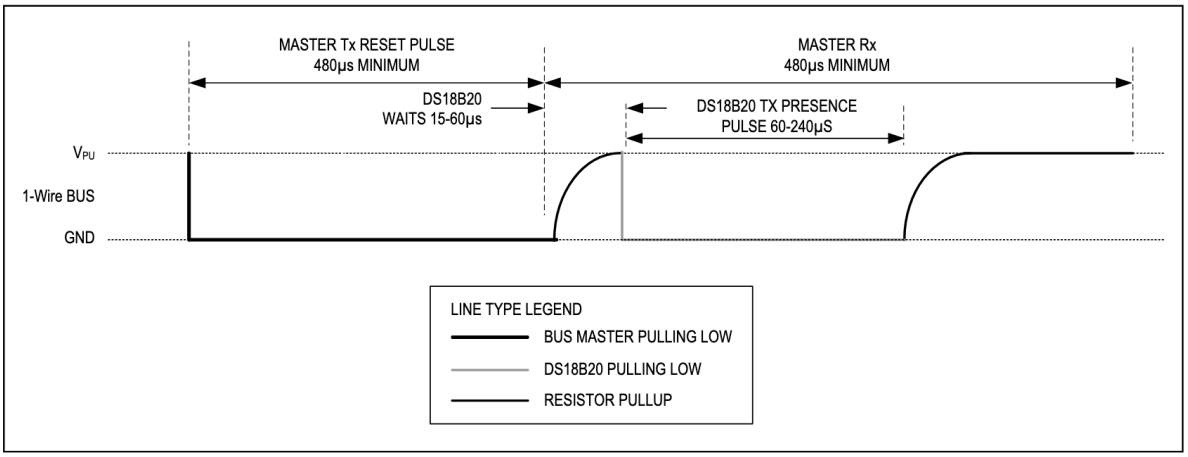

Figure 4.15: One Wire initialization/reset sequence [42]

minimum $480\mu s$ transmission window and the slave has a $480\mu s$ minimum receive window. The master pulls down the line for at least $480\mu s$. Then it releases the line and the slave generates a pulse from 60 to $240\mu s$ pulling down the line and informing the master of its presence. Then it releases again the line. Figure 4.16 shows a block diagram of the function created for the initialization of the One Wire. Following the initialization sequence of the One Wire protocol it is necessary to create functions for the read and write in order to transmit and receive information from the slave. Figure 4.17 shows the writing and the reading operation using the One Wire protocol.

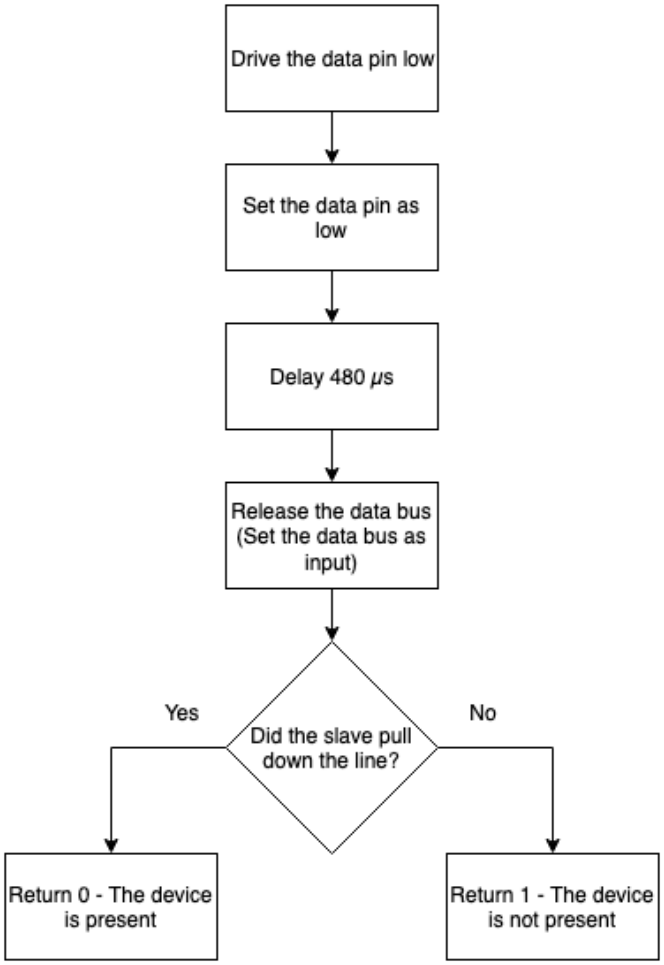

Figure 4.16: One Wire initialization function block diagram

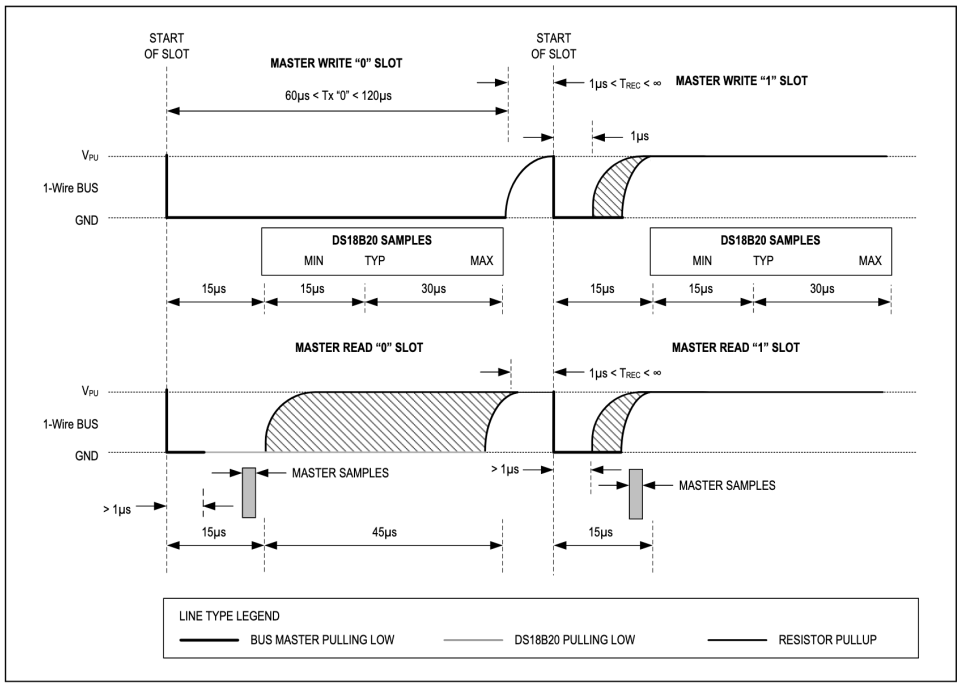

Figure 4.17: One Wire read and write sequence [42]

For the writing operation the master has a transmission window with a minimum of $60\mu s$. The transmission of a zero bit is accomplish by pulling down the line during at least $60\mu s$. For transmitting a one bit the master has the same minimum time window of $60\mu s$ in which the line must be pulled down and then released. The master needs to release the line after at maximum $15\mu s$. The line is then pulled up by the resistor for the rest of the $60\mu s$ transmission window. By following this sequence, the slave will know that a bit with a value of one is being written.

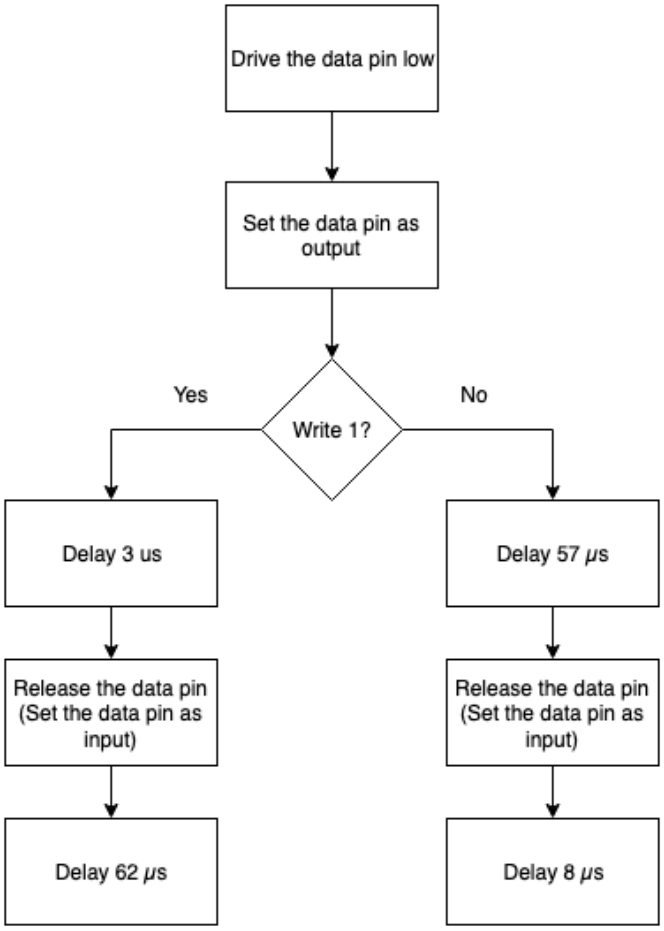

Figure 4.18: One Wire writing function block diagram

```
/*
 * Function:  OneWire_writeBit()
 * ----------------------
 * Writes a bit to the One Wire data line
 *
 * Arguments: The bit to be written to the data line
 *
 * Returns: Nothing
 *
 *
 */
void OneWire_writeBit(uint8_t b);
```

For the read part, the master needs to write a Read Scratchpad or Read Power Supply with corresponds to BEh and B4h respectively. After that, the slave generates a read slot that must have at least $60\mu s$ with a minimum of $1\mu s$ of recovery. The reading window is started by the master by pulling down the line for $1\mu s$ and then realising it. The slave starts transmitting information by pulling down the line (0 bit) or leave it high (1 bit). In Fig. 4.19 a block diagram of the read function followed by the header of the function created to read a bit from the One Wire data line is presented.

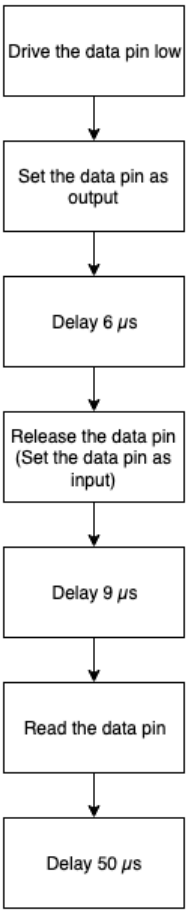

Figure 4.19: One Wire read function block diagram

```
/*
 * Function:  OneWire_readBit()
 * ----------------------
 * Reads a single bit from the One Wire data line
 *
 * Arguments: Nothing
 *
 * Returns: The bit read from the data line
 *
 *
 */
uint8_t OneWire_readBit(void);
```

With this operation in mind it is now possible to understand the code for the One Wire protocol.

4.2.4 Analog reads from sensors

The analog part requires the use of an ADC (Analog to digital converter) in order to convert an analog signal to a digital signal that can be interpreted by the microcontroller. The ADC is present in the PIC microcontroller and it is used to converter analog reads from sensors to a digital signal that can be transmitted using the transceiver. The operation of the ADC requires the definition of a sampling frequency and follow a specific conversion timing. It is also necessary to provide a reference positive and negative voltage. In addition it is also necessary to indicate the port from which the analog signal will be read. A full conversion of 10 bits requires at least 11 T_{AD} (ADC clock period) periods. The ADC clock period is generated from the microcontroller clock. It can be divided by 2, 4, 8, 16, 32, and 64 or use an internal dedicated oscillator. The TAD period must be at least $1\mu s$ long. Below this value a violation of the minimum required T_{AD} period exists and the ADC does not work properly. The Figure 4.20, taken from the datasheet of the microcontroller, represents an ADC acquisition. Figure 4.20 representes the

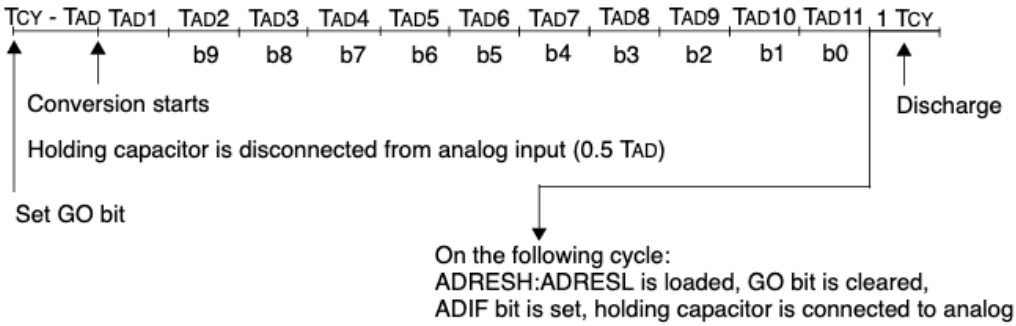

Figure 4.20: ADC acquisition without hold time [40]

minimum acquisition time. In this example the hold capacitor (see Figure 3.9 is disconnected from the input which means that there is no holding time. T_{CY} is the instruction cycle period and is equal to four times the input oscillator time base period for all configurations except the PLL (Phase Lock Loop). From the figure is possible to see the whole scheme of an analog conversion. The first instruction sets the GO bit and it takes one instruction cycle. Then it takes 1 T_{AD} clock period for the conversion to start. The conversion itself takes 10 T_{AD}, one per bit. For the last part, one instruction period is used for the discharge of the capacitor. In Figure 4.21 the hold capacitor is used for 4 T_{AD}. The acquisition time can be configured for 0, 2, 4, 6, 8, 12, 16 or 20 T_{AD}.

Having all the previous characteristics in mind, it is now possible to understand the code related to the ADC converter. First the initialization of the ADC module of the PIC microcontroller needs to be performed. In Figure 4.22, the combination of all the steps that need to be performed is presented. Following the diagram block, the header function of the initialization of the ADC is presented. After the initialization, a combination of two functions make the ADC work. The first one is called read value. It basically reads the value conversion from the two ADC register and merges it into a single variable. The second function is the retrieved value that starts a conversion, it uses the read value function and it returns the value of the conversion performed by the ADC of the microcontroller. In Figure 4.23, a block diagram of the working principle of the read ADC value is presented. It is followed by the header of the

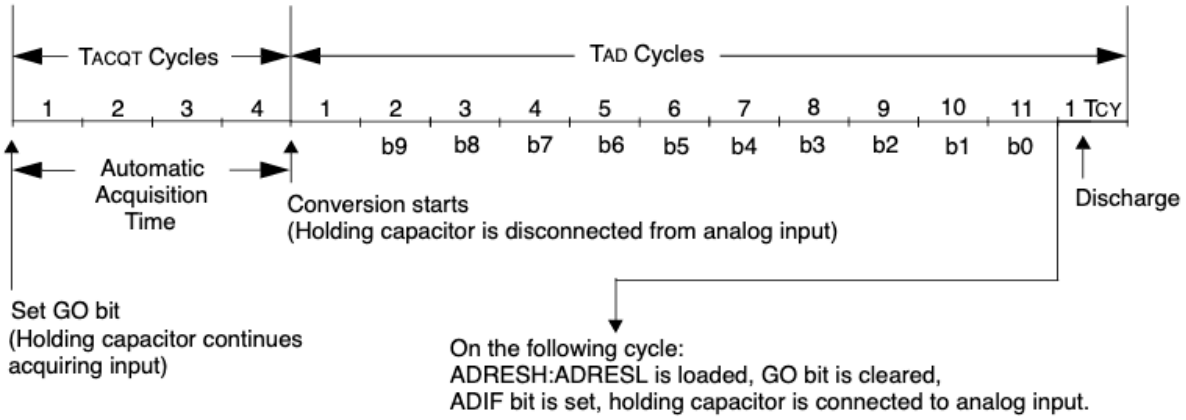

Figure 4.21: ADC acquisition with a holding time [40]

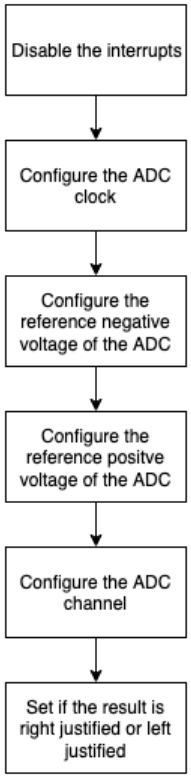

Figure 4.22: ADC initialization function

function. Finally the logic of the ADC retrieved function is showned in Figure 4.24.

```
/*Functions*/
/*
 * Function:  getStatusConversion
 * ----------------------
 *
 *
 * Arguments: None
 *
 * Returns: Returns the result of the conversion that was stored in the register ADRESH
```

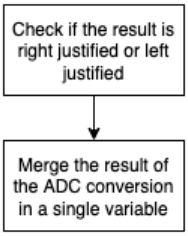

Figure 4.23: ADC read value function

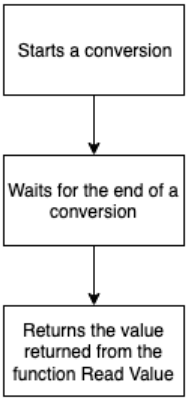

Figure 4.24: ADC retrieved function

```
    and ADRESL
10  *
11  *
12  */
13 uint16_t readADCValue();
```

4.2.5 LoRaWAN module

The LoRaWAN module requires the use of the EUSART module in order to send commands and read the responses from the RN2483 module. The list of commands that can be sent to the RN2483 module can be consulted here [38]. The module requires that all commands are terminated with a carriage return character followed by a new line character. The module presents several commands that can be used to perform different task. They are divided in three categories.

- System commands: For system level behaviour actions. The commands gather information from the firmware and hardware version or accesses the module of the user EEPROM.
- MAC commands: For LoRaWAN Class A protocol network commands. In this category, there are commands for communication, actions and mode of operation.
- Radio commands: For radio specific configurations, directly accessing and updating the transceiver setup.

Regarding the LoRaWAN protocol discussed in 2.2.2, the RN2483 only implements the Class A protocol. Additionally the module requires the setting of specific keys that are used in the LoRaWAN protocol. However, every module RN2483 has a different hardware EUI key that is used in the OTAA joining process. In addition to that, it is necessary to configure the device EUI key, application EUI key and the application key, in order to join the network. If the ABP is used, instead of the OTAA activation, it is also necessary to set the address of the device, the network session key and the application session key. These keys can be stored in the EEPROM of the RN2483 module in order to avoid the necessity of the microcontroller to send the keys every time the system powers up. The keys can be saved to the EEPROM by issuing the mac save command. This command stores not only the keys used for the LoRaWAN network but the band used and all parameters of all the available channels such as frequency, duty cycle, data rate range and status. For transmitting a message, the mac tx command can be used. It requires the definition of the type of message to be sent, confirmed or unconfirmed. The port number and the data are also need. The port is an information encapsulated inside the MAC payload and it can be used on the application server to distinguish different payload formats. Figure 4.25 represents the MAC payload of the LoRaWAN protocol where it is possible to see the Port field.

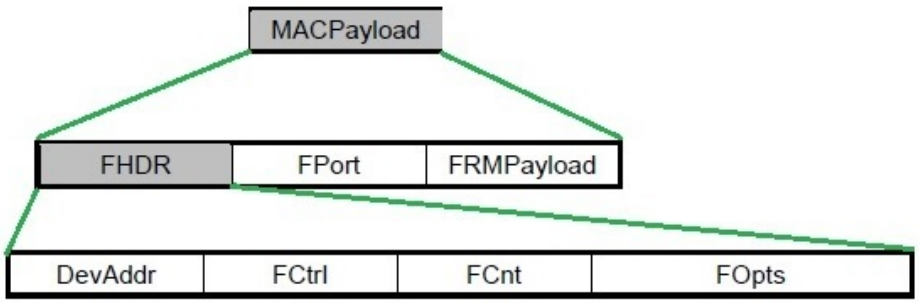

Figure 4.25: LoRaWAN MAC Payload [43]

Another useful command is the mac join which enables the RN2483 module to join a LoRaWAN network. It is possible to use OTAA or ABP in order to join the network. In the implemented system the first join is accomplished by using OTAA in order for the keys to be exchange between the module and the network server. After that, and having in consideration that the module now has its own address, the application session and network session key stored in its EEPROM the ABP activation is used for the following messages. It is necessary to join using ABP since the module is power down. The ABP sets the keys that are stored in the EEPROM and joins the network again. This join is necessary since the module is turned off after transmitting a message. If the module was not disabled it would not be necessary to join the network again. Since the code produce to communicate is too long to be presented here it will only be presented the headers of the function to join the network and to transmit a message to the network server.

```
/*
 * Function:  RN2483_MACTX
 * ----------------------
 * It transmit the message received to the Network server
 *
 * Arguments: message - A pointer to the message to be sent
 *            type - The type of message - Confirmed or Unconfirmed
 *            port - The port that is going to be used for the transmission
 *
 * Returns: 0 - if the message was sent to the RN2483 module
 *          1 - if the message was not sent to the RN2483 module
 *
 *
 */
int8_t RN2483_MACTX ( char *message, txModeE type, uint8_t port );

/*mac commands*/
/*
 * Function:  RN2483_macJOIN
 * ----------------------
 * It will join the network using OTAA - Over-the-Air Activation  or ADP - Activation by Personalization
 *
 * Arguments: Mode - If 0 it sets OTAA;
 *                   If 1 it sets ABP
 *
 * Returns: 0 - if the joining was sucessful
 *          1 - if the joining was not sucessful
 *
 *
 */
int8_t RN2483_macJOIN ( joinModeE mode );
```

4.2.6 Real time clock

The Real Time Clock is configured by the microcontroller through the I^2C communication protocol. It requires functions for setting the time and alarms of the RTC. It uses a Binaray Decimal Code (BCD), witch means that it uses 4 bits to count from zero to nine. At each new decimal unit, a new set of four bits is added. For example, the number 12 is 0001 0010 in BCD. For this reason, it is necessary to create functions that convert a decimal number to BCD and from BCD to decimal. Additionally the RTC uses two addresses. A writing address, with the value 0hD0 and a reading, with the value 0hD1. In order to write to the RTC it is necessary to generate a start condition using the I^2C library followed by the write address, the address of the register that is going to be written, followed by the data. Finally, a stop condition is issue by the master (microcontroller) to end the transmission. Figure 4.26 is a diagram of the writing function in the RTC. Reading the RTC requires first a writing operation from the master followed

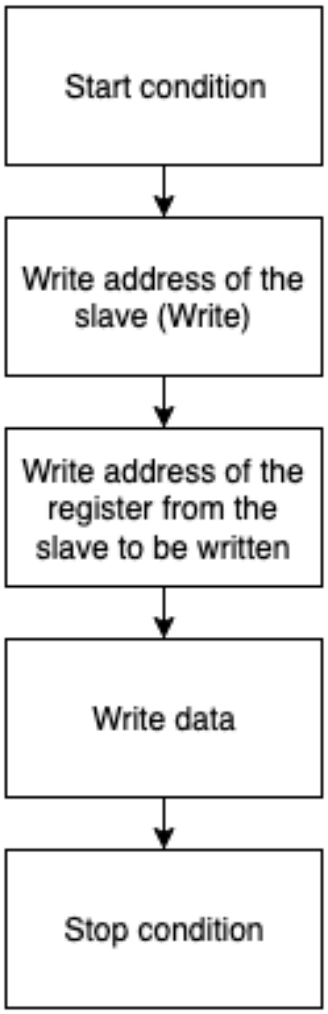

Figure 4.26: Write to the RTC using I^2C

by a repeated started. In the first operation, the microcontroller uses the writing address of the RTC followed by the address of the register that it wishes to read. Then, the master generates a repeated start

condition followed by a writing with the reading address. The RTC (slave) will now send the information that is present in the address given by the master and it will continue to send information until the master issues a not acknowledge. At the end the master issues a stop condition and the communication ends. In terms of the important registers the RTC has the following registers:

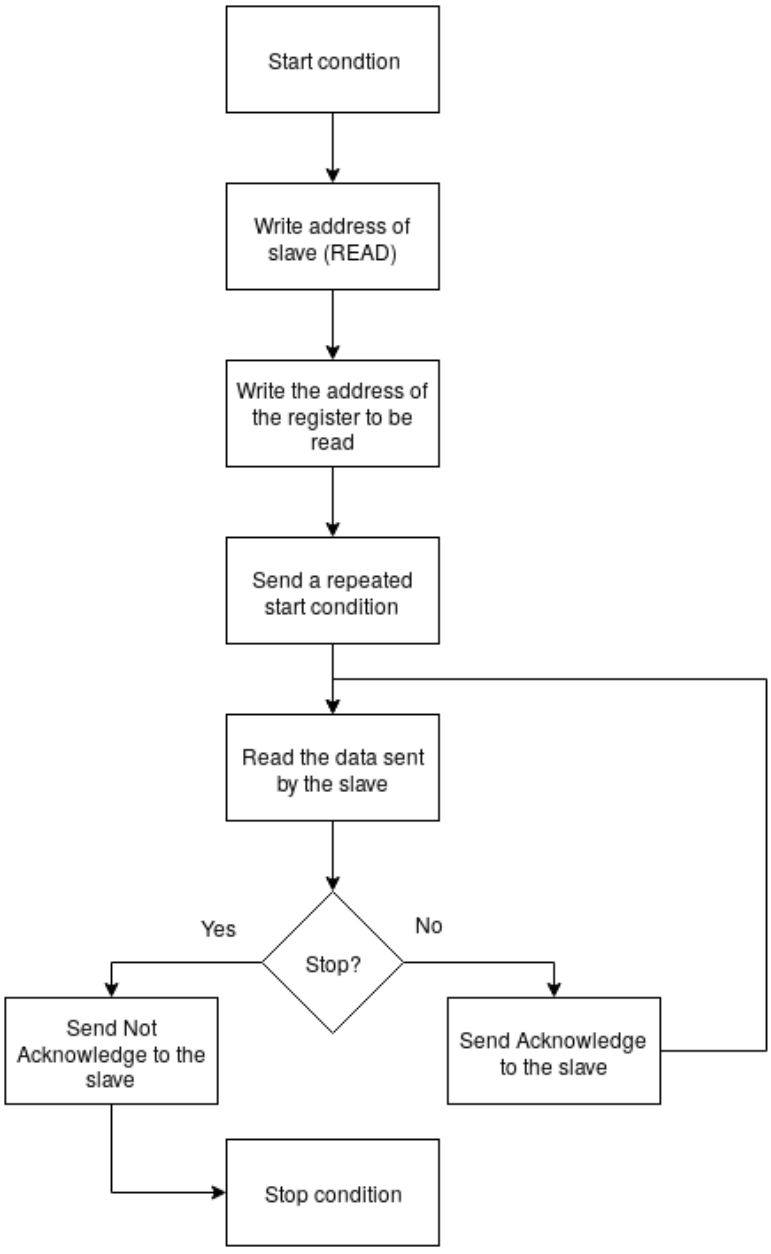

Figure 4.27: Read from to RTC using I^2C

- From the address 00h to 06h it has the memory positions related with the timekeeping.
- From the 07h to 0Ah it has memory positions that set the Alarm 1
- From the 0Bh to 0Dh it has the positions related to the Alarm 2

Moreover there are three more memory positions related with the Control, Status and Trickle Charger.

Since the Trickle Charge is not used in this system the libraries to control it were not implemented. It is however important to refer that Trickle Charge refers to a slow continuous charge for an electric storage battery. As for the control register it controls the enabling of the alarms, the oscillator and the module that controls the SQW/INT output pin. The bit 7 (EOSC) is used to enable or disable the oscillator. The bit 6 is the BBSQI and when set to 1 enables the SQW/INT output functionality while the part is powered by the backup power supply. When set to logic 0, this bit disables the SQW/INT output while the part is powered with the backup power supply. Then the RS2 and RS1 bits (5 and 4 bits) are used to control the frequency of the output squared wave. The second bit, called the interrupt control bit, controls interruptions. When set to zero, the SQW/INT port is used by the squared wave module. When set to 1, a match between the register alarm and the timekeeping will activate the SQW/INT output port. At the end, bit one and zero are, respectively, enable bits for the alarm 1 and 2. When set to one, it enables the corresponding alarm and when set to zero it disables it. Lastly on the status bits is present the Oscillator Stop Flag (bit 7) that when set to 1 by the hardware indicates that the oscillator has stop working which can be used to judge the validity of the calendar. Bit 1 and 0 are the alarm flags for the alarm 2 and alarm 1. When the alarm is set, the flag is set to one by the hardware. Additionally the SQW/INT is asserted and will only be cleared when the alarm flag is cleared by software.

4.2.7 DS18B20 temperature module

The temperature sensor from Maxim Integrated uses the One Wire protocol in order to communicate with a master device. There are many different commands available in the DS18B20 device. Not all commands were implemented. The skip ROM command is used to address all devices on the One Wire but without sending out any ROM code information. The Convert T temperature is used to initiate a single temperature conversion. The write scratchpad operation allows the master to write 3 bytes of data to the DS18B20's scratchpad. The first byte is written to the T_H register (byte 2 of the scratchpad), the second byte is written to the T_L register (byte 3 of the scratchpad) and the third byte is written into the configuration register. As for the read scratchpad it allows the master to read the contens of the scratchpad. It starts from the zero byte of the scratchpad until the 9th byte is read. The master can issue a reset command to terminate the reading at any time. Finally the read power supply command allows the master to determine if any of the DS18B20s sensors are using parasite power. The difference between parasite power and external power supply is presented in Fig. 4.28.

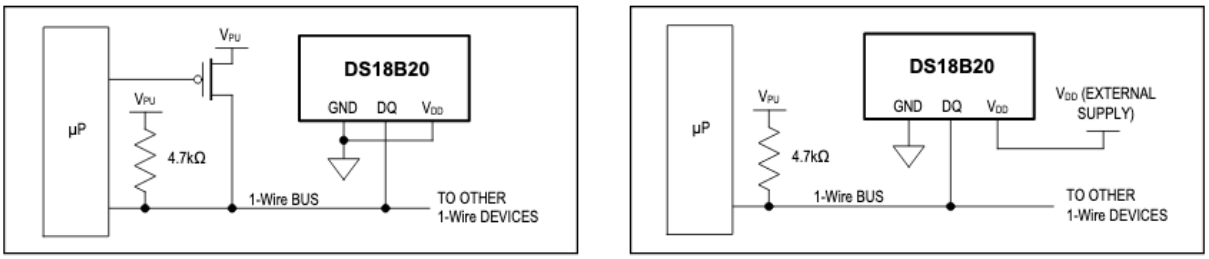

Figure 4.28: Parasitic and Normal Power DS18B20 [42]

In order to use the temperature sensor the Table 4.2 was used to program the microcontroller. The table presents a sequence of instructions to follow in order to measure the temperature.

Table 4.2: Sequence follow to read the temperature from the sensor

Master Mode	Data (LSB first)
TX	Reset
RX	Presence
TX	Skip ROM Command
TX	Write Scratchpad Command
TX	3 data bytes
TX	Reset
RX	Present
TX	Skip ROM Command
TX	Read Scratchpad Command
RX	9 data bytes
TX	RESET

Chapter 5

Results

The proposed embedded system, after begin designed and produced, was tested in order to check its performance and its power consumption. The system was connected to a LoRaWAN network and the information from the sensors connected to the board was transmitted to the network server. Moreover the system was tested in order to measure the sleeping current and the transmission current in order the evaluate the battery life of the proposed system.

5.1 Verification and Validation

After soldering the components basic tests were performed in order to test the different parts of the system. The first test was to power up the system and check if all the voltages were present. By using a multimeter it was possible to check all the voltages at the integrated circuits. Then a first attempt has made to program the microcontroller with a basic program in order to test if it was working properly. The program consisted of a single change in state of an I/O with a delay in order to see if the crystal and microcontroller were working properly. The system passed all the tests and was then used to develop the full code that would allow it to program the RTC and the sensors and send the information to the gateway.

5.1.1 Hardware measurements

In order to evaluate the consumption of the system a set of measurements were taken. The first measurement was the current consumption of the system in sleep mode. In order to obtain this measurement an ammeter was used to measure the current at the input of the system, in jumper 1 and in jumper 2. The jumper 1 is used to measure the current used by the LDO and the jumper 2 is used to measure the current of the microcontroller, LoRaWAN module and sensors. At the input of the system, a current measurement was also performed in order to check the performance of the DC-DC converter. At the input and on the jumper 1 the sleep current measured with an UT39B multimeter from UNI-T was $0.37\mu A$ which is equal to $370nA$. As for jumper 2, a probe current connected to an oscilloscope was used in order to measure the current consumption of the microcontroller, LoRaWAN module and sensors. In order to

see the different variations of time and current using different spreading factors a set of measurements was taken.

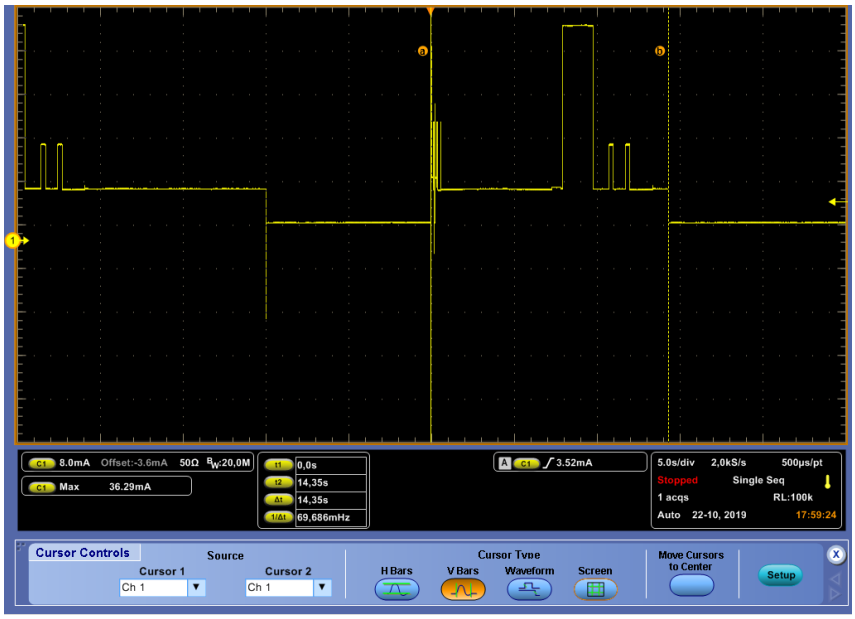

Figure 5.1: Oscilloscope image for a Spreading Factor of 12 with the wake up time

In Figure 5.1, it is possible to visualize the wake up time of the system. Moreover, it is also possible to visualize the current consumption when the system is transmitting a message. In order to better visualize the time that a transmission took, a second image of the oscilloscope was taken. In figure 5.2

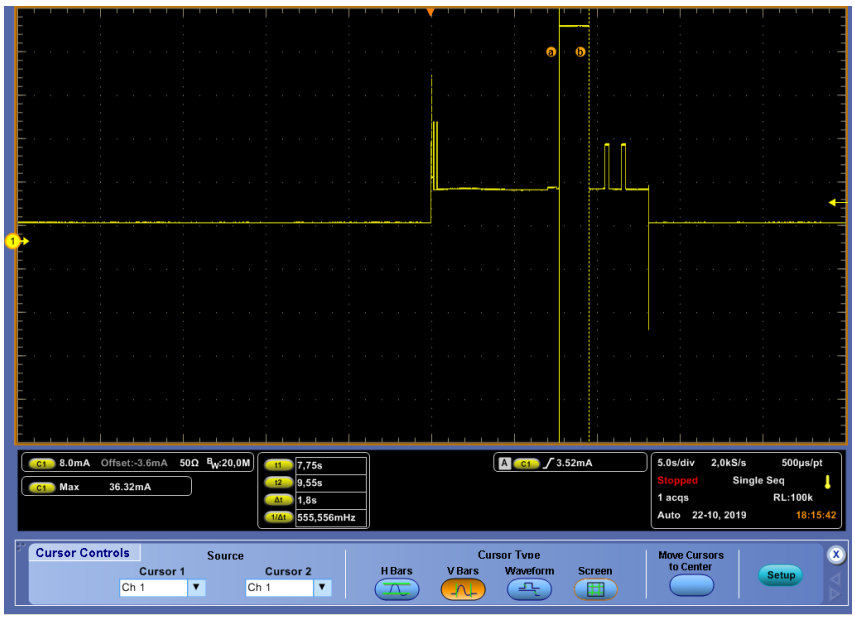

Figure 5.2: Oscilloscope image for a Spreading Factor of 12 with the transmission time

the horizontal cursors are used to measure the time of a transmission. It took the system 7,75 seconds to transmit a message with a spreading factor of 12. In addition, the system was awake for 14.35 seconds. The same measurements were made for a spreading factor of 11, 10, 9, 8 and 7.

In order to estimate the battery life of the system, it was necessary to calculate the average current

of the system using the equation:

$$I_{avg} = \frac{I_{on} \times T_{on} + I_{sleep} \times (T_{ci} - T_{on})}{T_{ci}}, \tag{5.1}$$

where the T_{ci} is the time cycle and T_{on} the ON time. After having the average current, the following equation was used to calculate the battery life in hours

$$Battery\ Life\ (Hours) = \frac{Battery\ Capacity\ (Ah)}{Average\ current\ drain} \tag{5.2}$$

With the two equations and the oscilloscope images, the battery duration was then calculated. It was considered the use of a battery with 3600 mAh of capacity. The table 5.1 shows, for different spreading factors the battery life expected in hours and years.

Table 5.1: Battery life for different spreading factors

Spreading Factor	Time ON	Time of cycle	Time transmitting	Transmitting current	Iddle current	Sleep current	Average current	Battery life (Hours)	Battery life (Years)
12	14,35s	3600s	1,8s	36,32mA	6,4mA	0,37 uA	40,8 uA	88149,6	10
11	13,15s	3600s	1,8s	36,32mA	6,4mA	0,37 uA	38,7 uA	93007,8	10
10	11,8s	3600s	450,0ms	36,22mA	6,4mA	0,37 uA	25,1 uA	143574,6	16
9	11,6s	3600s	240,0ms	36,21mA	6,4mA	0,37 uA	23,0 uA	156664,6	17
8	11,45s	3600s	140,0ms	36,27mA	6,4mA	0,37 uA	21,9 uA	164488,79	18
7	11,4s	3600s	80,0ms	36,24mA	6,4mA	0,37 uA	21,3 uA	169025,1	19

5.1.2 Comparison between similar products

Considering the Table 2.1 in the Chapter 2, a new entry can be added for the embedded system design in the scope of this thesis. Since a platform name is required, it was chosen the name Muvu Node. Table 5.3, at the end of the chapter, lists available products on the market and the node produced by the work of this thesis. Comparing with all the systems listed in Table 5.3, Muvu Node presents the second lowest sleeping current. However, considering the platforms that use the LoRaWAN network the Muvu Node is the one that presents the lowest sleep current. As for the connections to the sensors, the system has the standard protocols used.

5.1.3 LoRaWAN deployment

In order to test the LoRaWAN network, a set of nodes were deploy by Muvu in an agriculture field. The field is located in Alcobaça more precisely in Quinta da Ruiva. Figure 5.3 shows the localization of the nodes and of the gateway. The gateway is an OLG02 Outdoor Dual Channels LoRa IoT Gateway. Despite of the name of the gateway, it only uses one channel to transmit and another channel to receive. Since the gateway used is a single channel gateway, it is not possible to full evaluate the LoRaWAN network. A gateway with at least three channels should be consider in order to measure the performance of the system. However, and considering the limitations of the gateway, the same gateway was configured with a spreading factor of 9 and a bandwidth of 125 kHz. The frequency of the receiving channel is 868.3MHz. For the transmitting channel the frequency is also the same. In order for the nodes to work with the

Figure 5.3: Sensor nodes localization using Google Maps, Quinta da Ruiva, Alcobaça

gateway all channels were disable excepted the channel that has the frequency of 868.3MHz. After the deployment of the nodes, the network server was used in order to measure the average RSSI (Received signal strength indication) and the average SNR (Signal to Noise Ratio). The Received Signal Strength Indication (RSSI) is the received signal power in milliwatts and is measured in dBm. This value can be used to measure how well the gateways can hear the sensor node. The Signal-to-Noise Ratio (SNR) is the ratio between the received power signal and the noise floor power level. In Figure 5.4, 5.5, 5.6, 5.7, 5.8 and 5.9 the value of the x coordinate represents the number of messages received.

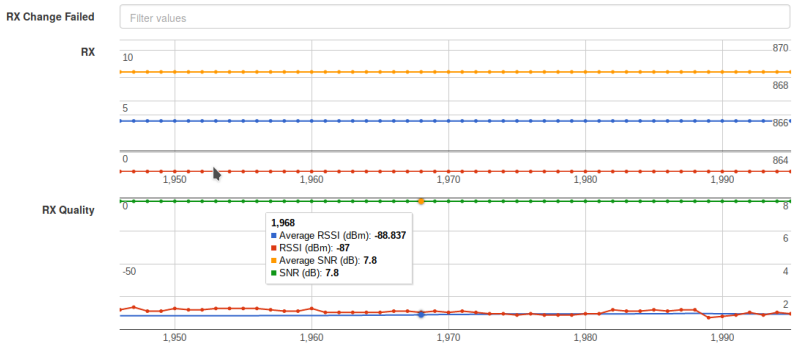

Figure 5.4: SNR and RSSI of sensor node AAA00000

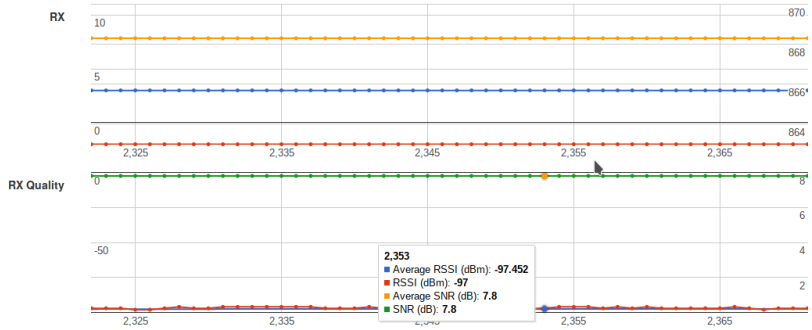

Figure 5.5: SNR and RSSI of sensor node AAA00002

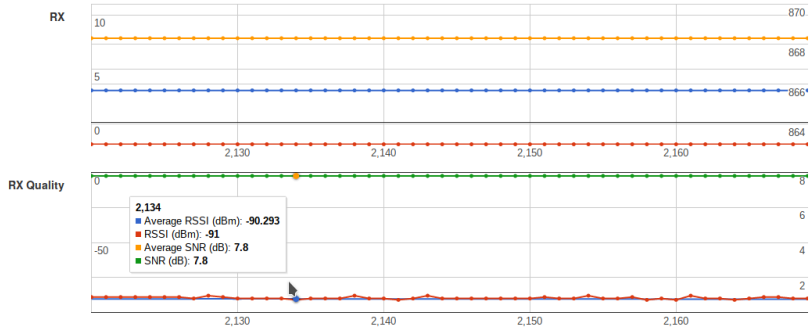

Figure 5.6: SNR and RSSI of sensor node AAA00004

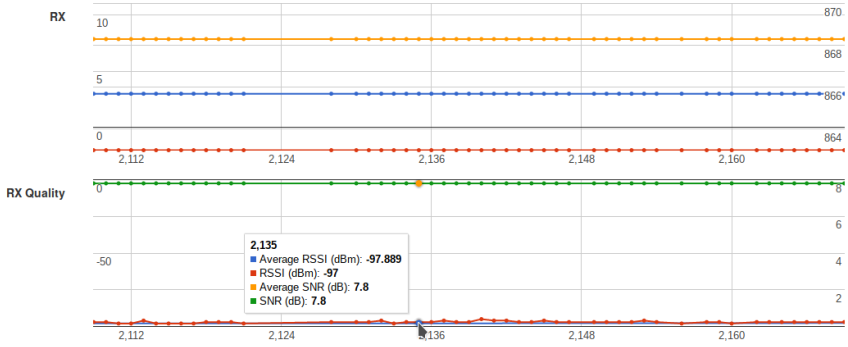

Figure 5.7: SNR and RSSI of sensor node AAA00005

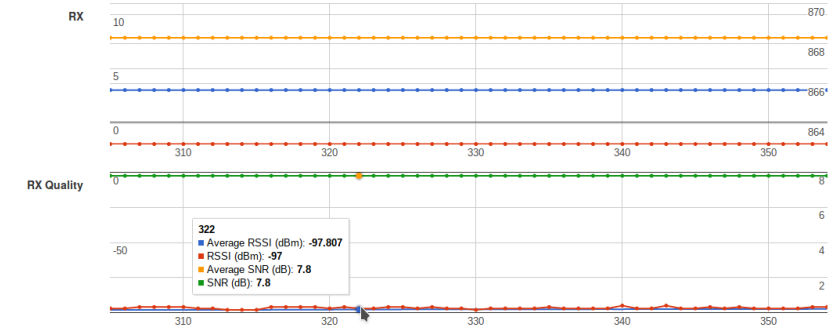

Figure 5.8: SNR and RSSI of sensor node AAA00006

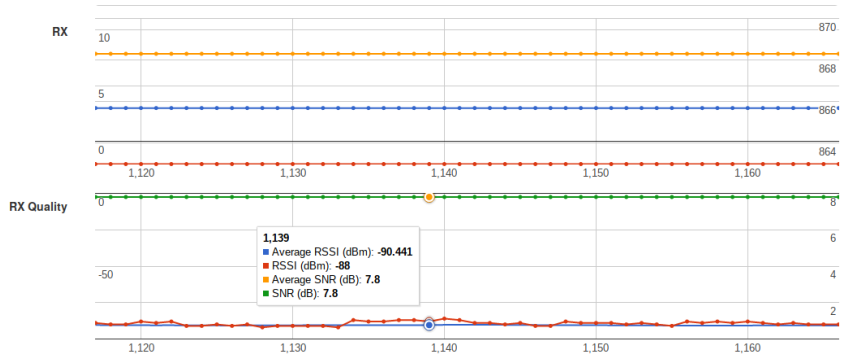

Figure 5.9: SNR and RSSI of sensor node AAA00008

The Table 5.2 shows the average value of the SNR and RSSI for the different nodes.

Table 5.2: Average SNR and RSSI for different nodes

Node	Average RSSI (dBm)	Average SNR (dB)
AAA00000	-88.837	7.8
AAA00002	-97.452	7.8
AAA00004	-90.293	7.8
AAA00005	-97.889	7.8
AAA00006	-97.807	7.8
AAA00008	-90.441	7.8

It is possible to see that the nodes AAA00002, AAA00005 and AAA00006 present the weakest signal. On the other hand the node with the strongest signal is the AAA00000. The nodes AAA00005 and AAA00006 are, from the set of nodes, the ones that are far apart from the gateway. It is important to refer that the nodes AAA00001, AAA00003 and AAA00007 suffered from external factors, such as humidity and condensation and did not work properly. For that reason they are omitted from the table. Since the gateway used has a single channel, the LoRaWAN network is not fully deploy and limited conclusions can be obtained. It is necessary to use a gateway with at least three channels to evaluate the performance of the network. However, the test shows that the sensors were able to transmit information to the gateway only by using a single channel. In order to avoid collisions between nodes, they where powered at different times. This allowed the nodes to transmit at different times and avoid collisions.

Table 5.3: Comparison between available products on the market and the system of the thesis

Platform name	Microcontroller	Transceiver	Program, Data Memory	Flash, EEPROM, Ext. Memory	Sensor Connections	Sleep Current
IMote 2.0	Marvell PXA271 ARM 11-400 MHz	TI CC2420 IEEE 802.15.4/ZigBee compliant radio	32 MB SRAM	32 MB	UART, SPI, I2C, GPIOS	-
Iris Mote	ATmega 1281	Atmel AT86RF230 802.15.4/ZigBee compliant radio	8 KB RAM	128 KB	ADC, UART, GPIOS, I2C, SPI	$8\mu A$
TelosB/T-Mote Sky	Texas Instruments MSP430 microcontroller	250 kbit/s 2.4 GHz IEEE 802.15.4 Chipcon Wireless Transceiver	8 KB RAM	48 KB	UART, SPI, I2C, USB, ADC	$1\mu A$
Zolertia Remote	CC2538 ARM Cortex-M3	Dual Radio: 802.15.4/CC1200 869/915 MHz	32 KB RAM	512 KB	UART, I2C, SPI, ADC	$1\mu A$ *to* $150nA$
Zolertia Z1	Texas Instruments MSP430 microcontroller	Chipcon Wireless Transceiver 2.4 GHz IEEE 802.15.4	8 KB RAM	92 KB	GPIOS, SPI, I2C, UART, USB	-
WiSMote	Texas Instruments MSP430 microcontroller	TI CC2520 2.4 GHz IEEE 802.15.4	16 KB RAM	1-8 MB, 128, 192 or 256 KB	-	-
Waspmote	ATmega 1281	ZigBee/IEEE 802.15.4 DigiMesh RF, 2.4 GHz/868 MHz/915 MHz	8 KB SRAM	128 KB, 4 KB EEPROM, 2 GB SD card	Analog, GPIOS, UART, I2C, SPI, USB	$7\mu A$
Arduino Uno/Mega/Nano	ATmega328P ATmega168 ATmega328P	External modules	2 KB SRAM/8 KB SRAM/2 KB SRAM	32 KB, 1 KB/256 KB, 4 KB/32 KB, 1 KB	Analog, I2C, SPI, UART, Digital	-
Arduino Yun (2 processors)	ATmega32U4/Atheros AR9331	Ethernet, Wifi	2.5 KB, 64 MB DDR2	1 KB/16 MB	Analog, I2C, SPI, UART, Digital	-
Raspberry Pi (various versions)	ARMv6 (1-core, 700MHz) ARMv7 (4-cores, 900MHz) ARMv8 (4-cores, 1.2 GHz)	Onboard LAN, "Wifi/Bluetooth" ("RPi 3 only")	256 MB - 1 GB SRAM (@400 MHz)	SD card	I2C, SPI, UART, GPIOS	-
LoPy (2 processors)	Xtensa (2-cores, 160 MHz)	Onboard Wifi, SX1272 LoRa, Bluetooth (BLE)	256 KB	1 MB (internal) 4 MB (external)	Analog, GPIO, UART, SPI	$10\mu A$
NodeMCU	ESP8266/LX106	Onboard Wifi	20 KB RAM	4 MB Flash	Analog, GPIO, UART, SPI	$20\mu A$
Arietta G25	ARMv9 (4-cores, 400 MHz)	External Wifi adapter	128-256 MB RAM	SD card	Analog, I2C, UART, SPI	$9.1mA$
WIOT Board	ATmega32U4 ESP8266 (for Wifi)	Wifi	2.5 KB SRAM	32 KB, 1 KB	Analog, GPIOS	-
Muvu Node	**PIC18LF46K22**	**RN2483**	**3896 Bytes**	**64 kB, 1024 Bytes**	**I2C, SPI, EUSART, Analog**	**0.37 uA**

Chapter 6

Conclusions

This chapter presents the achievements of the work done. It also includes ideas for future work that can improve the performance of the system.

6.1 Achievements

The main achievement of this work was the development of an embedded system with an ultra low sleeping current. There are many of embedded systems on the market, although generally they do not present such a low sleeping current. With a sleeping current of 370 nA, the system produced in the scope of this thesis can operate for several years, with a single battery charge, depending on the capacity of the battery used. By using a Real Time Clock in order to turn off the microcontroller, a LoRaWAN module and sensors, with optimal power management, the system is able to reach a ultra low sleeping current. The main difference to other available on the market is the ability to turn off completely the microcontroller. In addition, the RTC is used to enable the DC-DC that turns on the microcontroller, transceiver and sensors. Most of the systems used in precision agriculture use the sleep mode of the microcontroller instead of power gating it. The solution implemented uses the RTC to wake up the microcontroller from sleep mode. Moreover, by using a buck DC-DC convert, the efficiency of high power modes can reach 90%, which also improves the overall performance of the system. Another important aspect is the way the embedded system uses the LDO. The LDO only has a load when the RTC is in sleep mode. When the DC-DC wakes up, it releases the load from the LDO by powering the RTC from the VIN pin. It is also important to refer that the system developed can communicate using several protocols, such as UART, SPI, I^2C, One-Wire and it is able to convert analog signals to digital ones by using an ADC in the microcontroller. This means that, despite the target application for the design being an agriculture IoT node, the embedded the system designed is very flexible since it can work with several types of sensors and can be used for a wide range of applications.

6.2 Future Work

One way to reduce the time in idle mode is to create parts of the code using assembly. The MPASM from Microchip can be used to reduce the number of instructions required to perform certain actions. By reducing the idle time, the operation time with a single battery charge can be increased. On the other hand it is also possible to improve the C code produced and optimize it with assembly. A very interesting functionality of the MPLAB IDE is the ability to use assembly and C code in a single project. In terms of hardware it is important to reduce the volume of the system. The board produced for this thesis was a prototype and a proof of concept. A smaller board, with smaller components will allow the system to reduce its size considerable and make it able to fit in a smaller protection case. Another important aspect is the use of a good soil moisture sensor. The sensor used in this work is very simple and without a datasheet that relates the voltage measured to the humidity of the soil. There are on the market several humidity sensors that translate the voltage measured to a specific humidity. An important test that should be conducted is the use of a gateway with at least three channels in order to test the LoRaWAN protocol. The tests that were conducted used a single channel gateway and for that reason they do not represent the LoRaWAN protocol. Finally, a battery voltage monitoring system should be implemented in order to inform the farmer the battery is becoming discharged.

Bibliography

[1] FAO. Global agriculture towards 2050. *High Level Expert Forum-How to feed the world 2050*, pages 1–4, 2009. ISSN 0002-9505. doi: http://www.fao.org/fileadmin/templates/wsfs/docs/Issues_papers/HLEF2050_Global_Agriculture.pdf. URL `http://www.fao.org/fileadmin/templates/wsfs/docs/Issues{_}papers/HLEF2050{_}Global{_}Agriculture.pdf`.

[2] N. Alexandratos and J. Bruinsma. Food and Agriculture Organization, World agriculture towards 2030/2050: the 2012 revision. *ESA Working Paper No. 12-03*, (12), 2012.

[3] P. P. Ray. Internet of things for smart agriculture: Technologies, practices and future direction. *Journal of Ambient Intelligence and Smart Environments*, 9(4):395–420, 2017. ISSN 18761364. doi: 10.3233/AIS-170440.

[4] D. Murugan, A. Garg, and D. Singh. Development of an Adaptive Approach for Precision Agriculture Monitoring with Drone and Satellite Data. *IEEE Journal of Selected Topics in Applied Earth Observations and Remote Sensing*, 10(12):5322–5328, 2017. ISSN 21511535. doi: 10.1109/JSTARS.2017.2746185.

[5] M. Rouse, L. Rosencrance, M. Rouse, and M. Rouse. What is internet of things (iot) - definition from whatis.com. URL `https://internetofthingsagenda.techtarget.com/definition/Internet-of-Things-IoT`.

[6] A. Tzounis, N. Katsoulas, T. Bartzanas, and C. Kittas. Internet of Things in agriculture, recent advances and future challenges. *Biosystems Engineering*, 164(December):31–48, 2017. ISSN 15375110. doi: 10.1016/j.biosystemseng.2017.09.007. URL `https://doi.org/10.1016/j.biosystemseng.2017.09.007`.

[7] B. T. Inc. Leading types of iot wireless tech and their best use cases. URL `https://behrtechnologies.com/blog/6-leading-types-of-iot-wireless-tech-and-their-best-use-cases/`. Access on 18 March 2019.

[8] K. Mekki, E. Bajic, F. Chaxel, and F. Meyer. Overview of Cellular LPWAN Technologies for IoT Deployment: Sigfox, LoRaWAN, and NB-IoT. *2018 IEEE International Conference on Pervasive Computing and Communications Workshops, PerCom Workshops 2018*, pages 197–202, 2018. doi: 10.1109/PERCOMW.2018.8480255.

[9] A. Augustin, J. Yi, T. Clausen, and W. M. Townsley. A study of Lora: Long range & low power networks for the internet of things. *Sensors (Switzerland)*, 16(9), 2016. ISSN 14248220. doi: 10.3390/s16091466.

[10] SigFox. Coverage, . URL https://www.sigfox.com/en/coverage. Access on 19 March 2019.

[11] SigFox. Semiconductor companies, . URL https://partners.sigfox.com/companies/chip-maker. Access on 19 March 2019.

[12] STMicroelectronics. S2-lp - datasheet. URL https://www.st.com/resource/en/datasheet/s2-lp.pdf. Access on 19 March 2019.

[13] Microchip. Ata8520e - complete datasheet, . URL http://ww1.microchip.com/downloads/en/DeviceDoc/Atmel-9409-Smart-RF-ATA8520E_Datasheet.pdf. Access on 19 March 2019.

[14] N. Semiconductors. Ol2385 industrial rf receiver - product data sheet. URL https://www.nxp.com/docs/en/data-sheet/OL2385.pdf. Access on 19 March 2019.

[15] T. Instruments. Cc1310simplelink ultra-low-powersub-1ghz wirelessmcu, . URL http://www.ti.com/lit/ds/symlink/cc1310.pdf. Access on 19 March 2019.

[16] Microchip. Low-power long range lora® technologytransceiver module, . URL http://ww1.microchip.com/downloads/en/DeviceDoc/RN2483-Low-Power-Long-Range-LoRa-Technology-Transceiver-Module-Data-Sheet-DS50002346D.pdf. Access on 19 March 2019.

[17] SemTech. Sx1261/2 - long range, low power, sub-ghz rf transceiver. URL https://www.semtech.com/uploads/documents/DS_SX1261-2_V1.1.pdf. Access on 19 March 2019.

[18] BTI. Wireless connectivity for iiot - facilitate the last mile of communications with mioty lpwan technology. URL https://cdn2.hubspot.net/hubfs/4739964/Brochures/Brochure%20-%20MIOTY%20(digital%20only).pdf. Access on 19 March 2019.

[19] Pedro. Deep diving into mioty low power long range network. URL https://wattx.io/blog/research/2017/10/27/deep-diving-into-mioty--low-power-long-range-network---wattx.html. Access on 19 March 2019.

[20] A. Portugal. Narrowband-iot é o futuro e chega pelas mãos da altice portugal. URL https://www.telecom.pt/pt-pt/media/noticias/paginas/2018/novembro/narrowband-iot-.aspx. Access on 19 March 2019.

[21] Anacom. Frequências. URL https://www.anacom.pt/render.jsp?categoryId=382989. Access on 19 March 2019.

[22] S. Dawaliby, A. Bradai, and Y. Pousset. In depth performance evaluation of LTE-M for M2M communications. pages 1–8, 2017. doi: 10.1109/wimob.2016.7763264.

[23] A. Devices. Understand low-dropout regulator (ldo) concepts to achieve optimal designs. URL https://www.analog.com/en/analog-dialogue/articles/understand-ldo-concepts.html. Access on 28 October 2019.

[24] *TPS61291 Low Iq Boost Converter with Bypass Operation*. Texas Instruments, 09 2014. URL http://www.ti.com/lit/ds/symlink/tps61291.pdf. Revision 2014.

[25] *300/400 mA High Efficiency Buck Converter with Ultra-low Quiescent Current*. Texas Instruments, 6 2015. URL http://www.ti.com/lit/ds/symlink/tps62743.pdf. Revised May 2016.

[26] *TPS65023x Power Management IC (PMIC) With 3 DC/DCs, 3 LDOs, I2C Interface and DVS*. Texas Instruments, 06 2006. URL http://www.ti.com/lit/ds/symlink/tps65023.pdf. Revision 2018.

[27] *Ultra-Low Quiescent Current LDO Regulator*. Microchip, 6 2016. URL http://ww1.microchip.com/downloads/en/DeviceDoc/20005623A.pdf.

[28] *TLV755P 500-mA, Low IQ, Small Size, Low Dropout Regulator*. Texas Instruments, 11 2017. URL http://www.ti.com/lit/ds/symlink/tlv755p.pdf. Revision 2018.

[29] *150 mA low quiescent current and low noise voltage regulator*. ST Microelectronics, 07 2015. URL https://www.st.com/resource/en/datasheet/ld39015.pdf. Revision 5.

[30] *Low Quiescent Current, PFM/PWM Synchronous Boost Regulator with True Output Disconnect or Input/Output Bypass Option*. Microchip, 03 2013. URL http://ww1.microchip.com/downloads/en/devicedoc/20005173b.pdf. Revision B.

[31] *4MHz PWM Buck Regulator with HyperLight Load and Voltage Scaling*. Microchip, 07 2009. URL http://ww1.microchip.com/downloads/en/DeviceDoc/mic23051.pdf.

[32] *TPS65024x PowerManagementICs for Li-Ion PoweredSystems*. Texas Instruments, 6 2007. URL http://www.ti.com/lit/ds/symlink/tps650243.pdf. Revision 2016.

[33] *TPS65021 Power Management IC For Li-Ion or Li-Polymer Powered Systems*. Texas Instruments, 10 2005. URL http://www.ti.com/lit/ds/symlink/tps65021.pdf. Revision 2015.

[34] *MAX14720/MAX14750*. Maxim Integrated, 12 2015. URL https://datasheets.maximintegrated.com/en/ds/MAX14720-MAX14750.pdf. Revision 10.

[35] *Low-Current, I2C, Serial Real-Time Clock*. Maxim Integrated, 1 2015. URL https://datasheets.maximintegrated.com/en/ds/DS1339A.pdf. Rev. 2.

[36] *Battery-Backed I2C Real-Time Clock/Calendar with SRAM*. Microchip, 04 2011. URL http://ww1.microchip.com/downloads/en/DeviceDoc/MCP7940N-Battery-Backed-I2C-RTCC-with-SRAM-20005010G.pdf. Revision G.

[37] *TinyLogic UHS Inverter with Schmitt Trigger Input*. ON Semiconductor. URL https://www.mouser.com/ds/2/149/NC7SZ14-1011406.pdf. Rev. 1.0.3.

[38] *LoRa^{TM} Technology ModuleCommand Reference User's Guide*. Microchip, 2015. URL https://ww1.microchip.com/downloads/en/DeviceDoc/40001784B.pdf. Revision A.

[39] *Low-Power Long Range LoRa Technology Transceiver Module*. Microchip, 3 2015. URL https://www.microchip.com/stellent/groups/picmicro_sg/documents/devicedoc/cn547043.pdf. Revised March 2019.

[40] *28/40/44-Pin, Low-Power, High-Performance Microcontrollers with XLP Technology*. Microchip, 2 2010. URL https://www.microchip.com/stellent/groups/picmicro_sg/documents/devicedoc/cn547043.pdf. Revised August 2016.

[41] *Single-Supply, Low Power, Precision FET Input Quad Buffer*. Analog Devices, 12 2014. URL https://www.microchip.com/stellent/groups/picmicro_sg/documents/devicedoc/cn547043.pdf. Revision A.

[42] *Programmable Resolution1-Wire Digital Thermometer*. Maxim Integrated, 7 2019. URL https://datasheets.maximintegrated.com/en/ds/DS18B20.pdf. Revision 6.

[43] R. W. World. Lorawan mac layer messages meaning. URL https://www.rfwireless-world.com/Tutorials/LoRaWAN-MAC-layer-inside.html. Access on 28 October 2019.

[44] E. Viciana, A. Alcayde, F. G. Montoya, R. Baños, F. M. Arrabal-Campos, and F. Manzano-Agugliaro. An Open Hardware Design for Internet of Things Power Quality and Energy Saving Solutions. *Sensors (Basel, Switzerland)*, 19(3), 2019. ISSN 14248220. doi: 10.3390/s19030627.

[45] J. Palacín, M. Tresanchez, E. Clotet, D. Martínez, T. Pallejà, and A. Pujol. A proposal of low-cost and low-power embedded wireless image sensor node for IoT applications. *Procedia Computer Science*, 134:99–106, 2018. ISSN 18770509. doi: 10.1016/j.procs.2018.07.149. URL https://doi.org/10.1016/j.procs.2018.07.149.

[46] M. Cerchecci, F. Luti, A. Mecocci, S. Parrino, G. Peruzzi, and A. Pozzebon. A low power IoT sensor node architecture for waste management within smart cities context. *Sensors (Switzerland)*, 18(4), 2018. ISSN 14248220. doi: 10.3390/s18041282.

[47] M. E. Moulat, O. Debauche, S. Mahmoudi, L. A. Brahim, P. Manneback, and F. Lebeau. Monitoring System Using Internet of Things for Potential Landslides. *Procedia Computer Science*, 134:26–34, 2018. ISSN 18770509. doi: 10.1016/j.procs.2018.07.140.

[48] F. A. Aoudia, M. Gautier, M. Magno, M. L. Gentil, O. Berder, and L. Benini. Long-short range communication network leveraging LoRa^{TM} and wake-up receiver. *Microprocessors and Microsystems*, 56(December 2017):184–192, 2018. ISSN 01419331. doi: 10.1016/j.micpro.2017.12.004. URL https://doi.org/10.1016/j.micpro.2017.12.004.

[49] T. Lei, A. A. Mohamed, and C. Claudel. An IMU-based traffic and road condition monitoring system. *HardwareX*, 4:e00045, 2018. ISSN 24680672. doi: 10.1016/j.ohx.2018.e00045. URL https://doi.org/10.1016/j.ohx.2018.e00045.

[50] B. Wolbert. Designing With Low-Dropout Voltage Regulators. 1(408):944–970, 1998.

[51] J. Tollefson. The Truth about Power Consumption in PIC® MCUs with XLP Technology vs. TI's MSP430. page 8, 2010. URL http://www.microchip.com/stellent/groups/picmicro{_}sg/documents/devicedoc/en551263.pdf.

[52] I. L C Ng and S. Y. L. Wakenshaw. warwick.ac.uk/lib-publications. *The Warwick Research Archive Portal (WRAP)*, 34:3–21, 2017. URL http://wrap.warwick.ac.uk/84544/7/WRAP-Internet-of-Things-research-directions-Ng-2017.pdf.

[53] Semikron. Effect of Humidity and Condensation on Power Electronics Systems, application note AN 16-001. pages 1–17, 2016.

[54] T. Ameloot, P. Van Torre, and H. Rogier. A compact low-power LoRa IoT sensor node with extended dynamic range for channel measurements. *Sensors (Switzerland)*, 18(7):10–13, 2018. ISSN 14248220. doi: 10.3390/s18072137.

[55] M. Gaudenzi Asinelli, M. Serra Serra, J. Molera Marimòn, and J. Serra Espaulella. The smARTS_Museum_V1: An open hardware device for remote monitoring of Cultural Heritage indoor environments. *HardwareX*, 4, 2018. ISSN 24680672. doi: 10.1016/j.ohx.2018.e00028. URL https://doi.org/10.1016/j.ohx.2018.e00028.

[56] N. Ahmed, D. De, and I. Hussain. Internet of Things (IoT) for Smart Precision Agriculture and Farming in Rural Areas. *IEEE Internet of Things Journal*, 5(6):4890–4899, 2018. ISSN 23274662. doi: 10.1109/JIOT.2018.2879579.

[57] G. T. Netto and J. Arigony-Neto. Open-source Automatic Weather Station and Electronic Ablation Station for measuring the impacts of climate change on glaciers. *HardwareX*, 5:e00053, 2019. ISSN 24680672. doi: 10.1016/j.ohx.2019.e00053. URL https://doi.org/10.1016/j.ohx.2019.e00053.

[58] A. Srilakshmi, J. Rakkini, K. Sekar, and R. Manikandan. A Comparative study on Internet Of Things (IoT) and its applications in Smart Agriculture. *Pharmacognosy Journal*, 10(2):260–264, 2018. doi: 10.5530/pj.2018.2.46.

[59] R. Hienonen and R. Lahtinen. *Corrosion and climatic effects in electronics*. Number 413. 2000. ISBN 9789513869915.

[60] R. Want, B. N. Schilit, and S. Jenson. Enabling the internet of things. *Computer*, 48(1):28–35, 2015. ISSN 00189162. doi: 10.1109/MC.2015.12.

[61] C. Pham. Low-cost, low-power and long-range image sensor for visual surveillance. pages 35–40, 2016. doi: 10.1145/2980147.2980156.

[62] S. Oberloier and J. M. Pearce. Open source low-cost power monitoring system. *HardwareX*, 4, 2018. ISSN 24680672. doi: 10.1016/j.ohx.2018.e00044.

[63] C.-h. Wang, C.-h. Chen, X.-y. Zheng, and C.-p. Chen. An Agricultural-Cloud Based Greenhouse Monitoring System. (June):24–27, 2013.

[64] A. Khanna and S. Kaur. Evolution of Internet of Things (IoT) and its significant impact in the field of Precision Agriculture. *Computers and Electronics in Agriculture*, 157(December 2018):218–231, 2019. ISSN 01681699. doi: 10.1016/j.compag.2018.12.039.

[65] M. Magno, F. A. Aoudia, M. Gautier, O. Berder, and L. Benini. WULoRa: An energy efficient IoT end-node for energy harvesting and heterogeneous communication. *Proceedings of the 2017 Design, Automation and Test in Europe, DATE 2017*, pages 1528–1533, 2017. doi: 10.23919/DATE.2017.7927233.

[66] P. W. Cain and M. D. Cross. An open-source hardware GPS data logger for wildlife radio-telemetry studies: A case study using Eastern box turtles. *HardwareX*, 3(January):82–90, 2018. ISSN 24680672. doi: 10.1016/j.ohx.2018.02.002. URL `https://doi.org/10.1016/j.ohx.2018.02.002`.

[67] Aqeel-Ur-Rehman, A. Z. Abbasi, N. Islam, and Z. A. Shaikh. A review of wireless sensors and networks' applications in agriculture. *Computer Standards and Interfaces*, 36(2):263–270, 2014. ISSN 09205489. doi: 10.1016/j.csi.2011.03.004. URL `http://dx.doi.org/10.1016/j.csi.2011.03.004`.

[68] J. Jiang and C. Claudel. A high performance, low power computational platform for complex sensing operations in smart cities. *HardwareX*, 1:22–37, 2017. ISSN 24680672. doi: 10.1016/j.ohx.2017.01.001. URL `http://dx.doi.org/10.1016/j.ohx.2017.01.001`.

[69] T. Ŝimunić, L. Benini, and G. De Micheli. Energy-efficient design of battery-powered embedded systems. *IEEE Transactions on Very Large Scale Integration (VLSI) Systems*, 9(1):15–28, 2001. ISSN 10638210. doi: 10.1109/92.920814.

[70] J. Luomala and I. Hakala. Effects of Temperature and Humidity on Radio Signal Strength in Outdoor Wireless Sensor Networks. *Proceedings of the 2015 Federated Conference on Computer Science and Information Systems*, 5(September 2016):1247–1255, 2015. doi: 10.15439/2015f241.

[71] G. P. Colucci, M. Poletti, R. Stefanelli, and D. Trinchero. Internet of Things as a means to improve agricultural sustainability. *2017 IEEE Biomedical Circuits and Systems Conference, BioCAS 2017 - Proceedings*, 2018-Janua:1–4, 2018. doi: 10.1109/BIOCAS.2017.8325182.

[72] Y. E. Wang, X. Lin, A. Adhikary, A. Grövlen, and Y. Sui. A Primer on 3GPP Narrowband Internet of Things(NB-IoT). pages 1–8, 2017. ISSN 01636804. doi: 10.1109/MCOM.2017.1600510CM.

[73] Quectel. Quectel bg96, . URL `https://www.quectel.com/UploadFile/Product/Quectel_BG96_LTE_Specification_V1.5.pdf`. Access on 19 March 2019.

[74] Quectel. Quectel bc66, . URL `https://www.quectel.com/UploadFile/Product/Quectel_BC66_NB-IoT_Specification_V1.0_Preliminary_20180201.pdf`. Access on 19 March 2019.

[75] Libelium. Waspmote hardware general characteristics, . URL `http://www.libelium.com/products/waspmote/hardware/`. Access on 28 October 2019.

[76] Libelium. Waspmote plug and sense, . URL http://www.libelium.com/products/plug-sense/technical-overview/. Access on 28 October 2019.

[77] pycom. Lopy4. URL https://pycom.io/product/lopy4/. Access on 28 October 2019.

[78] Dragino. Lsn50 - waterproof long range wireless lora sensor node. URL https://www.dragino.com/products/lora-lorawan-end-node/item/128-lsn50.html. Access on 28 October 2019.

[79] T. Instruments. Layout review techniques for low power rf designs by suyash jain, . URL http://www.ti.com/lit/an/swra367a/swra367a.pdf. Access on 28 October 2019.

[80] IPC. Generic standard onprinted board design. URL http://www.ipc.org/TOC/IPC-2221A.pdf. Access on 28 October 2019.

Appendix A

Electrical Schematic

See next page

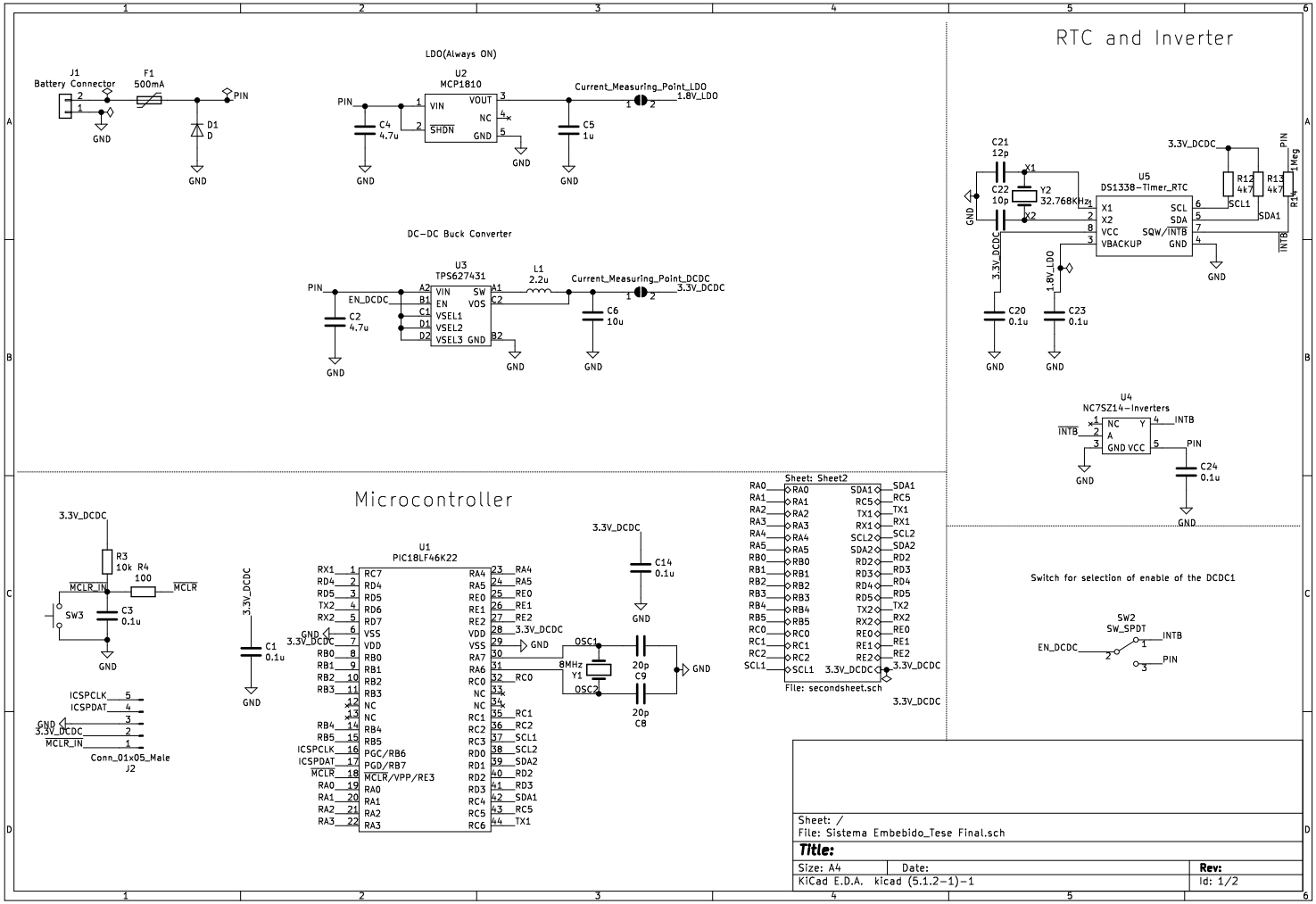

Figure A.1: Schematic of embedded system - page 1

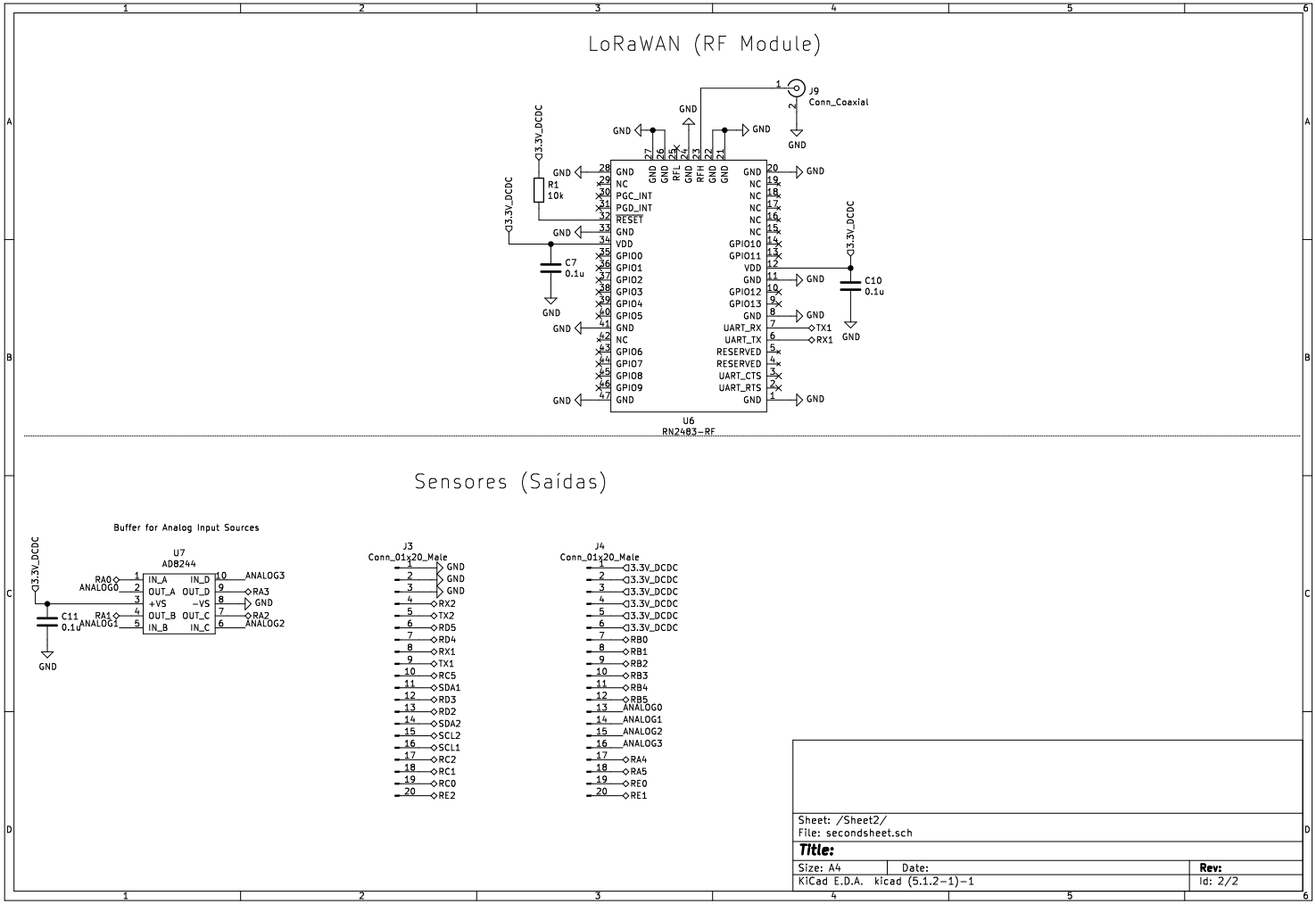

Figure A.2: Schematic of embedded system - page 2

Appendix B

PCB design

B.1 Printed Circuit Board design

After verifying the electrical schematic the next point was the design of a printed circuit board. A printed circuit board is made by several vias, tracks and layers that all together allow the connection of the different elements of the electrical schematic. There is also different components such as through hole technology (THT) or surface mounted devices (SMD) that have different sizes and proprieties. Furthermore the size of the tracks and vias depends on several parameters such as capacitance, inductance and the current that flows through them. In the following sections it will be presented the different problems to take in consideration when designing a PCB and what lead to the final design.

B.1.1 Number of layers used

A PCB can have several layers or a single layer. The possible combinations are 1, 2, 4, 6, 8, 10, 12, 14 and 16 layers. The number of layers on a PCB is normally called the stack up. A layer refers to a plane of a PCB. They can be conductive and be made with copper or be non-conductive as the silkscreen, the solder mask, etc.. The following list presents the different types of layers present in a printed circuit board.

- Silkscreen - The color letters present in a PCB that are used to identify the components, write company logos, putting warning symbols, manufacturer marks and others. Normally they present a white color and are useful to identify the different components in a board.

- Solder Mask - A coating that protects the circuit from corrosion and electrical shocks. It also gives electrical isolation between traces which allows higher voltage traces to be place near each other. This layer is what gives the color to the PCB. There are many different types of colors such as green, blue, white, yellow, dark and others.

- Copper - It is a copper foiled that is laminated to the PCB through heat and adhesive. Normally a double side PCB (two layers) has to copper foils. One in front and another on the back. It can

have different sizes such as 1 ounce, 2 ounce or 3 ounces (the last two for power electronics). It provides the electrical connection between the different elements of the circuit.

- Substrate - It is made of fiberglass and there are different types of materials that can be used. The most common rigid PCB materials are FR-2 and FR-4. For flexible PCBs, Kapton and Pyralux are the most common used materials. FR stands for flame retardant and denotes that the material complies with the standard UL94V-0. This layer gives rigidity or flexibility and thickness to the PCB.

Normally the number of layers that the stack up refers are the conductive layers. This means that a 4 layer stack up corresponds to the use of 4 layers of conductive material (cooper). For the design of an IoT node and having in consideration that the board needs to have radio frequency capabilities it was choose a 4 layer PCB based on [79]. The stack up proposed is the following

1. Layer - Components and Routing
2. Layer - Ground Plane
3. Layer - DC Power Supply Plane
4. Layer - Ground Plane and Routing

It is possible to see that the DC Power Supply Plane is between two ground planes allowing for distributed RF decoupling.

B.1.2 Vias

Vias allow the connection from a given plane to another. There are three types of vias.

- Platted through hole vias - It crosses the PCB from the top layer to the button layer. A good way to verify if a via is a through hole via is by leaning the PCB towards light. If it is possible to see the light on the via it means is a through hole via.
- Blind Via Hole - Connect an outside layer of the PCB to an adjacent inner layer with plated through-hole
- Burried Via Hole - Buried via hole connects to any layer of PCB but do not pass to the outer layer. It connects two inner layers. These vias need more time than the original through-hole and blind hole, which means that has an higher manufacturing price.

A via has two diameters. The hole diameter and the via diameter. A good rule of thumb is to have the diameter of the via equal to the track with. For example if a track has a width of 0.35 mm the via diameter should be 0.35 mm. Most of the vias used in this design are blind via holes that connect the top layer (components layer) to the inner layers of ground and DC power supply.

B.1.3 Track width

The IPC (Association Connecting Electronics Industries) has a document, the IPC-2221A that defines, among others, different formulas for calculating the track width. The document can be consulted here [80] and on page 40 it presents the following equation

$$I = k * \Delta T^{0.44} A^{0.725} \tag{B.1}$$

where I is the current in amperes, A the cross section in square mils and ΔT the temperature rise in deg C and k a constant that varies with the position of the layer. For outer layers the k value is 0.048 and for inner layers the value is 0.024. The conductors permissible temperature rise is defined as the difference between the maximum safe operating temperature of the printed board laminate material and the maximum temperature of the thermal environment to which the printed board will be subjected. This formula is only available for currents up to 35 Amps. For currents that are larger than 35 Amps other techniques are required. For the design of this system the maximum current is 2 A which is in range of the 35 Amps limit. The maximum width is 1 mm for the input power line. This line can handle a maximum current of 3.2444 A (outer layer). The smallest track width is 0.20 mm which can handle a maximum current of 1 A (outer layer). For inner layers the values are smaller but since the design of the node only uses the tracks in outer layers these values are omitted.

B.1.4 Line Impedance - Transmission lines

When having circuits that have radio frequency capabilities the proprieties of the lines change. The tracks start acting like transmission lines meaning that it is necessary to take in consideration the impedance of the line to avoid losses. The wavelength is equal to the propagation velocity divided by the frequency.

$$\lambda = \frac{v}{f} \tag{B.2}$$

The propagation velocity depends on the propagation medium. For this reason a better equation should be used since the medium of a PCB depends on the materials used. The Microwaves101 site provides a wavelength calculator that uses the relative dielectric of medium to calculate the wavelength of a transmission signal.

$$\lambda = \frac{300}{F \times \sqrt{\epsilon}} \tag{B.3}$$

where F is the frequency of the wave and lambda is given in millimetres. In order to properly calculate the wavelength is necessary to look for the stackup of the PCB and the dielectric constant of the different materials used. In Fig. B.1 the stackup of the AllPCB for a 4 layer PCB is presented. The manufacturer is based on China and it was proposed by Muvu to be used for the manufacturing process of the PCBs.

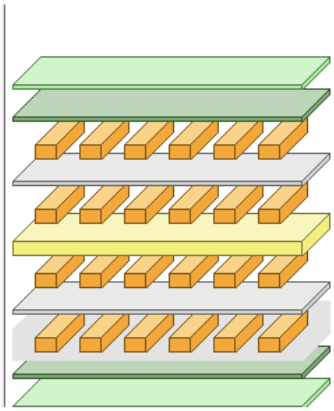

Layer Name	Type	Material	Thickness (mm)	Dielectric Material	Dielectric Constant
Top Overlay 1	Overlay				
Top Solder 1	Solder Mask/...	Surface Mate...	0.01016	Solder Resist	3.5
Top Layer	Signal	Copper	0.035		
Dielectric1	Dielectric	Prepreg	0.185		4.2
Signal Layer 1	Signal	Copper	0.035		
Dielectric 3	Dielectric	Core	1.15	FR4	4.2
Signal Layer 2	Signal	Copper	0.035		
Dielectric 2	Dielectric	Prepreg	0.185		4.2
Bottom Layer	Signal	Copper	0.035		
Bottom Solder 1	Solder Mask/...	Surface Mate...	0.01016	Solder Resist	3.5
Bottom Overl...	Overlay				

Figure B.1: ALLPCB stackup

If the length of the line is less than one tenth of the wavelength the line is not considered a transmission line. Having that for the 868 MHz frequency used by the LoRaWAN network the minimum trace length is 16.8 mm. Since the module is closed to the RF connector and the distance between the two is less than 16.8 mm the line that goes from the module to the RF antenna is not a transmission line. However it is important to see how the parameters of a transmission line are calculated for a PCB. The IPC-2141, Transmission Line Design Handbook by Wadell or the Single and Coupled Microstrip Lines in APLAC 1997 used by Kicad are numerical models that are used to calculate the impedance of a transmission line. For this project and using the Kicad calculator and considering a coplanar wave guide with ground plane the length for a transmission line of 50 Ω impedance is 0,31 mm. (inserir imagem da calculadora aqui)

B.1.5 Footprints

A footprint or land pattern is the arrangement of pads (in surface-mount technology) or through-holes (in through-hole technology) used to physically attach and electrically connect a component to a printed circuit boar [reference to Wikipedia]. Having this in mind the following process was followed. First a list with all the components present in the electrical schematic has made. Then a search in different electronics stores such as DigiKey, Mouser and others was conducted in order to find the components need. When the component was selected a looking in different libraries for the right footprint was conducted. There are several different components available on the market which leads to multiple footprints. Using the SnapEDA website [reference to the website] and the libraries present at KICAD the right footprints were choose to fit the components. Table B.1 shows the different footprints used for the each of the components in the design.

Table B.1: Components and footprints

Component	Footprint
All Capacitors	0805 [2012 Metric]
All resistors	0805 [2012 Metric]
L1	2.5mm x 2mm x 1.2mm
Y1	3.2mm x 1.5mm
Y2	5mm x 3.2mm
PIC microcontroller - PIC18LF46K22 - (U1)	44-PIN TQFP
Low Drowpout Regulator - MCP1810 - (U2)	5 Lead-SOT23
DC-DC buck converter - TPS627431 - (U3)	8-Pin DSBGA
Inverter - NC7SZ14 - (U4)	SOT23
Real Time Clock - DS1339AU - (U5)	8-MSOP
LoRaWAN module - RN2483 - (U6)	Specific footprint
Buffers - AD8244 - (U7)	10-MSOP
Diodes (D1)	DO-214AC (SMA)
Fuse (F1)	0805 [2012 Metric]

In the table for components such as resistors and capacitors it is possible to see two values. This is related to the units of measure used. The world presents two measurement systems, one called the metric system and another called the imperial system. The imperial system is used in the United States of America, Liberia, Myanmar and the United Kingdom. The rest of the world uses the metric system. The numbers represent the length and the width of the component. The first two numbers represent the length and the other two the width. Fig B.2 is a graphical representations of the sizes of a SMD component.

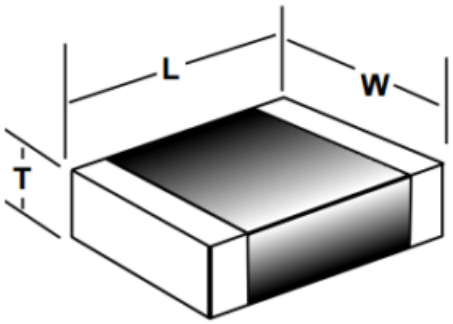

Figure B.2: Graphical representation of an SMD component

Where L represents the length, W the width and T the thickness. So the number 0805 refers to a component that as length of 0.08 inches and a width of 0.05 inches. A inch is equal to 2.54 cm leading to 2.0 mm and 1.2 mm for the length and width respectively. It is now understandable the number 2012 and the word metric after it. Is a form to tell the user that the 2012 corresponds to the dimensions in meters. When the package doesn't follow the standard packages the dimensions are presented in the same order.

So the inductor L1 has 2.5 mm of length, 2 mm of width and 1.2 mm of thickness. Sometimes the value of thickness can be omitted as the crystals presented in the table show. It is also important to take in consideration the solder pad land pattern. The solder pad land patter is where the component makes contact with the PCB. The Fig. B.3 is a representation of a solder pad land patter. where a is the pad

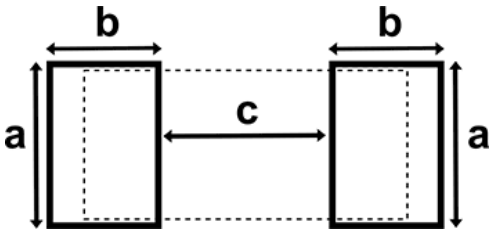

Figure B.3: Solder pad land patter

length, b the pad width, and c the gap between pads. The values of a, b and c are also tabulated and can be found online for different SMD components.

B.1.6 Final design

By having in consideration all the aspects that where mention in the last subtopics related to a PCB design the layers present in section B.2 represent the final PCB board for the embedded system of this thesis.

B.2 Layers of the printed circuit board

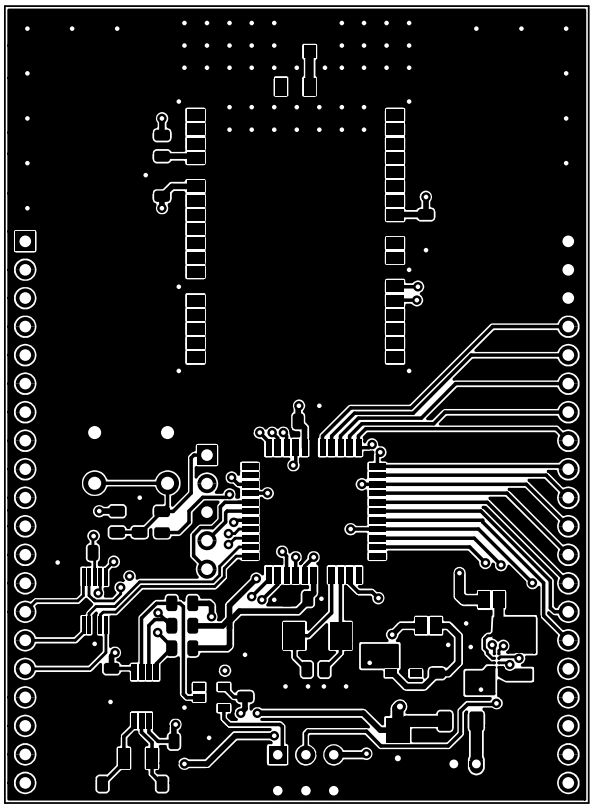

Figure B.4: Front Copper Mask

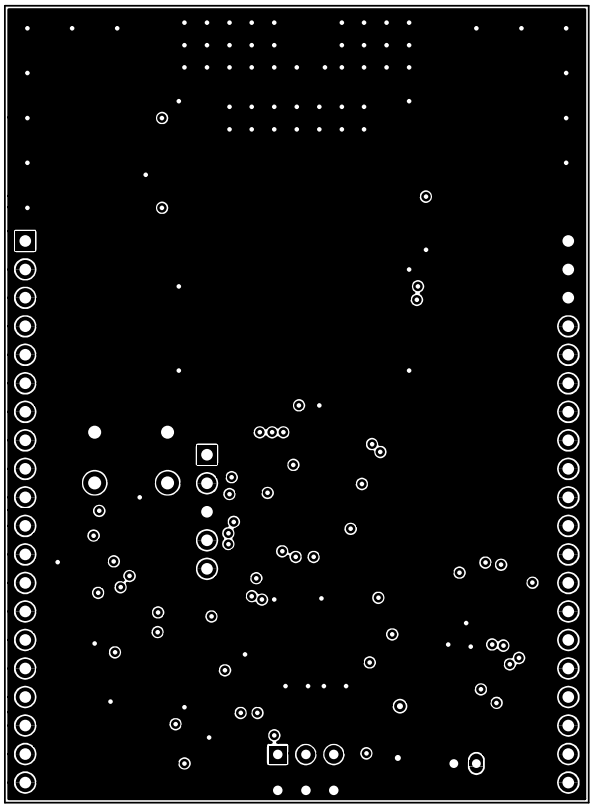

Figure B.5: Second layer of copper - Ground plane

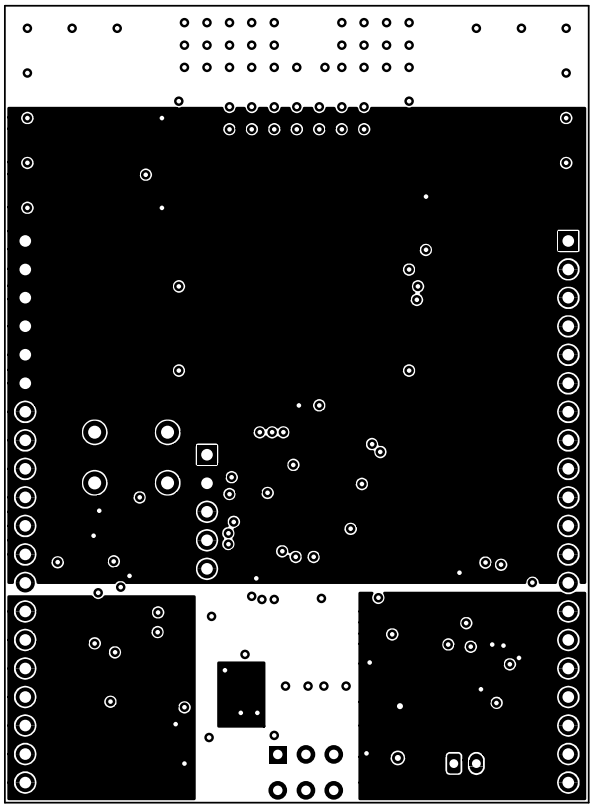

Figure B.6: Third layer of copper - Power plane

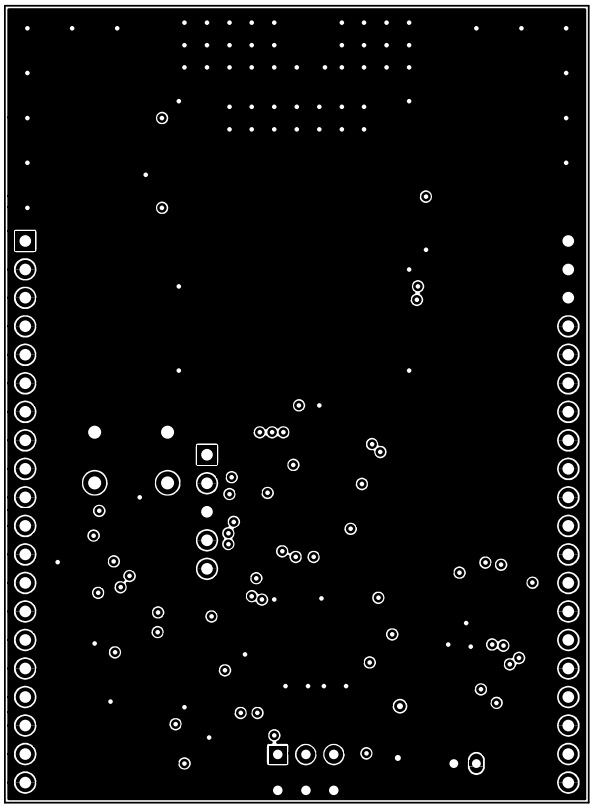

Figure B.7: Fourth layer of copper - Ground plane